LIPID KERATOPATHY IN THE DOG

VOLUME III

SHEILA CRISPIN,

M.A., Vet.M.B., B.Sc., M.R.C.V.S., D.V.A.

MAY, 1984

DEGREE OF DOCTOR OF PHILOSOPHY,

UNIVERSITY OF EDINBURGH.

VOLUME III

PHOTOGRAPHIC FIGURES

5.8/1 - 5.9/67

Figure 5.8/1

Squash Preparation in Prescence of Excess Water at 33 C (73R)

Isotropic droplets (A) and (B). The latter have formed from anisotropic droplets which have swelled in the presence of excess water.

Polarised light with first order red gypsum accessory plate X 390 (8)

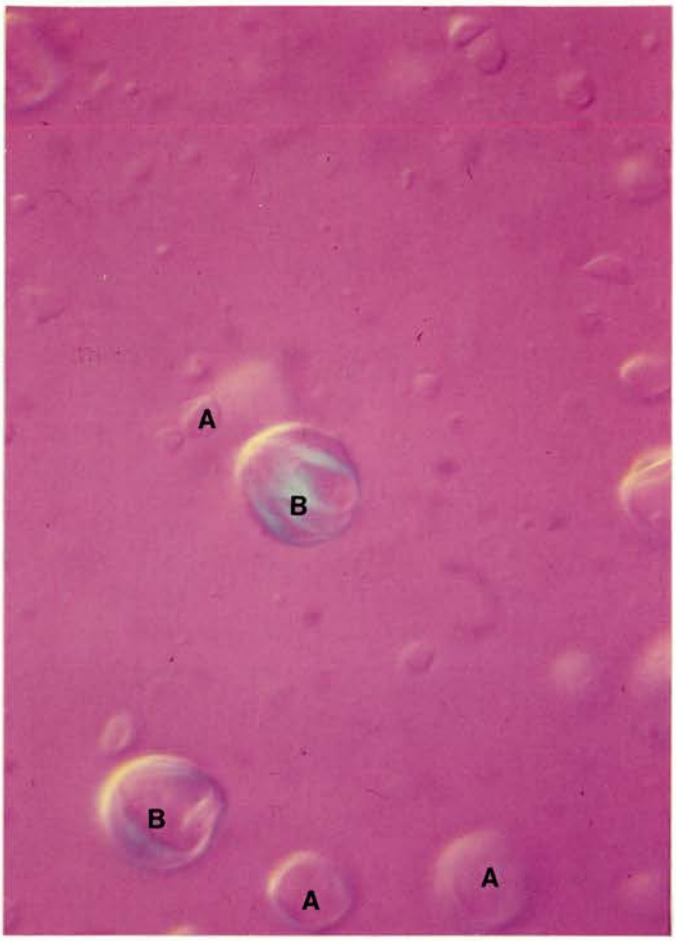
A
B
B
A
A

Figure 5.8/2 & 5.8/3

Squash Preparation of Anisotropic Droplets in 80% Glycerol at 33°C (42)

5.8/2 is rotated through 180° with respect to 5.8/3.

Polarised light with first-order red gypsum accessory plate X 390 (8)

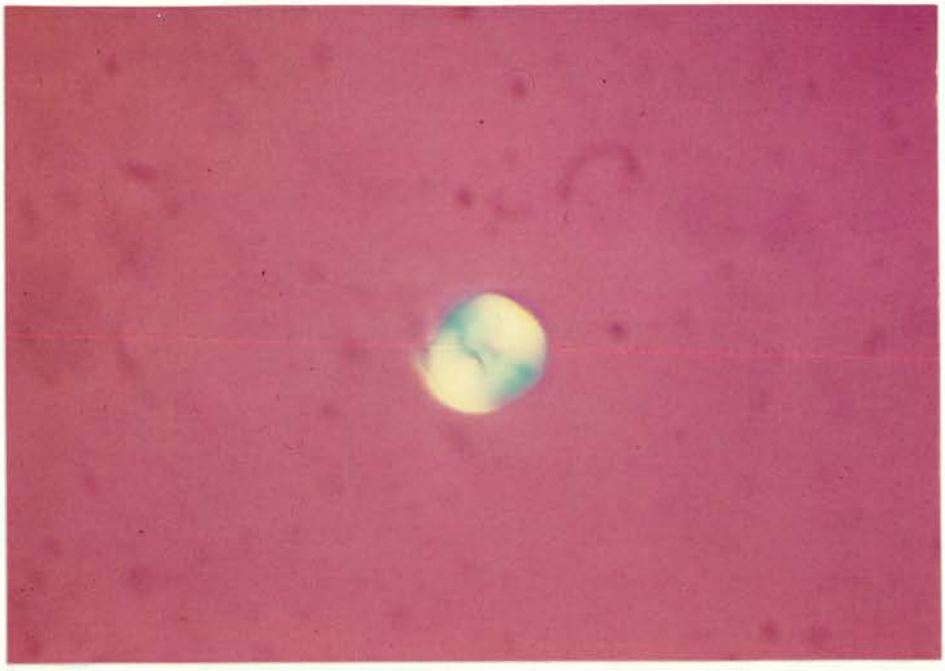

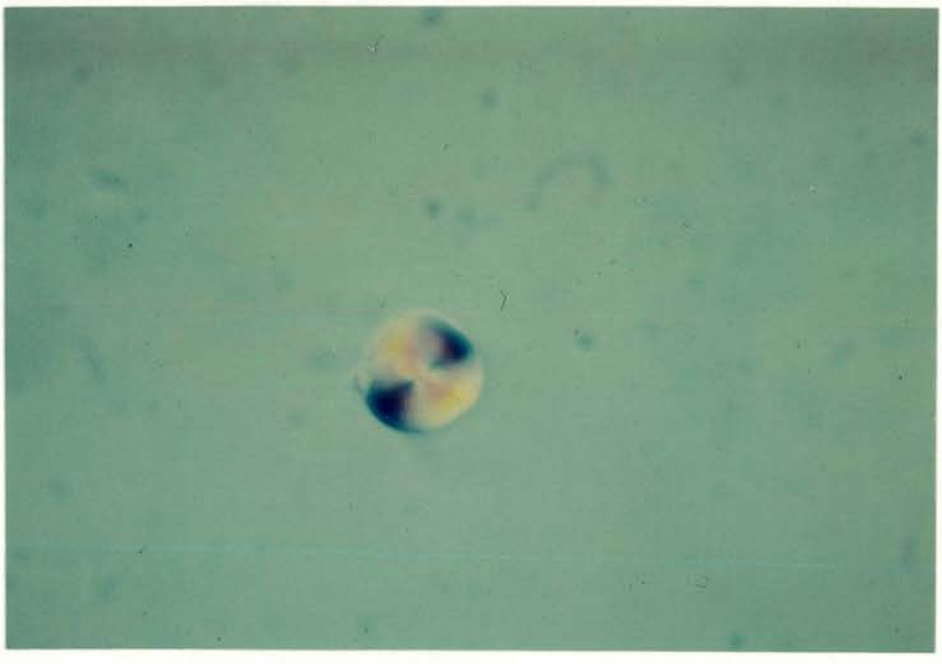

Figure 5.8/4

Squash Preparations of Crystals of Free Cholesterol (36R)

Polarised light with first-order red gypsum accessory plate X 390 (4).

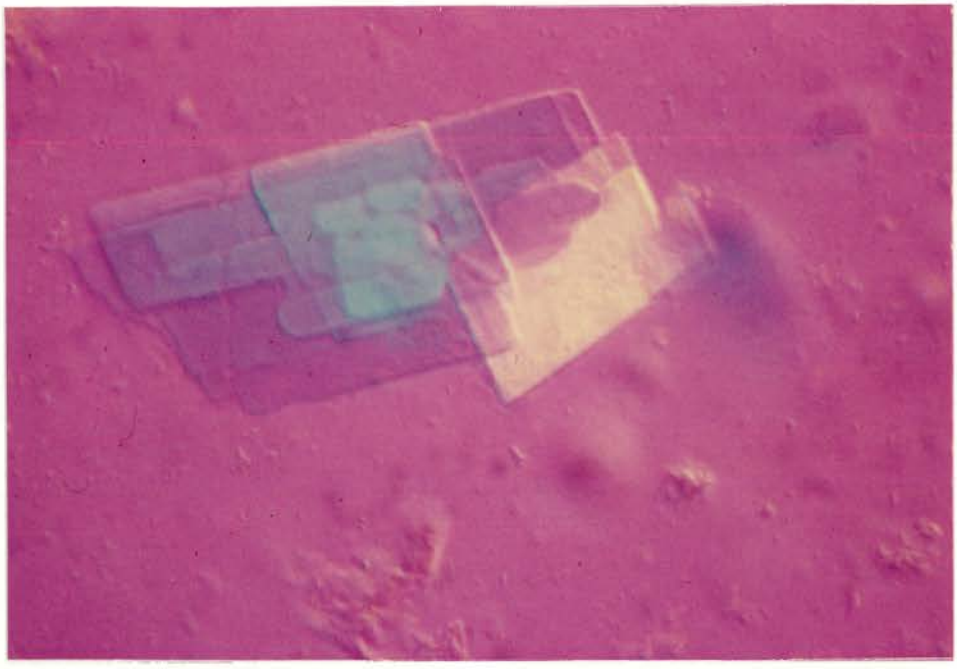

The following photomicrographs from clinical cases are meridional sections unless otherwise stated.

Figure 5.8/5

English Springer Spaniel (65R)

Intracytoplasmic vacuoles visible within fibroblasts (arrows) in a lesion of fine granular slit lamp appearance.

Toluidine Blue X 310 (4)

Figure 5.8/6

Golden Retriever (1R)

Tangential section of the anterior stroma in a zone of granular slit lamp appearance. Fibroblasts are of irregular shape and contain intracytoplasmic vacuoles (arrows).

Toluidine Blue X 280 (4)

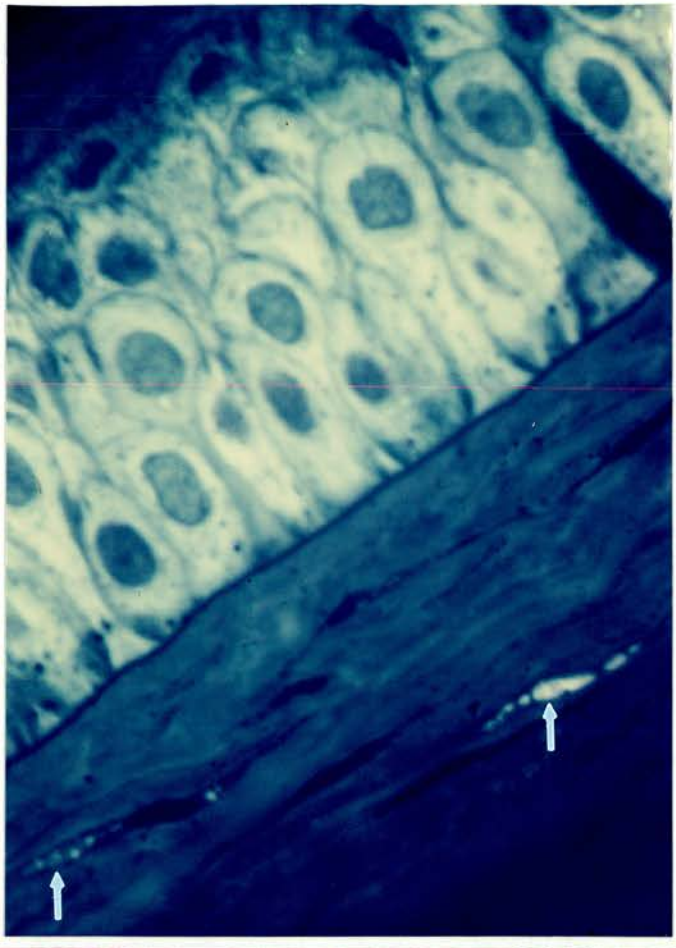

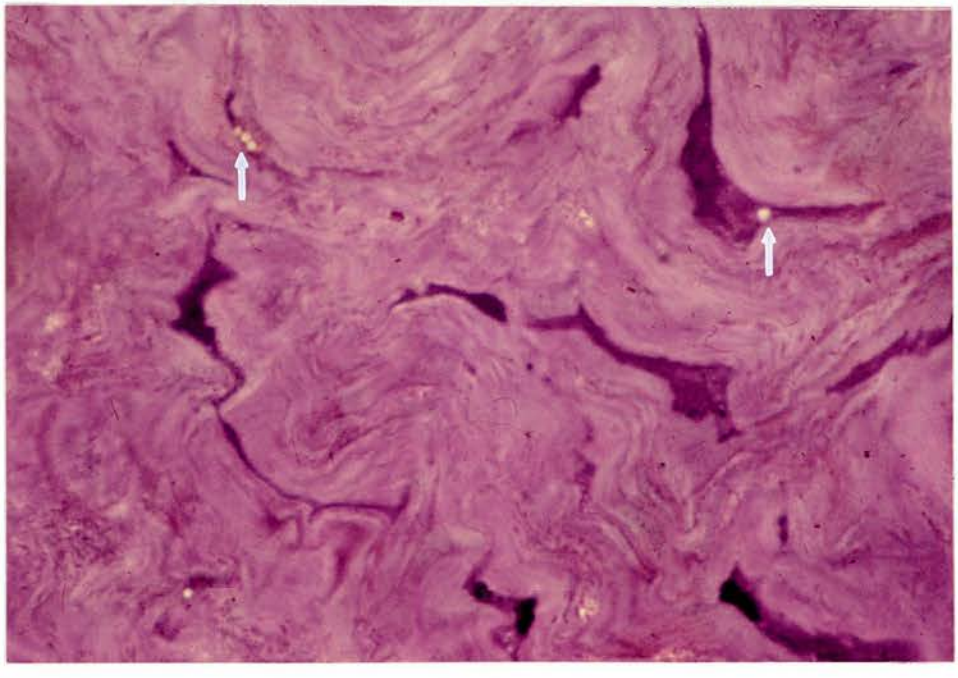

Figure 5.8/7

Welsh Springer Spaniel (42R1)

Non-vascularised, diffuse lesion of hazy slit lamp appearance. Mild changes are denoted by sparse intracellular vacuoles (arrows) and little stromal disruption at the edge of the lesion.

Alcian Blue, pH 0.5, Nomarski Differential Interference

Contrast X 280 (4)

Figure 5.8/8

Welsh Springer Spaniel (42L)

Numerous vacuoles; the majority appear to be intracellular (arrows) whereas others may be genuinely extracellular. There is considerable stromal disruption with separation of collagen lamellae in this, the densest part of the lesion.

Alcian Blue, pH 0.2, Nomarski Differential Interference

Contrast X 280 (4)

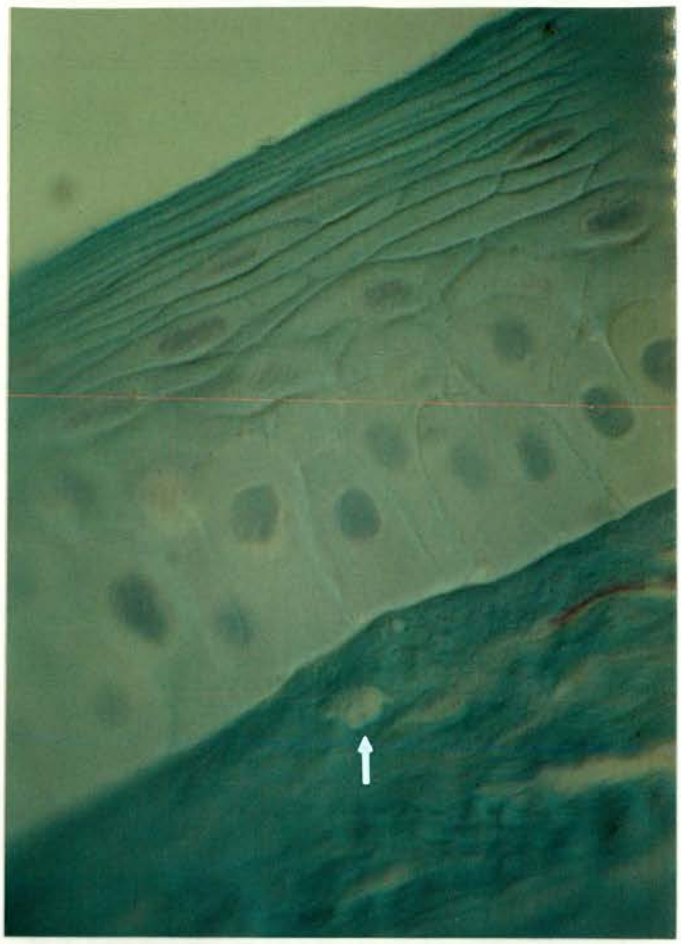

Figure 5.8/9

English Springer Spaniel (65R)

Granular zone of an early lipid keratopathy. Enhanced staining of basement membrane region (arrow). Fibroblasts (A) also stain more heavily than usual.

Bromine Sudan Black B X 155 (4)


A

Figure 5.8/10

English Cocker Spaniel (24L)

Dense opacity of recent origin.

Alcian Blue/PAS X 70 (4)

Figure 5.8/11

English Cocker Spaniel (24L)

Dense opacity of recent origin.

Sakaguchi Method X 100 (4)

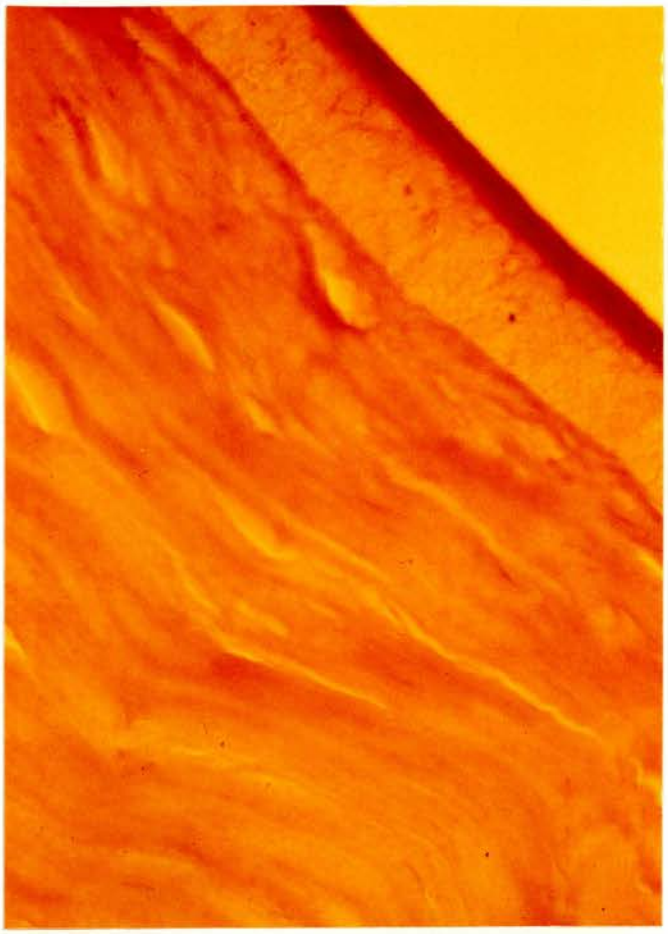

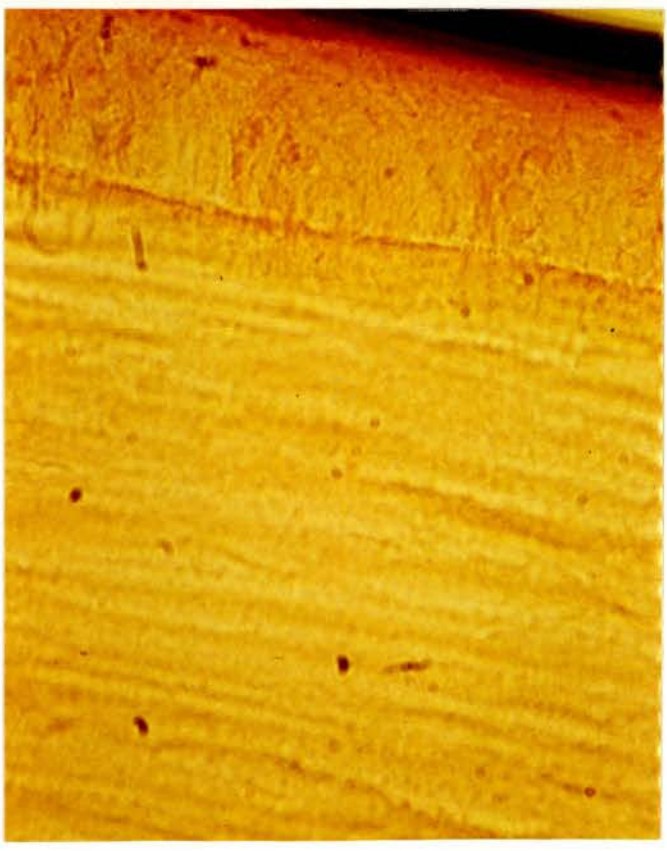

Figure 5.8/12

English Springer Spaniel (65R)

Early opacity of granular appearance. Intracytoplasmic vacuoles within fibroblast (arrowed). The vacuoles are not positive with the Holczinger technique, whereas the epithelium is more darkly stained than control cornea.

Holczinger Technique, Nomarski Differential Interference Contrast X 90 (4)

Figure 5.8/13

Welsh Springer Spaniel (42L)

Early granular opacity.

PAN X 90 (4)

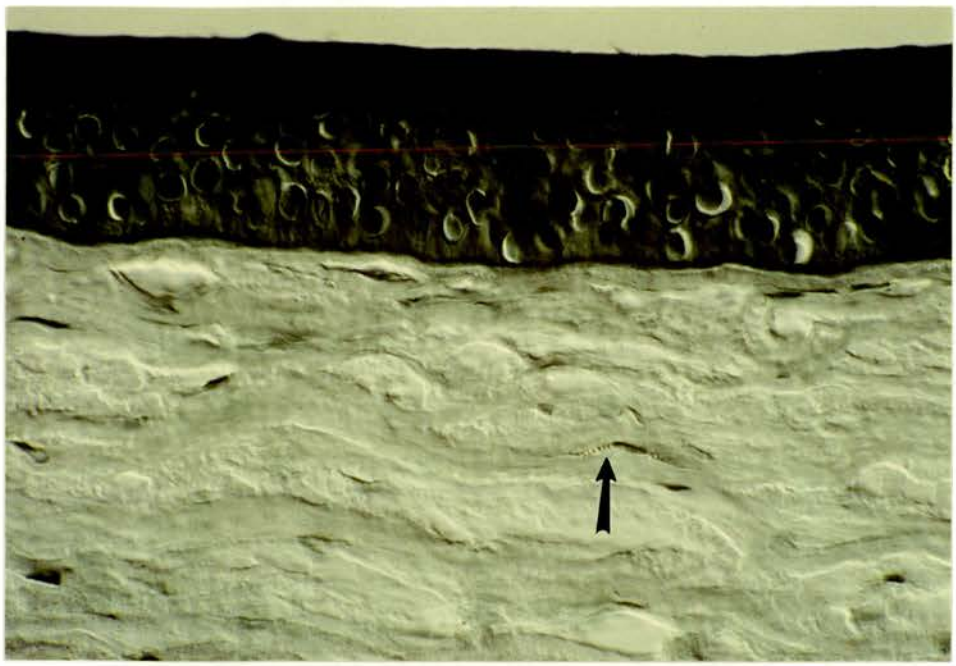

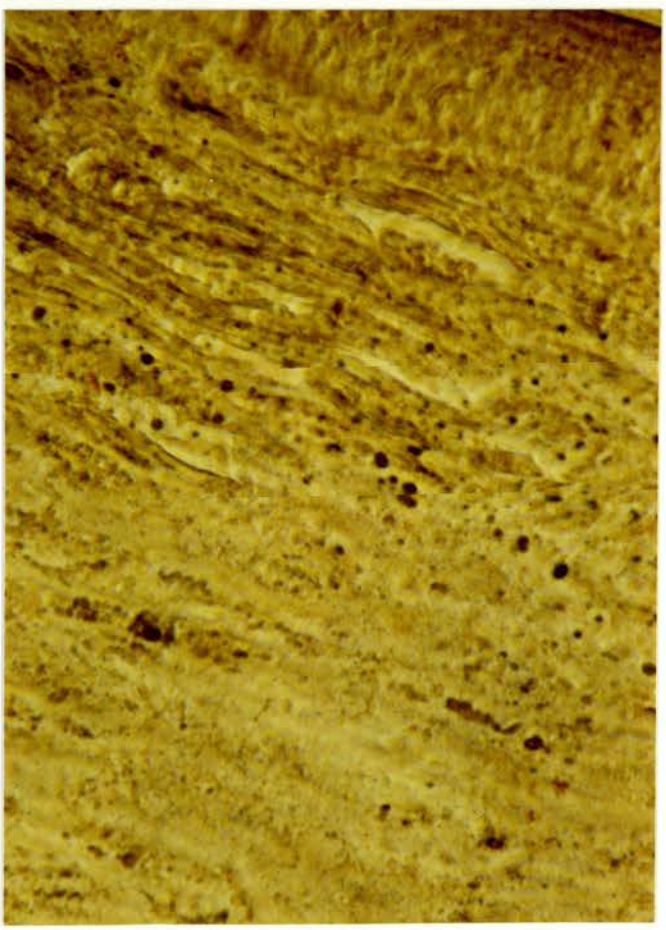

Figure 5.8/14

English Springer Spaniel (24L)

Granular part of opacity. Fibroblast with coarse intracellular lipid globules (A) and rather finer extracellular, diffuse, perifibrous, more granular lipid (B). Other fibroblasts (C) are stained grey and do not apparently contain globular lipid.

Acid Haematein-Oil Red O X 125 (4)

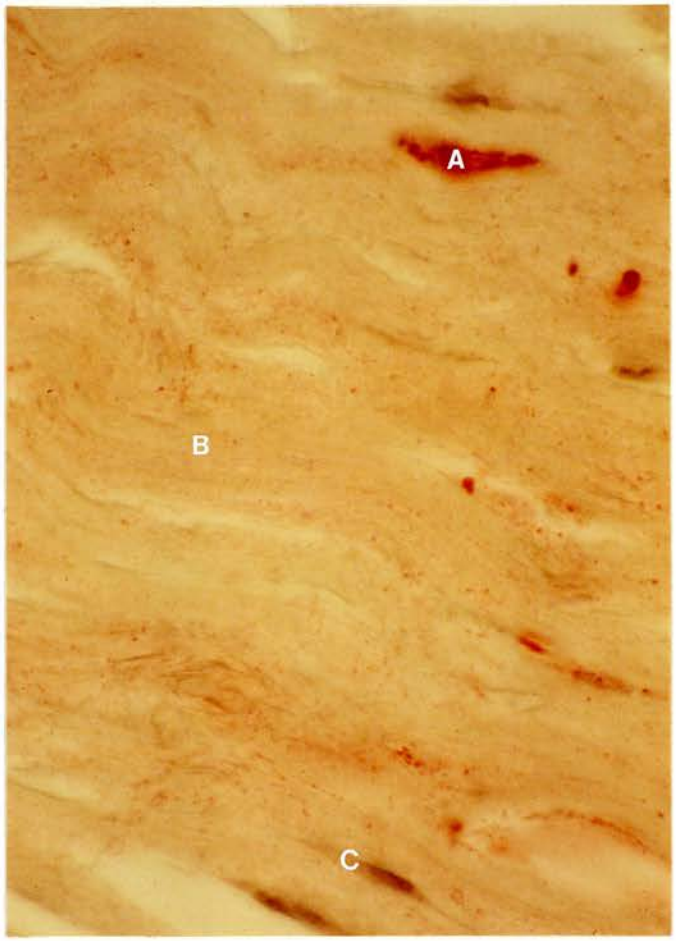
A
B
C

Figure 5.8/15

Alsatian X (150R)

The appearance of a superficial lesion. There is epithelial melanosis and mitosis with some disruption of lamellae and vacuolation of stromal fibroblasts.

Toluidine Blue X 280 (4)

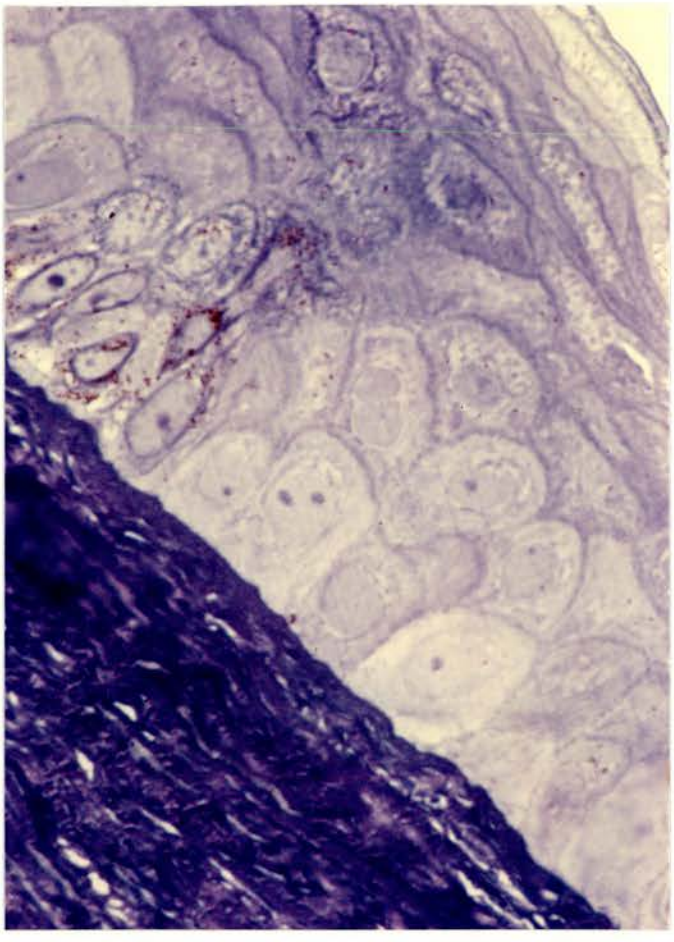

Figure 5.8/16

Golden Retriever (14L)

Slightly tangential section from a lesion with the densest opacity at mid-stromal level. Both fibroblasts and collagen lamellae are degenerate and there is obvious disorganisation.

Toluidine Blue X 280 (4)

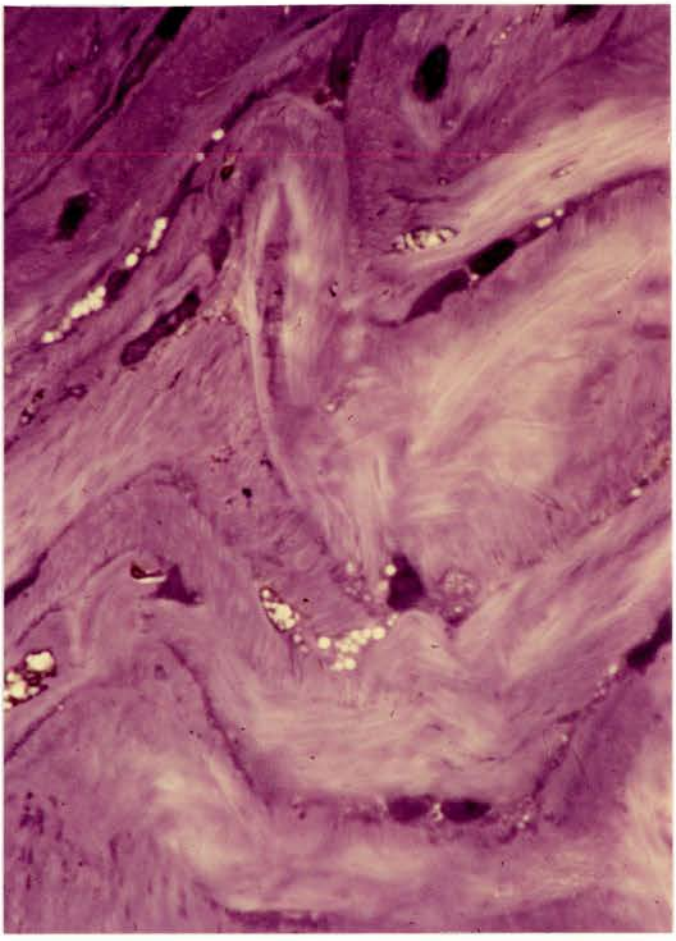

Figure 5.8/17

Alsatian (36L)

A dense lesion of granular and crystalline appearance. Numerous small, clear, spaces in the epithelial cells (A). The basement membrane is poorly defined (arrowed). Degenerate fibroblasts are prominent and there are acicular spaces (B), in addition to circular spaces (C), throughout the stroma.

Toluidine Blue X 280 (4)

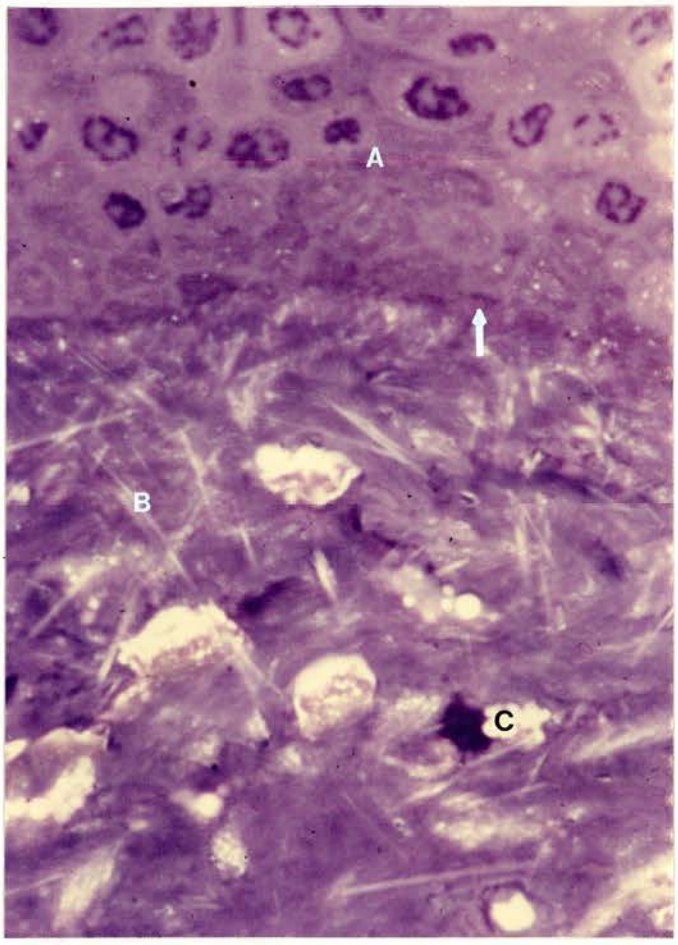
A
B
C

Figure 5.8/18

Alsatian (36R)

The other eye of the dog shown in Figure 5.8/17. The right eye has been affected for longer. The slightly tangential section emphasises the intense staining of the subepithelial zone and irregularity of the basement membrane. There are numerous clear spaces which were previously occupied by crystals or droplets of lipid. The region of heaviest lipid deposition is relatively acellular, whereas the surrounding region is hypercellular.

Toluidine Blue X 100 (4)

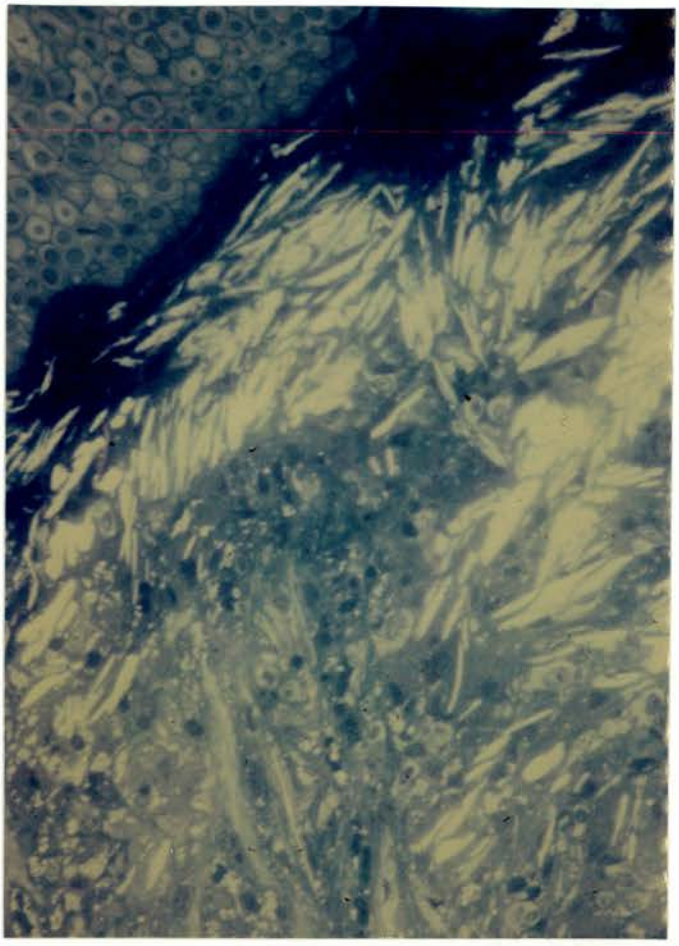

Figure 5.8/19

Welsh Springer Spaniel (42R2)

Dense, white, poorly vascularised plaque. Large, almost circular, intracellular spaces which are poorly separated (A). They probably represent poorly emulsified, saturated, lipid to judge from lipid histochemistry. There is little evidence of membranous lamellae which accords with the lack of phospholipid found with histochemical techniques.

Toluidine Blue. Nomarski Differential Interference Contrast X 310 (4)

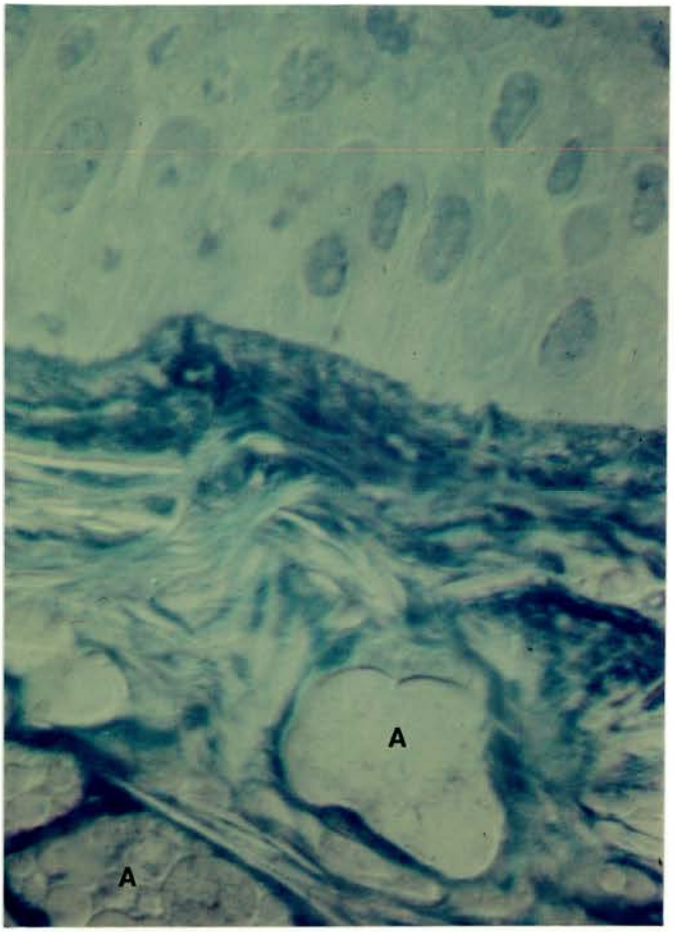
A
A

Figure 5.8/20

Welsh Springer Spaniel (42R3)

In a later keratectomy specimen, when the lesion was regressing in comparison with the expanding lesion seen in Figure 5.8/19, there was evidence of clearing in some zones and dense opacification in others. In this section there is superficial (A) and deep (B) vascularisation and extensive accumulation of lipidic debris (C) beneath crenated and irregular basement membrane. Collagen lamellae are thickened and separated in the anterior stroma, degenerate and necrotic more deeply.

Toluidine Blue X 390 (4)

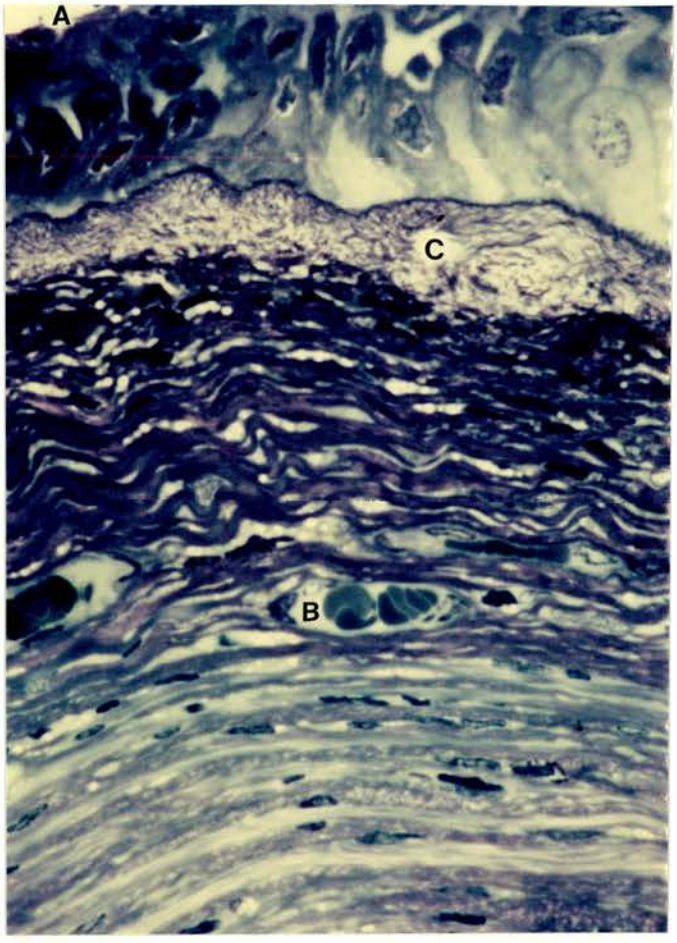
A
C
B

Figure 5.8/21

Golden Retriever (9L)

Numerous membranous lamellae or liposomes (A), many are associated with degenerate fibroblasts, whereas others have accumulated beneath the basement membrane.

Toluidine Blue X 180 (4)

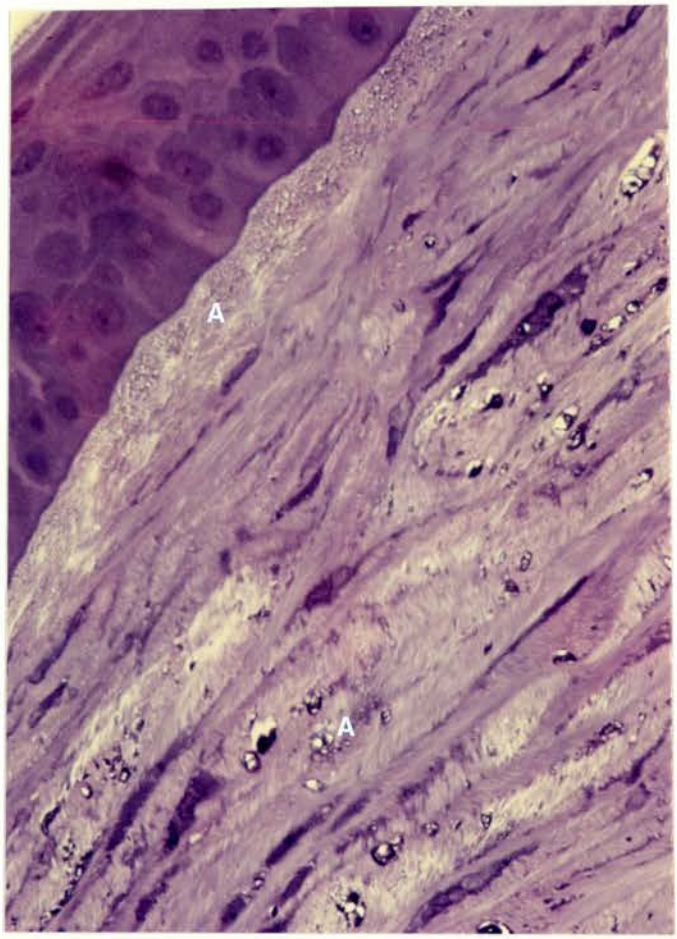
A
A

Figure 5.8/22

Alsatian X (150L)

Vascularised superficial lesion. Hydropic changes in some of the epithelial cells, no enhanced staining in the corneal stroma.

Sakaguchi Method X 70 (4)

Figure 5.8/23

English Cocker Spaniel (24R)

Dark staining regions present in anterior epithelium, basement membrane and fibroblasts. Heavy granular staining is closely related to the fibroblasts.

Holczinger Technique X 125 (4)

Figure 5.8/24

Alsatian (27L1)

Diffuse staining of epithelium and discrete staining of fibroblasts at the periphery of the lesion.

Holczinger Technique X 125 (4)

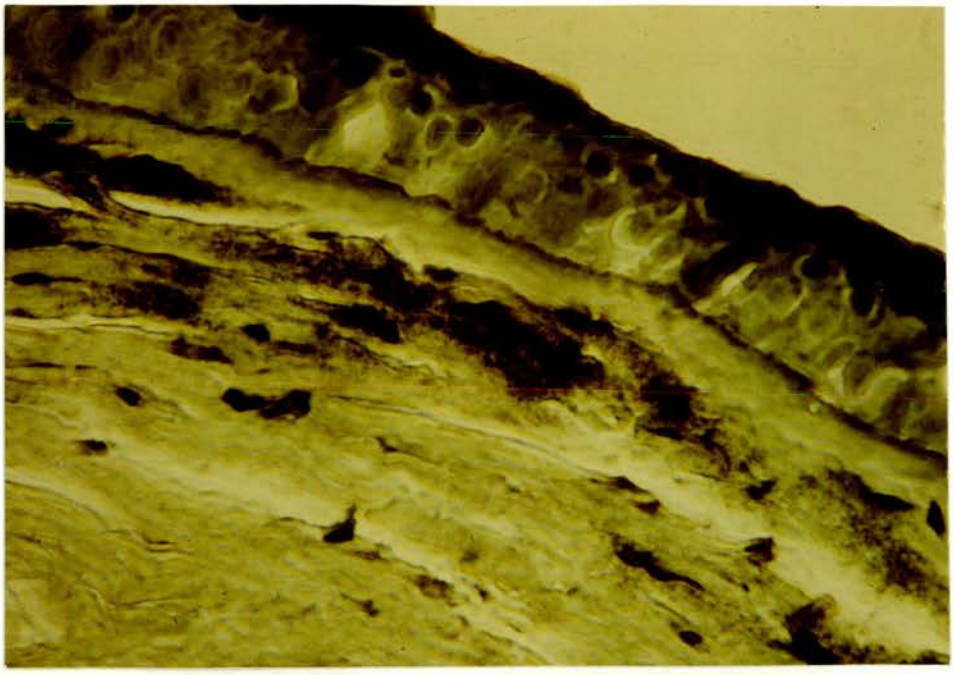

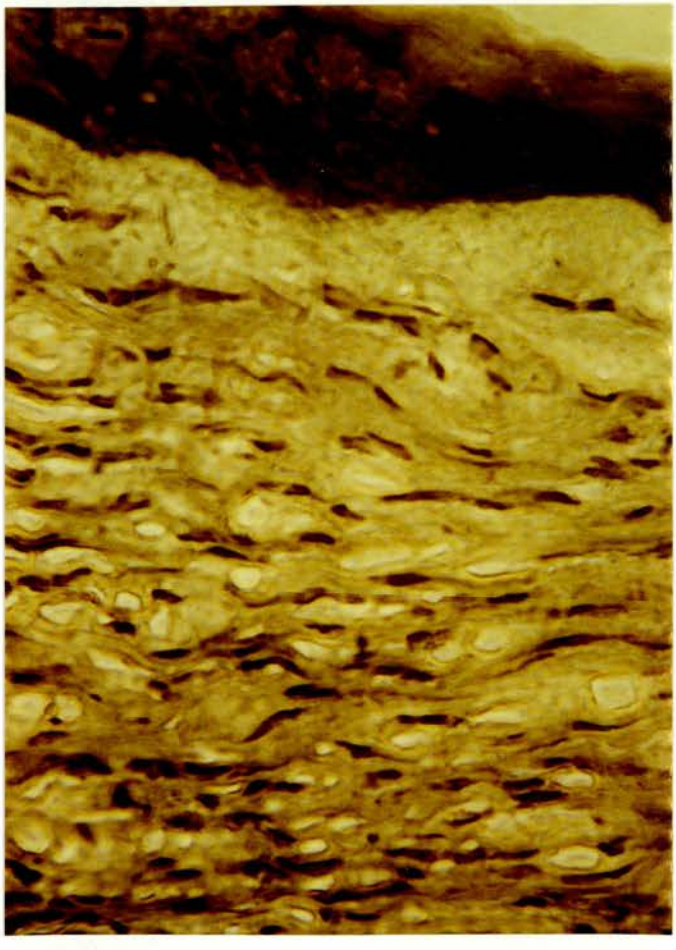

Figure 5.8/25

Welsh Springer Spaniel (42R2)

Very little stromal staining in relatively acellular, necrotic, region in the centre of the corneal opacity. Nuclei of posterior epithelial cells are strongly stained.

Holczinger Technique X 125 (4)

Figure 5.8/26

Alsatian (27L1)

Parallel section to Figure 5.8/24. Acetone-extracted section stained with Holczinger technique using carmalum counterstain.

Holczinger Technique X 125 (4)

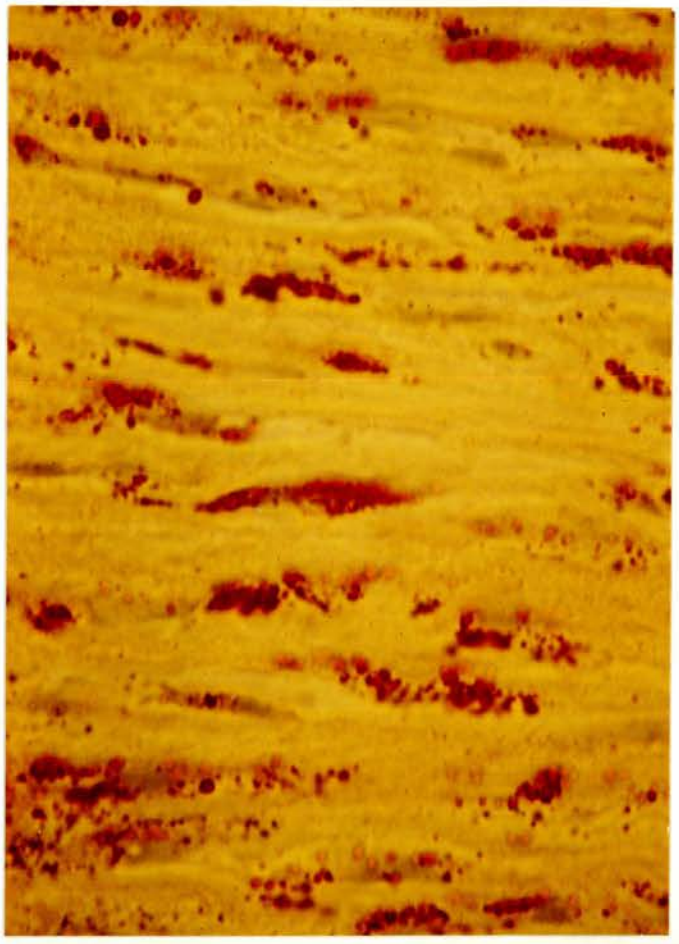

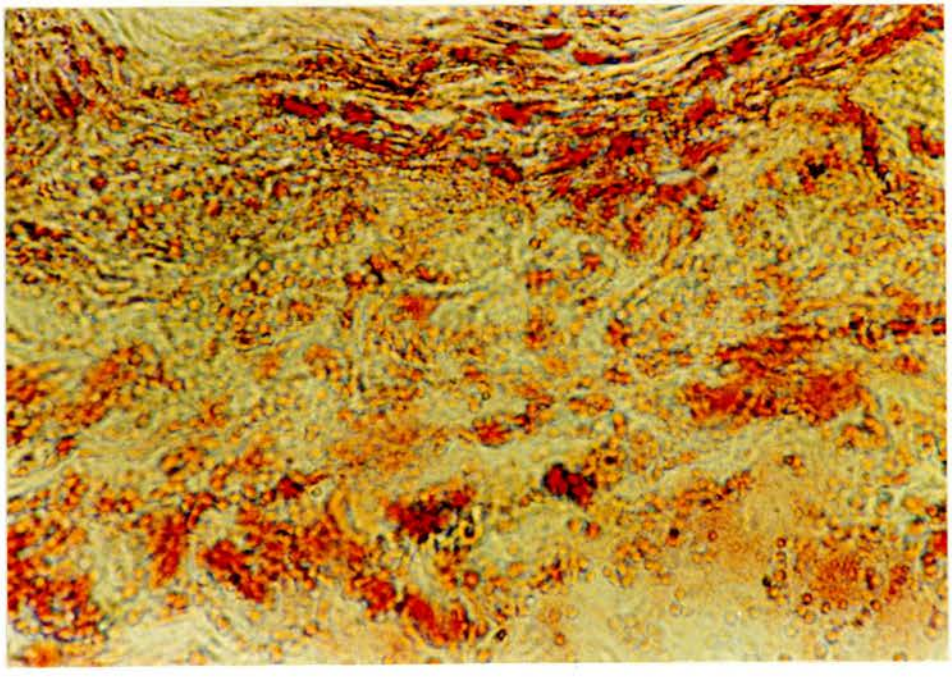

Figure 5.8/27

English Cocker Spaniel (24R)

Calcium Lipase-Lead Sulphide X 125 (4)

Figure 5.8/28

English Cocker Spaniel (24R)

Some positive staining is retained in the anterior epithelium of the control section. Compare the staining of this section with that for free fatty acids in Figure 5.8/23.

Non-enzyme treated parallel control section X 125 (4)

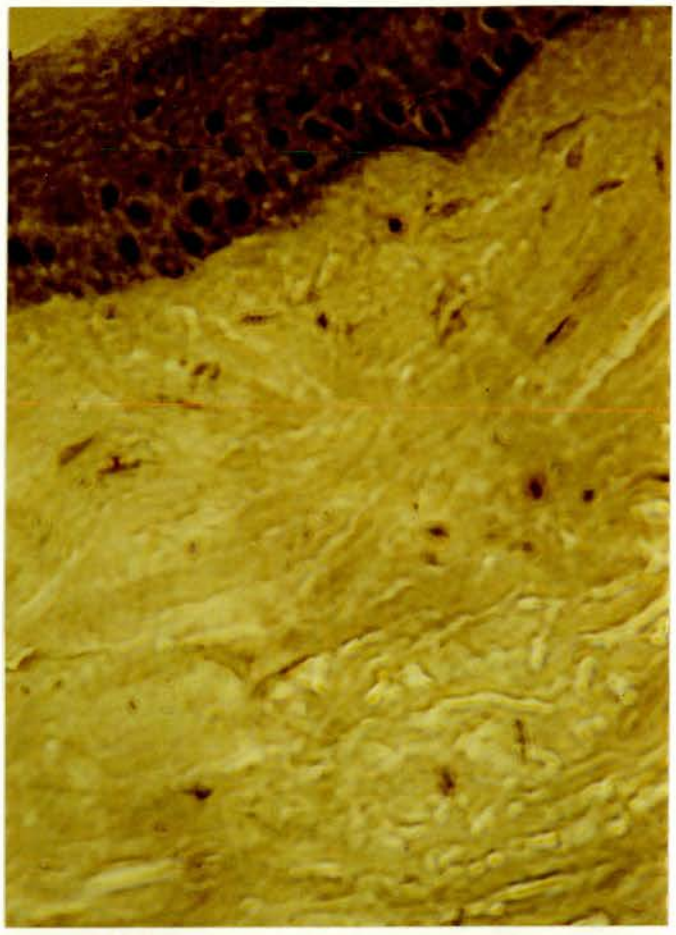

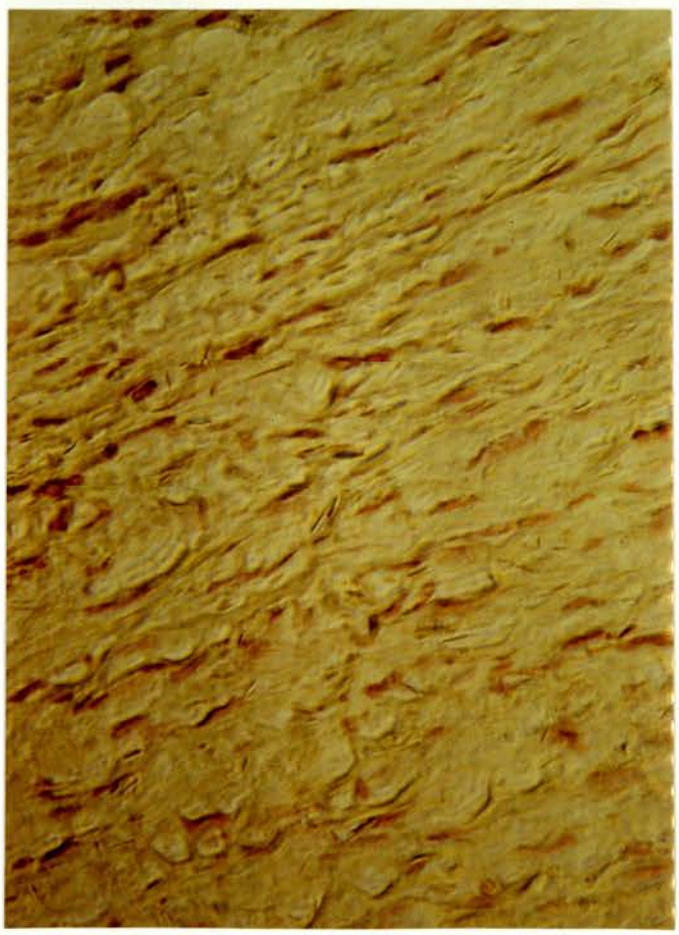

Figure 5.8/29

Alsatian (27L2)

In this animal triglyceride is apparently present in the anterior epithelium as fine granules (A). In the stroma there are occasional positive droplets (B) and diffuse patches (C). Cholesterol crystals are also present (D). The arrow delineates the basement membrane. Serum lipids and lipoproteins were in Group IV.

Calcium Lipase - Lead Sulphide X 90 (4)

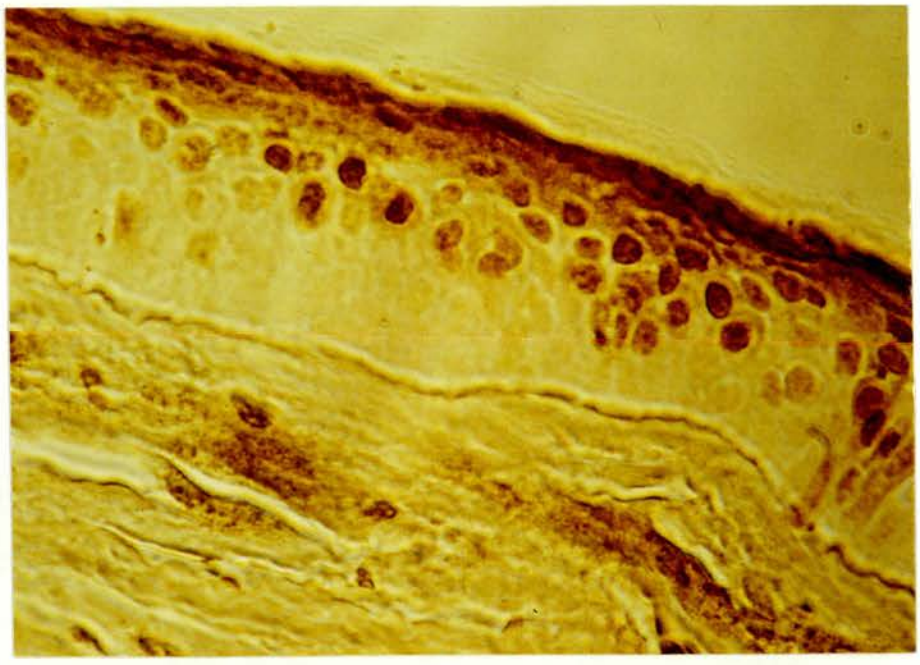

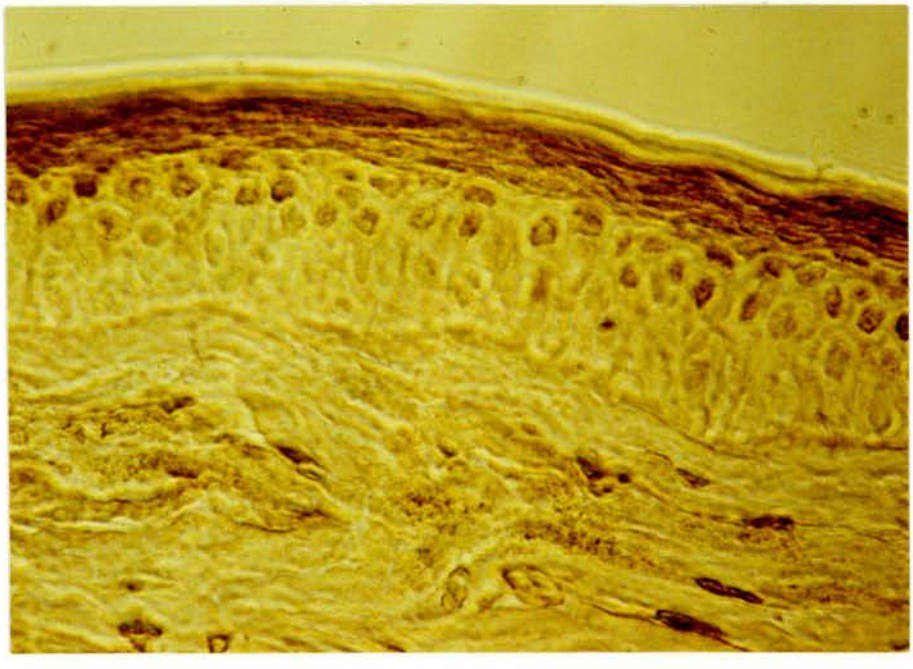

Figure 5.8/30

English Springer Spaniel (65R)

Intracellular lipid droplets predominate.

Oil Red O X 310 (4)

Figure 5.8/31

Alsatian (36L)

Compared with Figure 5.8/30 there are greater quantities of lipid droplets present and their exact location within the stroma is impossible to determine.

Oil Red O X 310 (4)

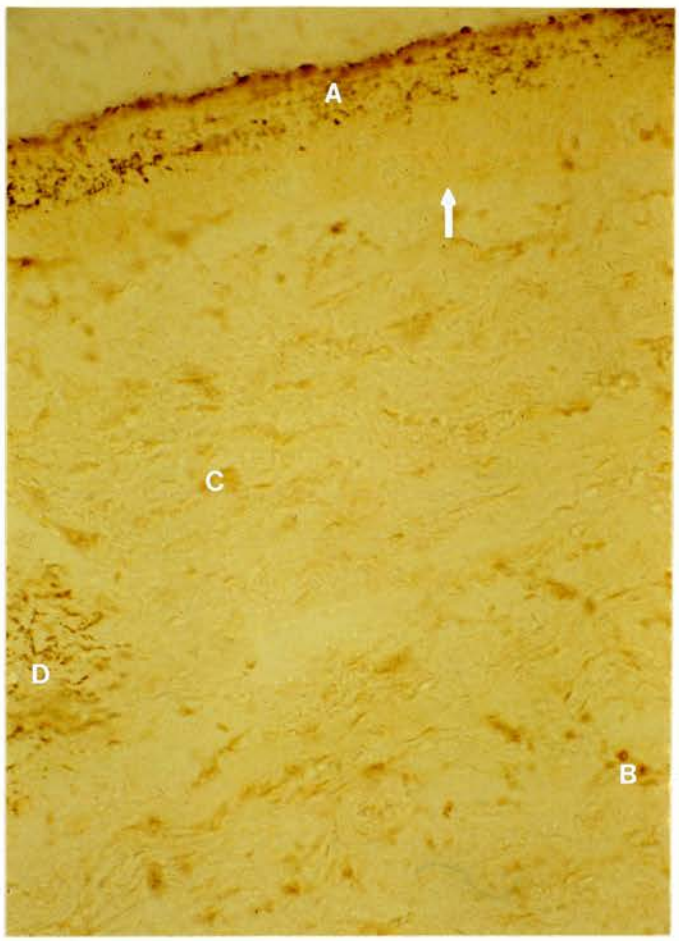
A
C
D
B

Figure 5.8/32

Alsatian (27R2)

Anisotropic and isotropic droplets with less frequent aggregates of birefringent solid crystals. The corneal epithelium appears devoid of lipids, whereas they are widely dispersed within the stroma.

PAN, Polarised Light X 40 (4)

Figure 5.8/33

Alsatian (36R)

Richly vascularised superficial lesion in a dog with hypercholesterolaemia (Group III). Numerous cholesterol crystals apparent within the stroma.

Unstained, short-fixed cryostat section,

Polarised Light X 90 (5)

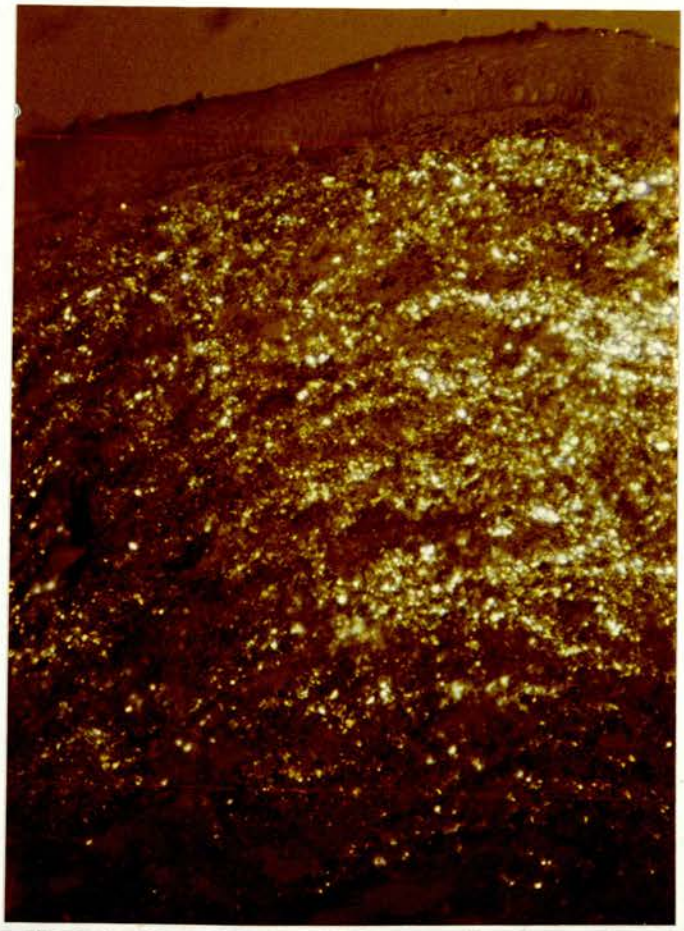

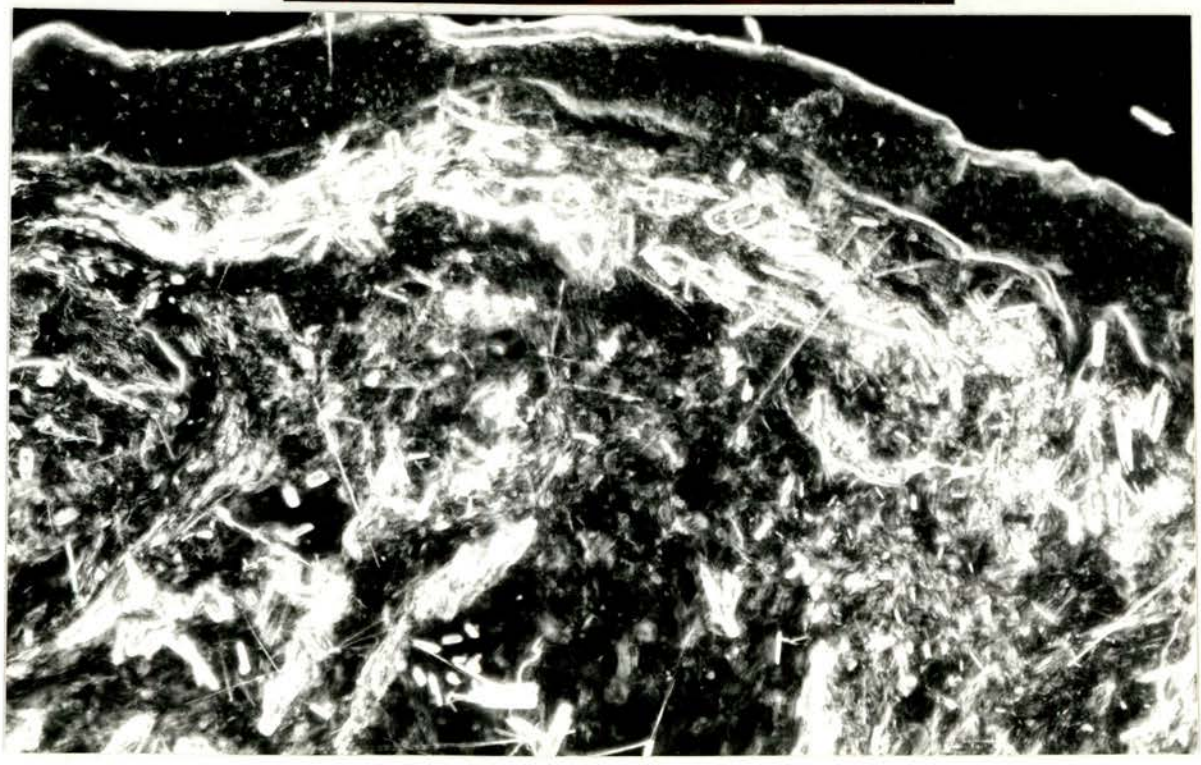

Figure 5.8/34

Great Dane (74R)

Occasional cholesterol crystals (A) and discrete fibroblasts containing mainly hydrophobic lipid droplets (B).

Acid Haematein - Oil Red O, Polarised Light X 60 (4)

Figure 5.8/35

English Springer Spaniel (65R)

Slightly tangential section in the region of crystalline and granular opacity with vascularisation nearby. There are cholesterol crystals (A) and degenerative fibroblasts containing large quantities of lipid (B).

Oil Red O, Polarised Light X 155 (4)

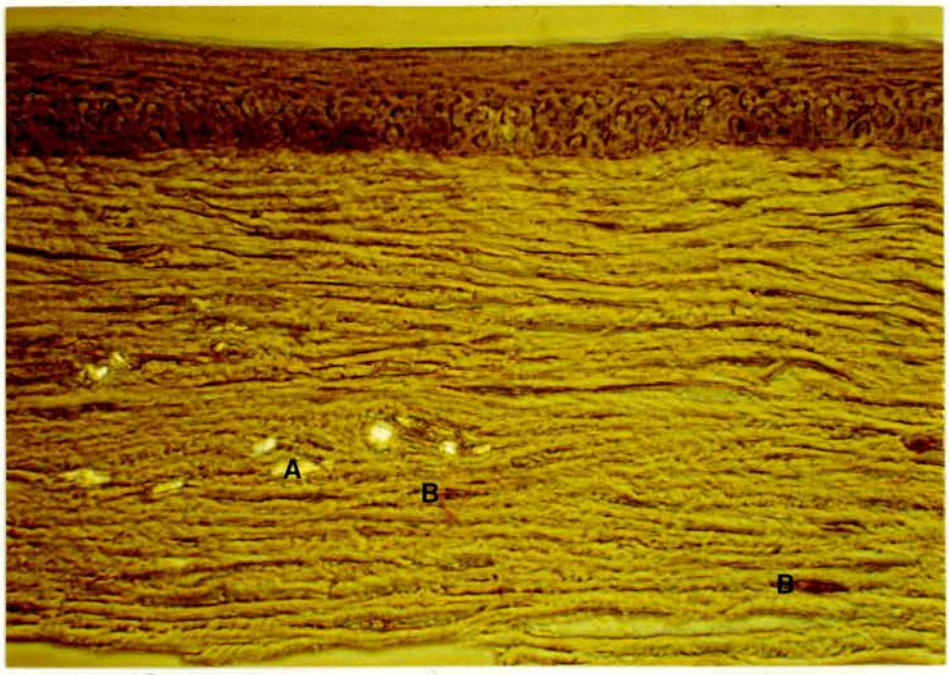
A
B
B

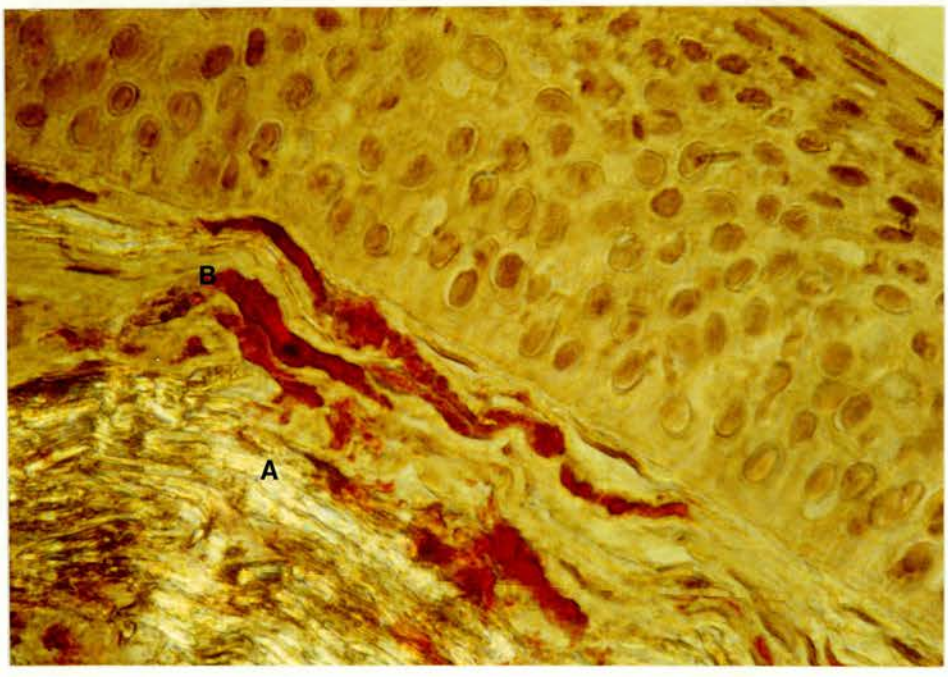
B
A

Figure 5.8/36

Welsh Springer Spaniel (42R2)

Large cholesterol granuloma (A) with hydrophobic lipid at its periphery and between the sheaves of cholesterol crystals.

Oil Red O X 70 (4)

Figure 5.8/37

Welsh Springer Spaniel (42R2)

The same granuloma as in Figure 5.8/36.

Nile Blue Sulphate, Polarised Light X 40 (4)

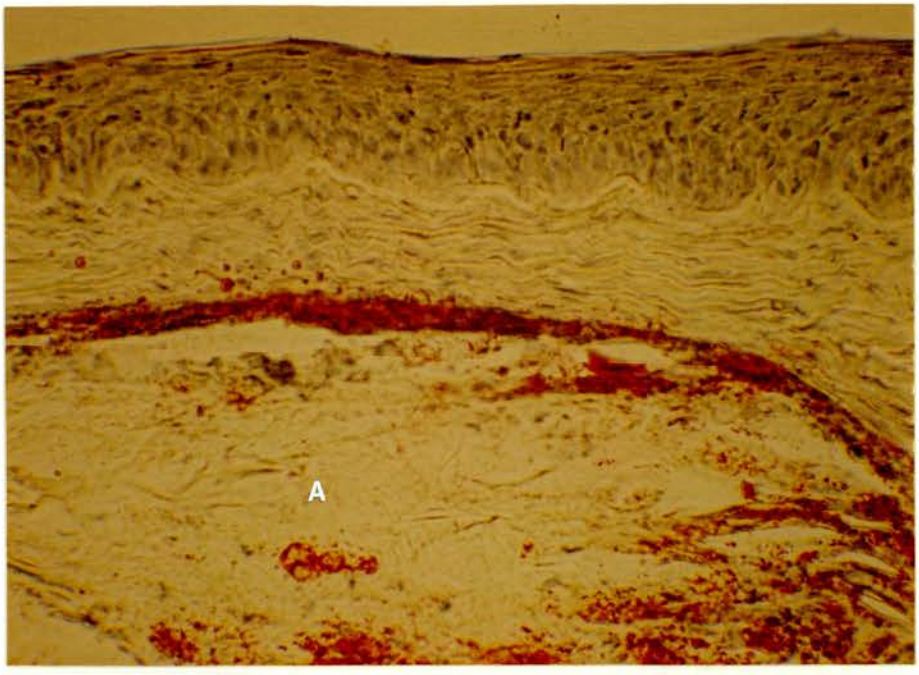
A

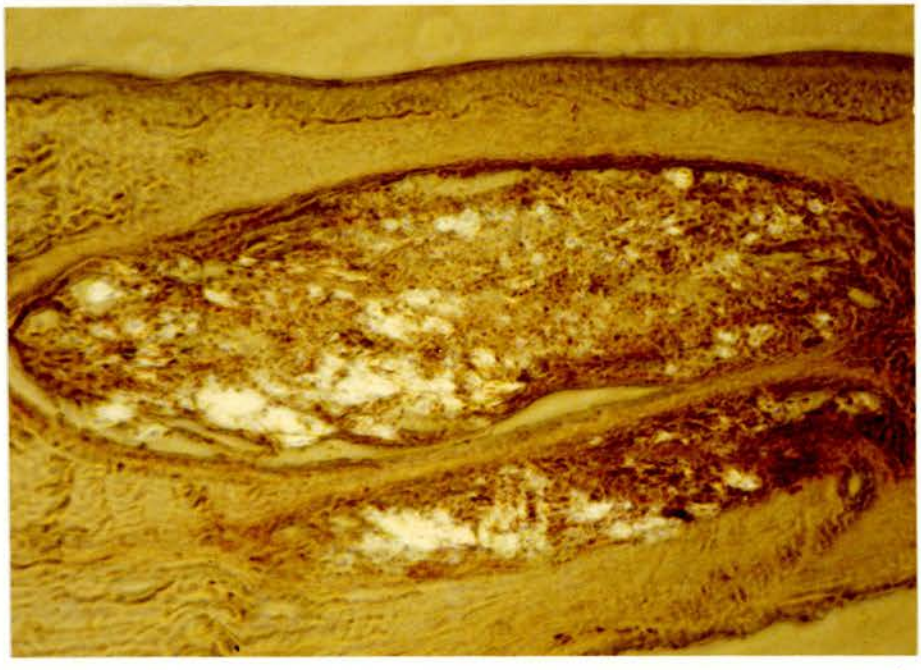

Figure 5.8/38

Welsh Springer Spaniel (42R3)

The majority of the discrete phospholipid staining is associated with fibroblasts.

Acetone - Acid Haematein X 125 (4)

Figure 5.8/39

Golden Retriever (6R)

Finely granular material (A) beneath the corneal epithelium and the basal epithelial cells are more darkly stained than in a normal control. Larger, phospholipid-positive, globules are present within the fibroblasts (B).

OTAN X 155 (4)

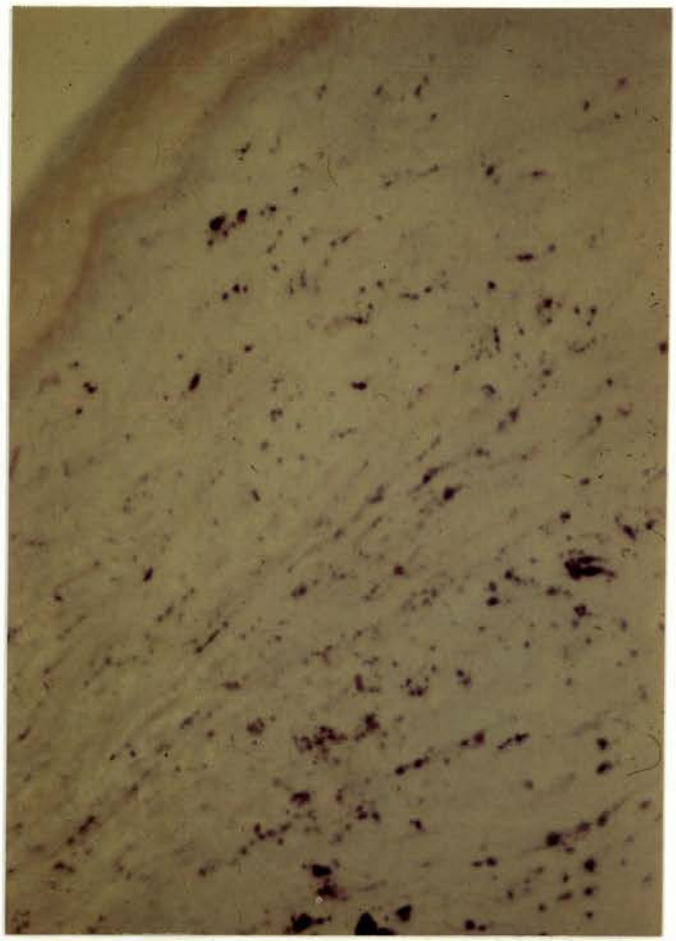

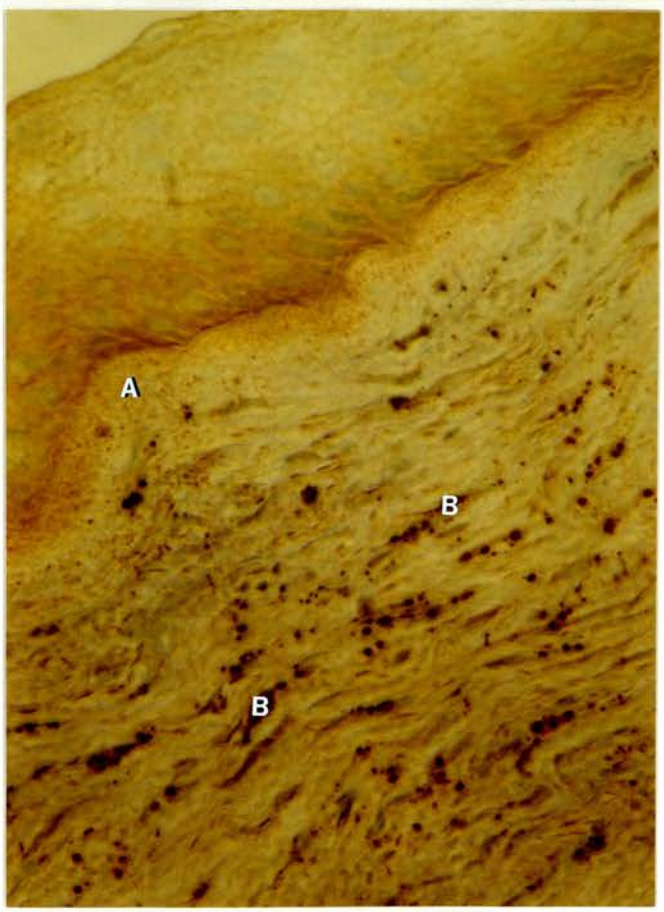
A
B
B

Figure 5.8/40

Welsh Springer Spaniel (42R3)

The persistence of staining in the fibroblasts with this technique indicates a high sphingomyelin content in the phospholipid. Compare this staining with that of Figures 5.8/38 and 5.8/39.

OTAN - NaOH X 125 (4)

Figure 5.8/41

Alsatian (36L)

Intense black staining of epithelium (A) and stroma (B). Cholesterol crystals are also present (C).

Acid Haematein, Partially Crossed Polarisers X 60 (4)

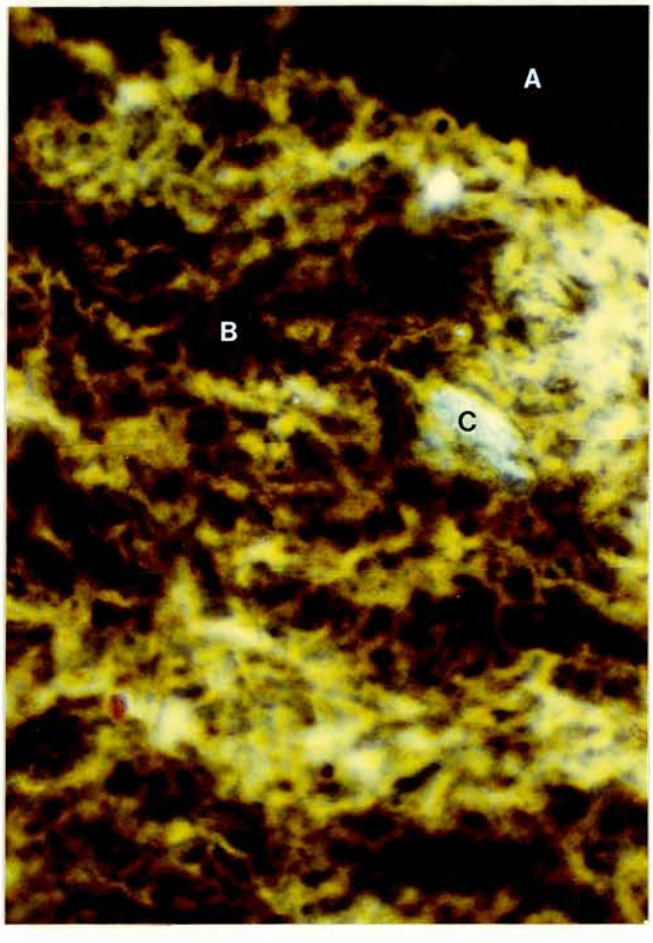
A
B
C

Figure 5.8/42

English Springer Spaniel (65R)

Degenerate fibroblasts contain mainly hydrophobic (red) lipid, but there is also some black staining phospholipid. There are considerable quantities of free cholesterol crystals.

Acid Haematein-Oil Red O, Nomarski Differential Interference Contrast X 390 (4)

Figure 5.8/43

Rough Collie (73L2)

Phospholipid (black) is present in excess of hydrophobic lipid (red). Cholesterol crystals are also present as are blood vessels with phospholipid-rich red cells in their lumen (arrows).

Acid Haematein-Oil Red O X 125 (4)

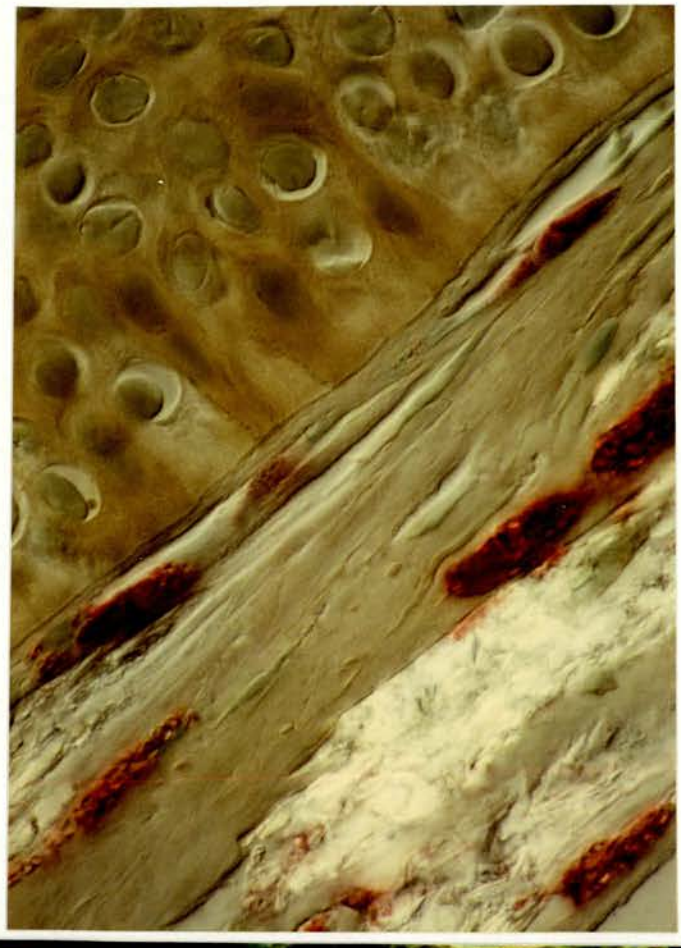

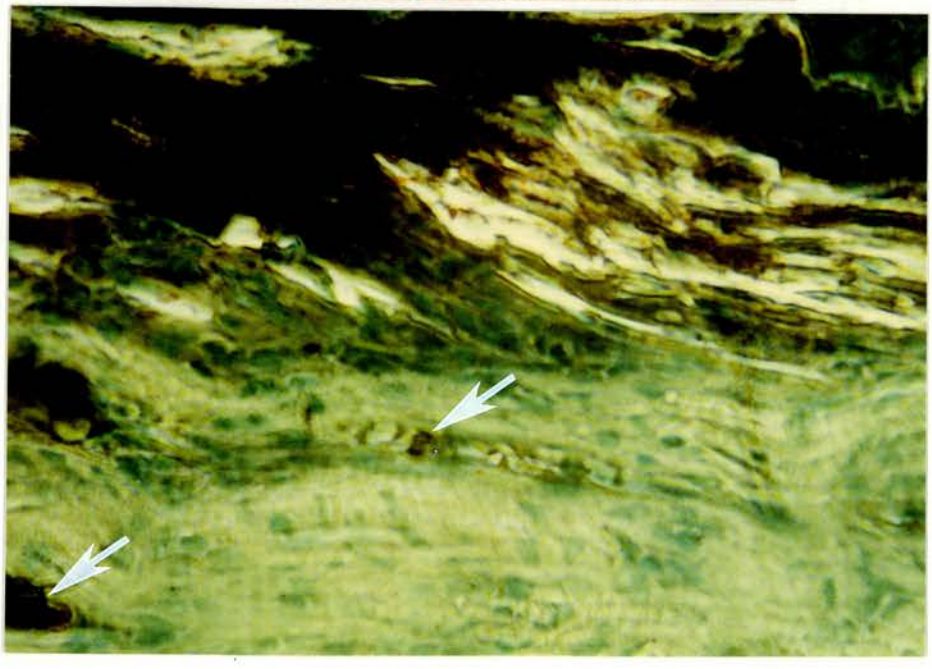

Figure 5.8/44

Welsh Springer Spaniel (42R3)

Numerous anisotropic droplets and sparse solid birefringent crystals, examined at 30°C.

Acid Haematein, Polarised Light with $\frac{1}{4}\lambda$ mica plate X 100 (4)

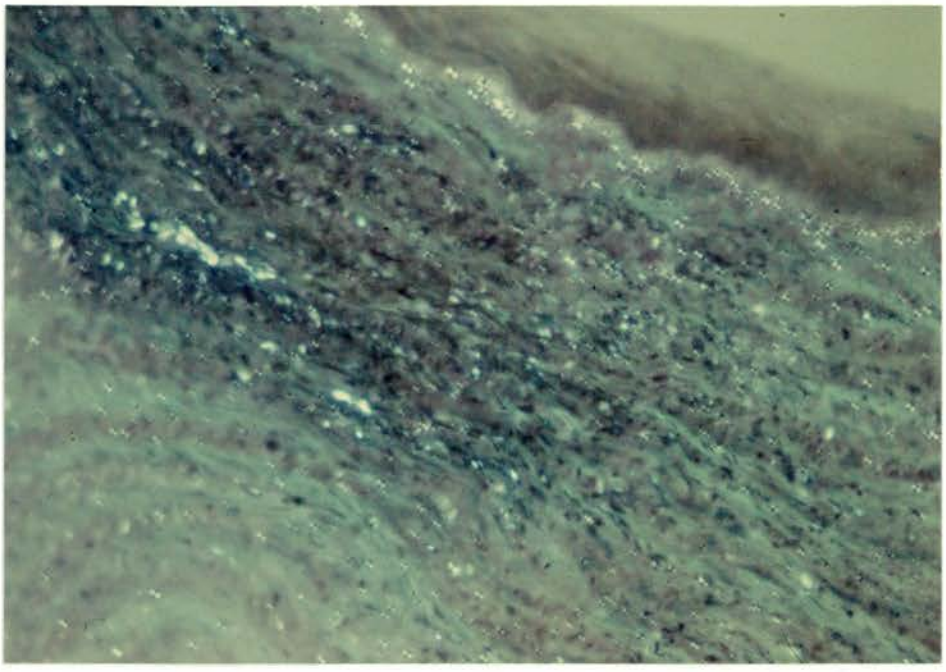

Figure 5.8/45

Golden Retriever (14L)

Cholesterol granuloma; PAS positive material is interposed between sites of previous occupancy by cholesterol crystals.

PAS X 125 (4)

Figure 5.8/46

Welsh Springer Spaniel (42R2)

Cholesterol granuloma; melanin pigment in corneal epithelium (A), dark staining lipofuscin in granuloma (B).

Schmorl X 125 (4)

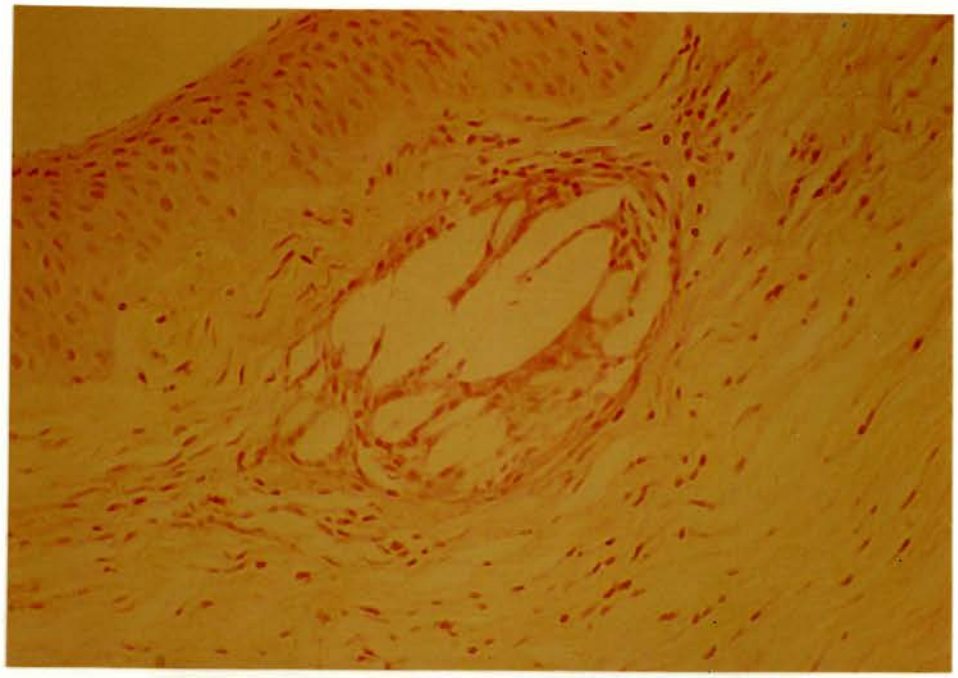

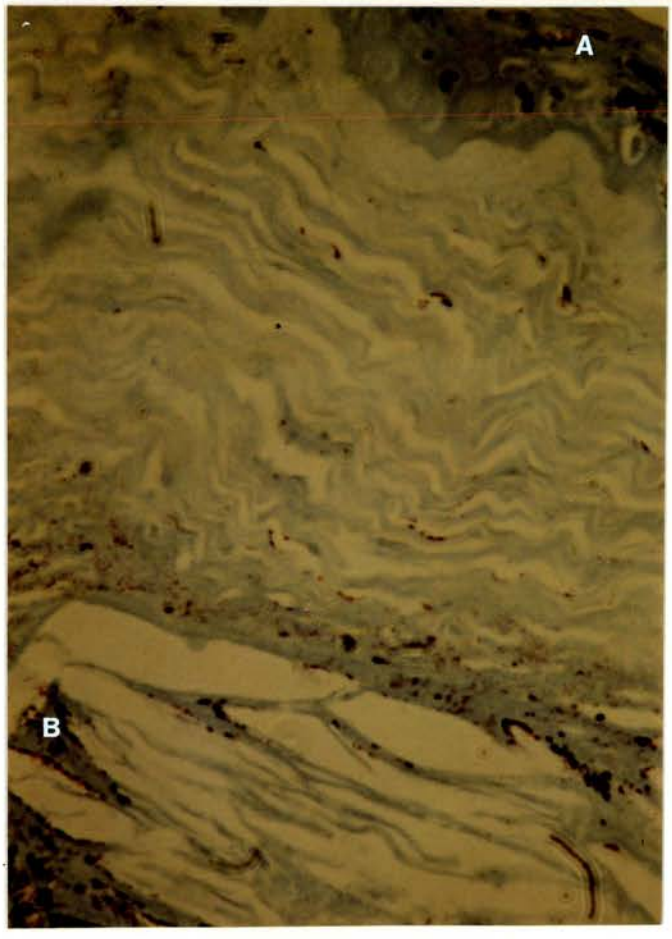
A
B

Figure 4.8/47

English Cocker Spaniel (24R)

Chloracetate Esterase Method for Non-Specific Esterases X 110 (4).

Figure 4.8/48

Welsh Springer Spaniel (42R2)

Positive enzyme activity in cells surrounding cholesterol granuloma.

Chloracetate Esterase Method for Non-Specific Esterases X 110 (4)

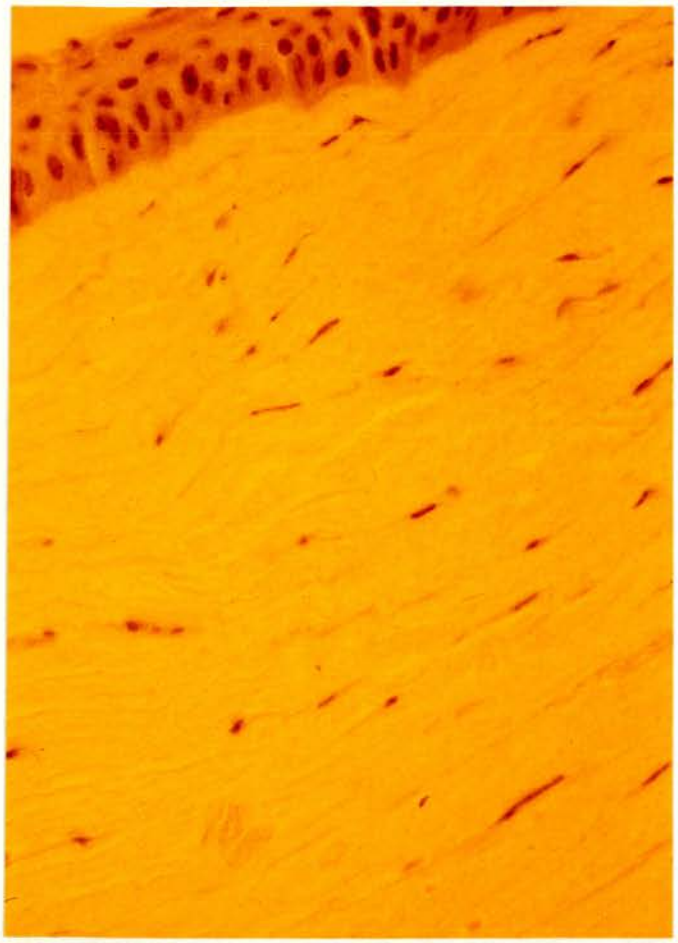

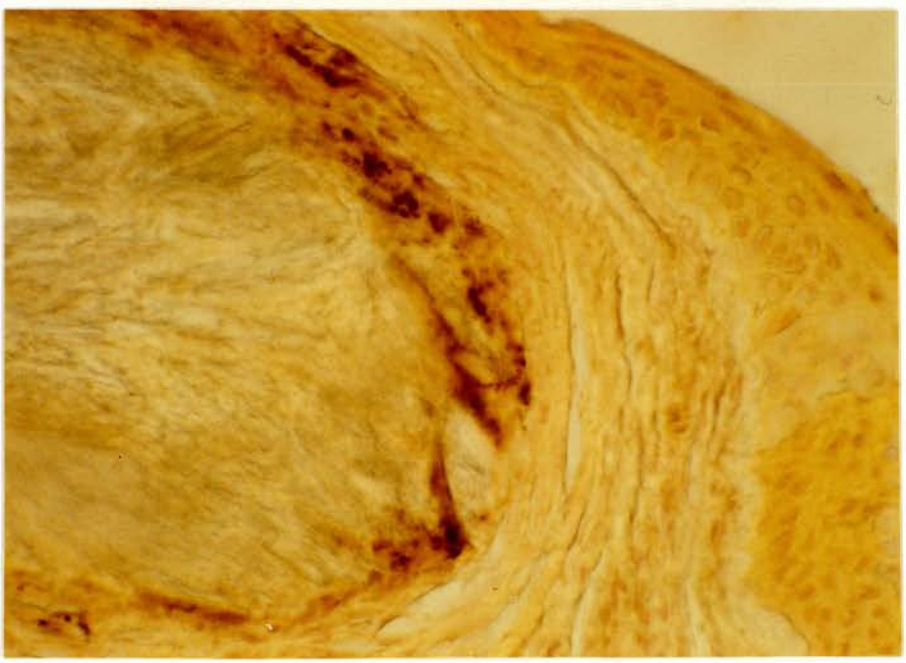

Figure 5.8/49

English Cocker Spaniel (24R)

Acid phosphatase activity in the immediate vicinity of fibroblasts. this section should be compared with a parallel section (5.8/23) stained for free fatty acids.

Gomori Lead Method for Acid Phosphatase X 100 (5)

Figure 5.8/50

Welsh Springer Spaniel (42R2)

Sparse acid phosphatase positive material (red-brown) in the corneal stroma near a cholesterol granuloma (A). Superficial vascularisation is also present (B).

Naphthol AS-BI Phosphate Method for Acid Phosphatase X 110 (4)

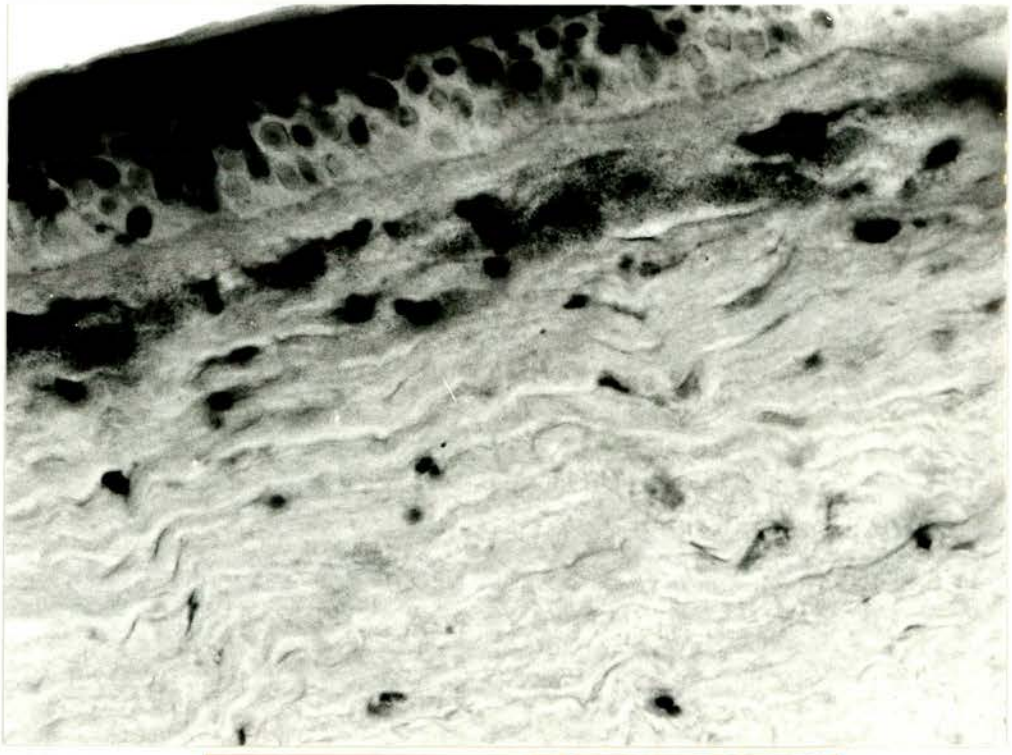

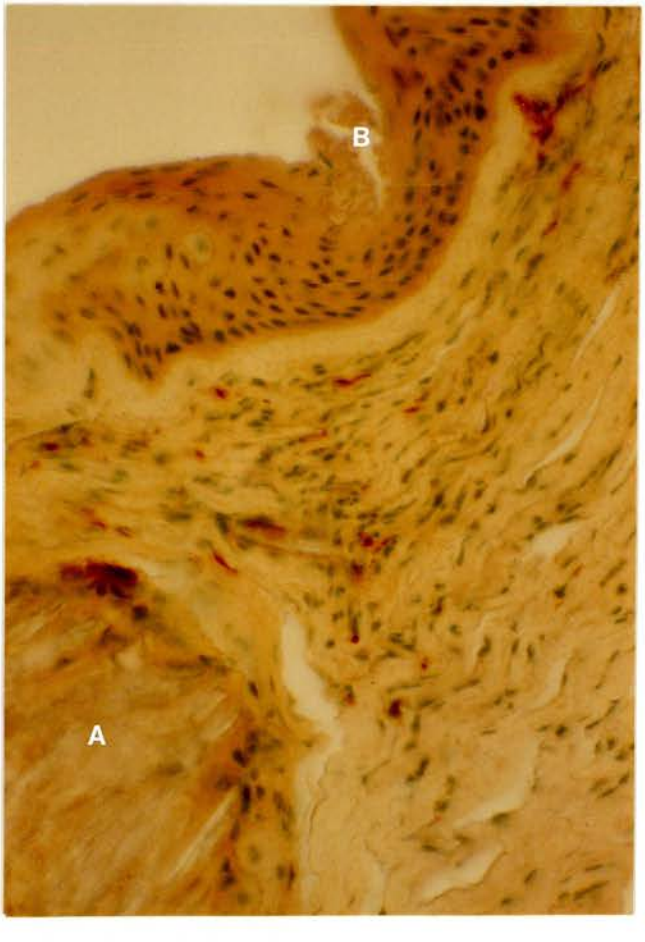
B
A

Figure 5.8/51

Golden Retriever (6R)

Corneal vascularisation (arrow) and cholesterol granuloma (A). There is a striking increase in the epithelial cell thickness in the hypercellular, granulomatous, region.

H & E X 30 (4)

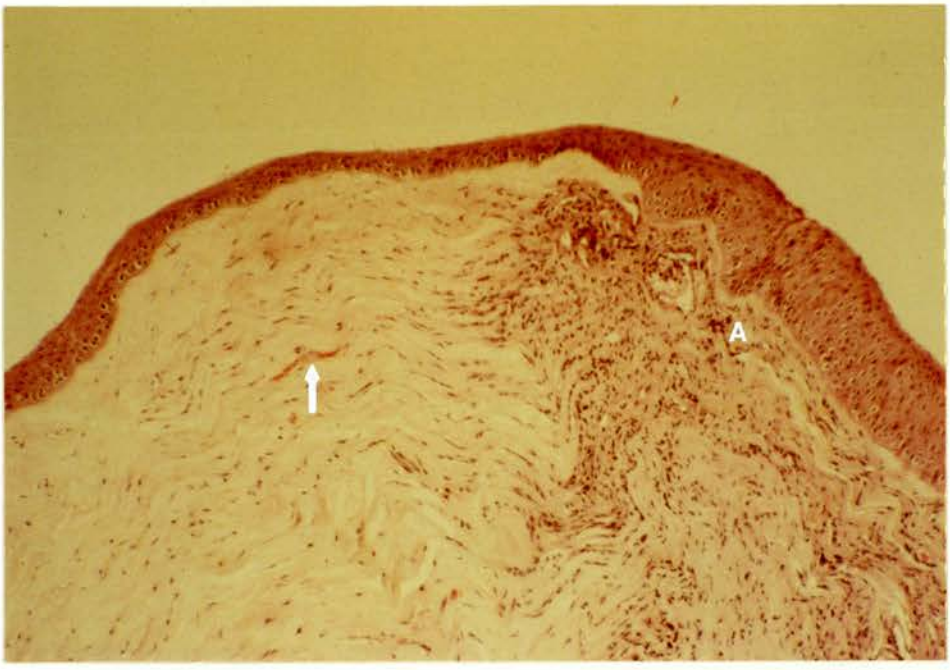
A

Figure 5.8/52

Alsatian (160R)

PAS positive thickenings and irregularities of epithelial basement membrane (A) and blood vessel walls (B).

PAS X 60 (4)

Figure 5.8/53

Welsh Springer Spaniel (42L)

Fibroblasts with lipid droplets outlined by acid mucin positive material (arrows) in addition to apparently extracellular material.

Hale's Dialysed Iron X 90 (4)

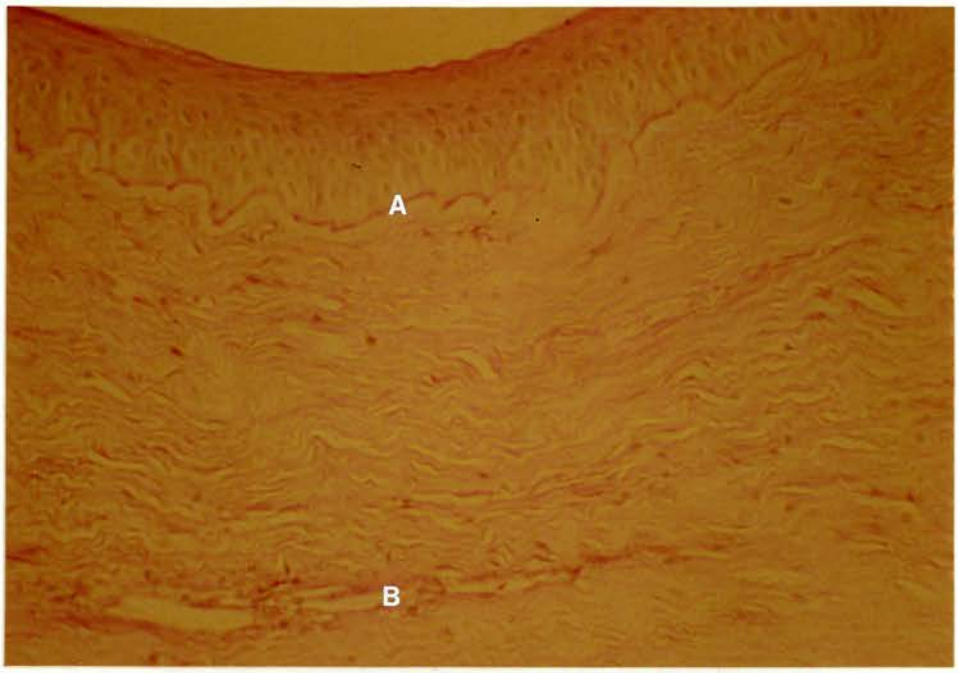
A
B

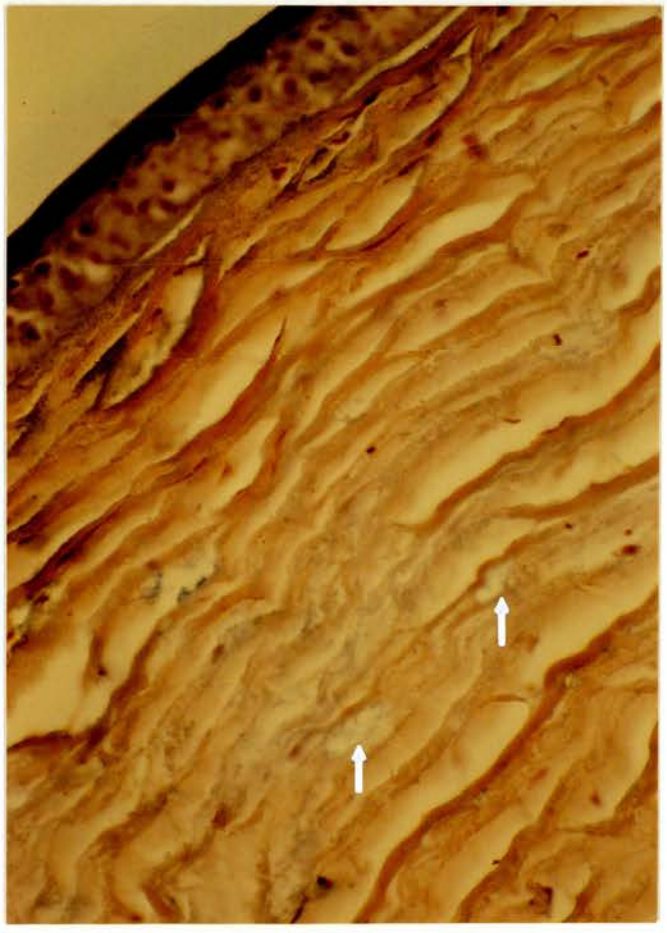

Figure 5.8/54

Welsh Springer Spaniel (42R2)

Cholesterol granuloma (A) and altered pattern of collagen staining in the affected stroma.

Mallory's X 110 (4)

Figure 5.8/55

Golden Retriever (14L)

Cholesterol granuloma (A) associated with amorphous pink material, which probably corresponds with the similarly located orange-red staining material of Figure 5.8/54 and the pink staining material of Figure 5.8/51.

A blood vessel (B) contains yellow-orange staining red blood cells.

MSB X 155 (4)

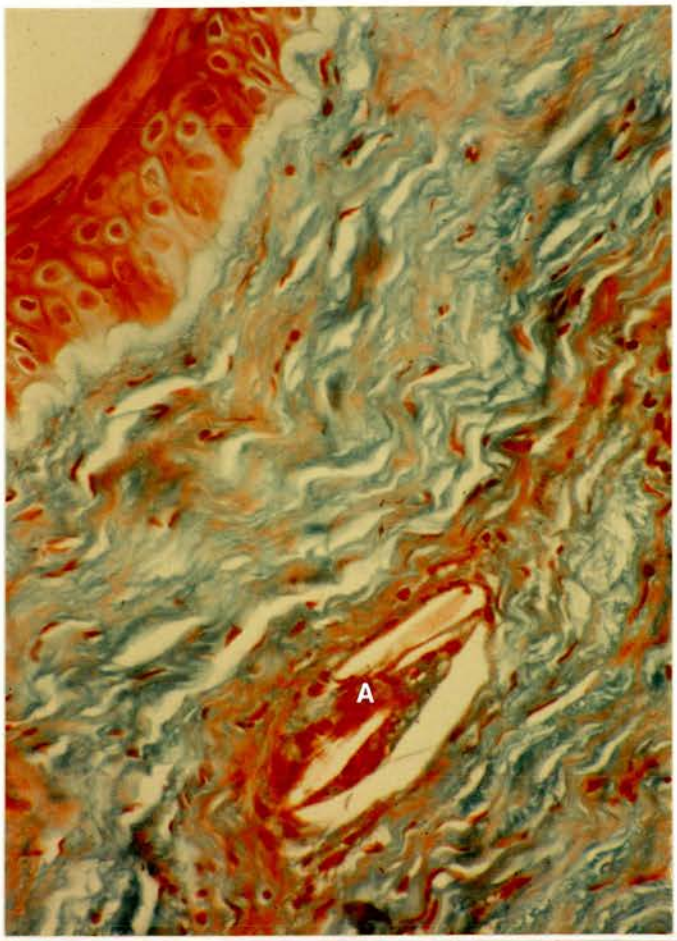
A

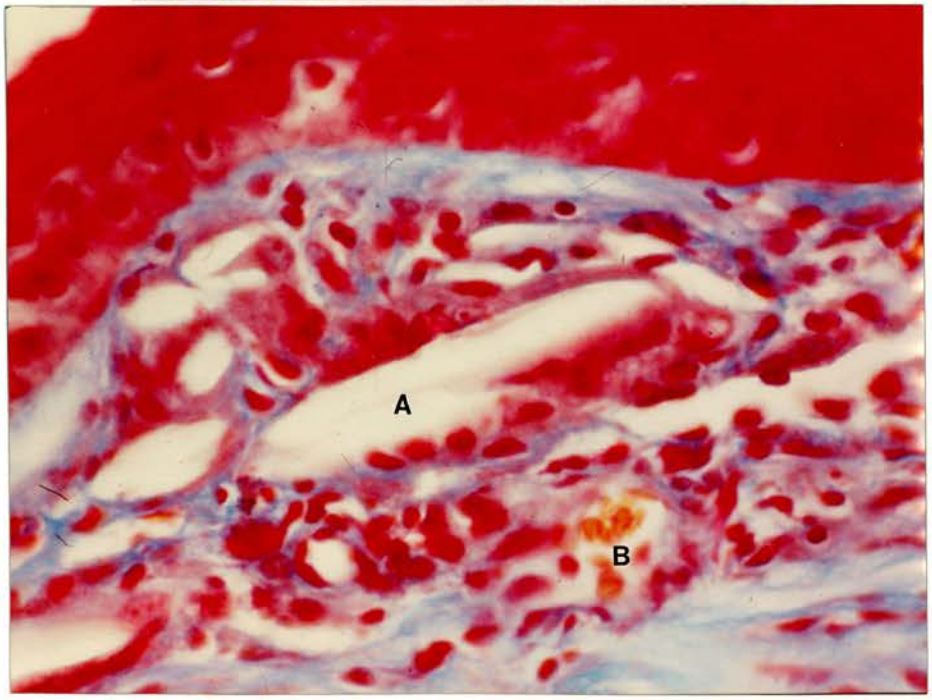
A
B

Figure 5.8/56

Alsatian (36R)

Superficial vascularisation (A) combined with considerable epithelial disruption has resulted in a line of cleavage between the epithelial cells and communicating with the stroma. Some lipid droplets (arrows) can be seen apparently in transit from the stroma to the precorneal tear film.

Toluidine Blue, Nomarski Differential Interference Contrast X 390 (4)

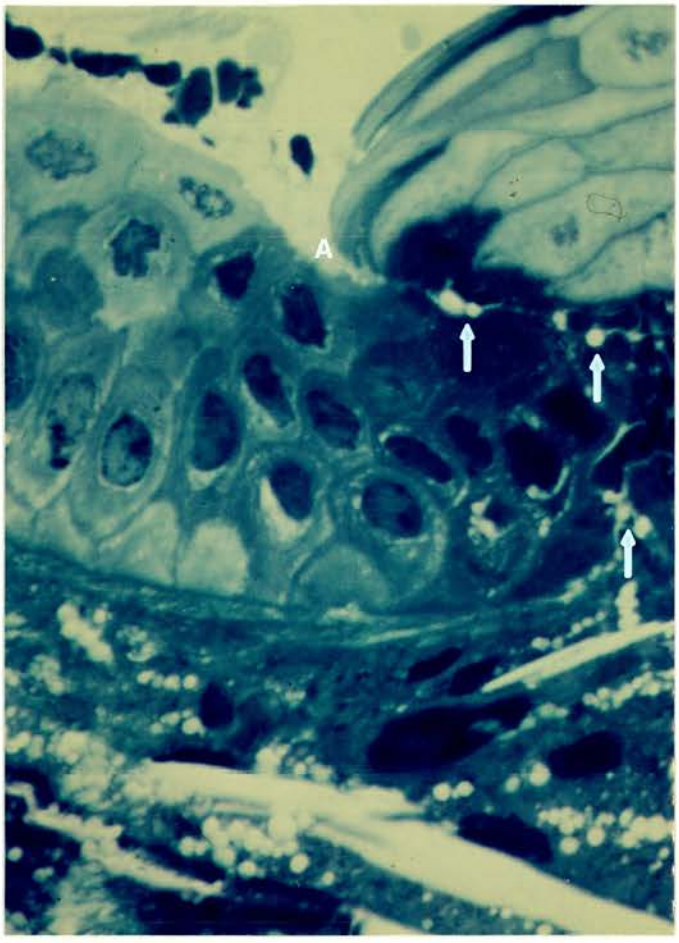
A

Figure 5.8/57

Alsatian (36L)

Round spaces indicate sites of lipid droplets in the corneal stroma (A) and blood vessel lumen (B). Numerous small, clearly defined, round spaces at (C) denote the presence of a giant cell which surrounds acicular and rhomboidal shaped spaces (D) which were previously occupied by crystals of free cholesterol.

Toluidine Blue, Nomarski Differential Interference Contrast X 390 (4)

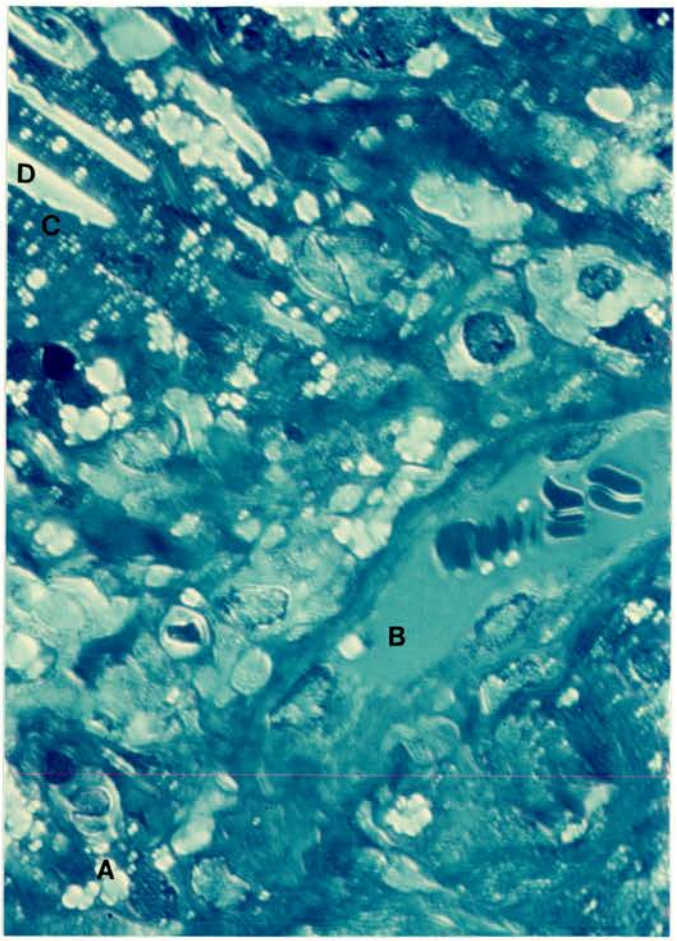
D
C
B
A

Figure 5.8/58

Old English Sheepdog (38R)

Mononuclear macrophages and giant cells surround characteristic cholesterol clefts. The clearly defined round, intracellular, spaces, correspond with well emulsified unsaturated, or polyunsaturated, cholesterol esters.

Toluidine Blue, Nomarski Differential Interference Contrast X 390 (4)

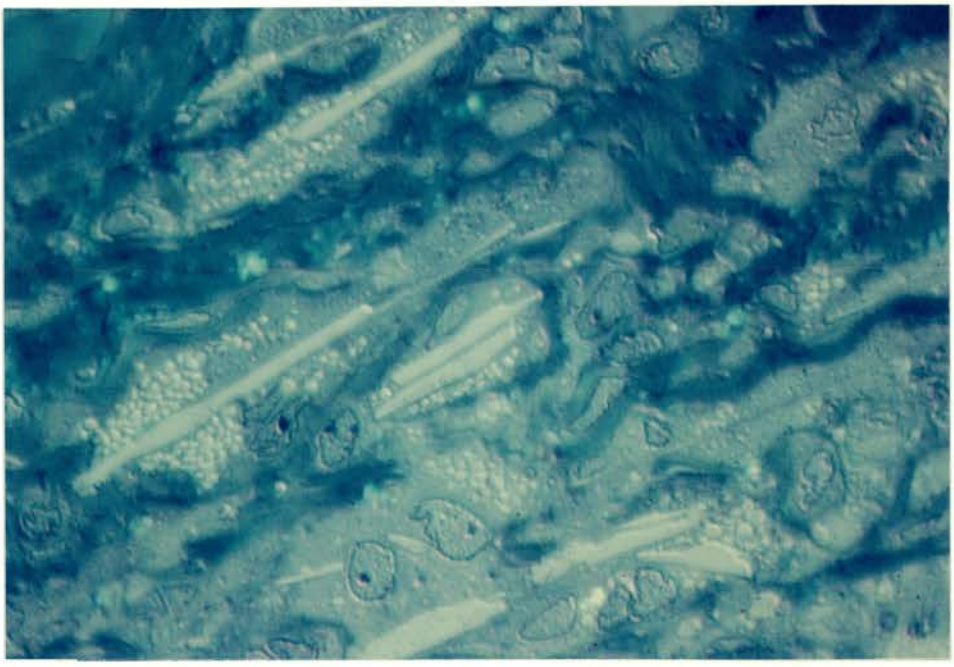

Figure 5.8/59

Golden Retriever (6R)

Typical cholesterol granulomata.

H & E X 90 (4)

Figure 5.8/60

Golden Retriever (9L)

Xanthomatous type of granulomatous reaction
Arrows indicate polymorphonuclear leukocytes.

H & E X 110 (4)

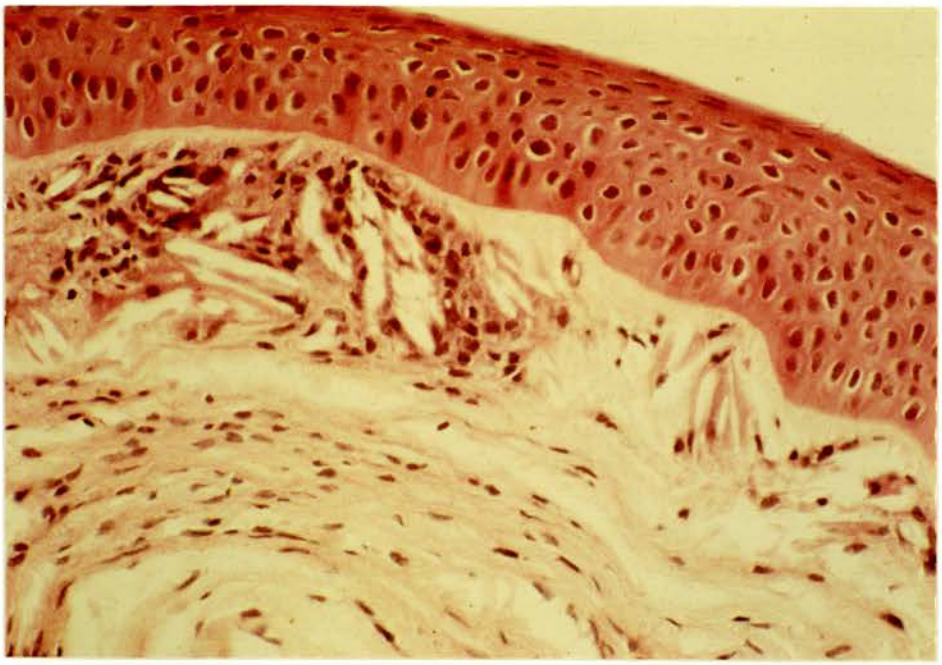

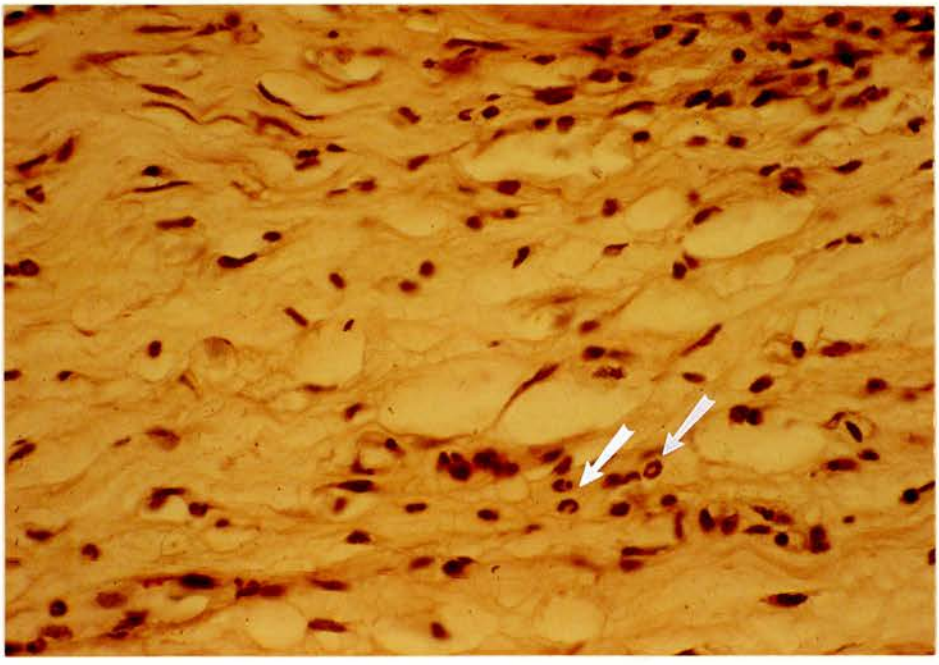

Figure 5.8/61

Rough Collie (73L2)

Occasional fatty acid positive cells surround characteristic cholesterol clefts.

Holczinger Technique, Nomarski Differential Interference Contrast X 390 (4)

Figure 5.8/62

Alsatian (27R1)

Giant cell (A) demonstrating minimal darkening with the Holczinger technique.

Holczinger Technique, Partially Crossed Polarisers X 125 (4)

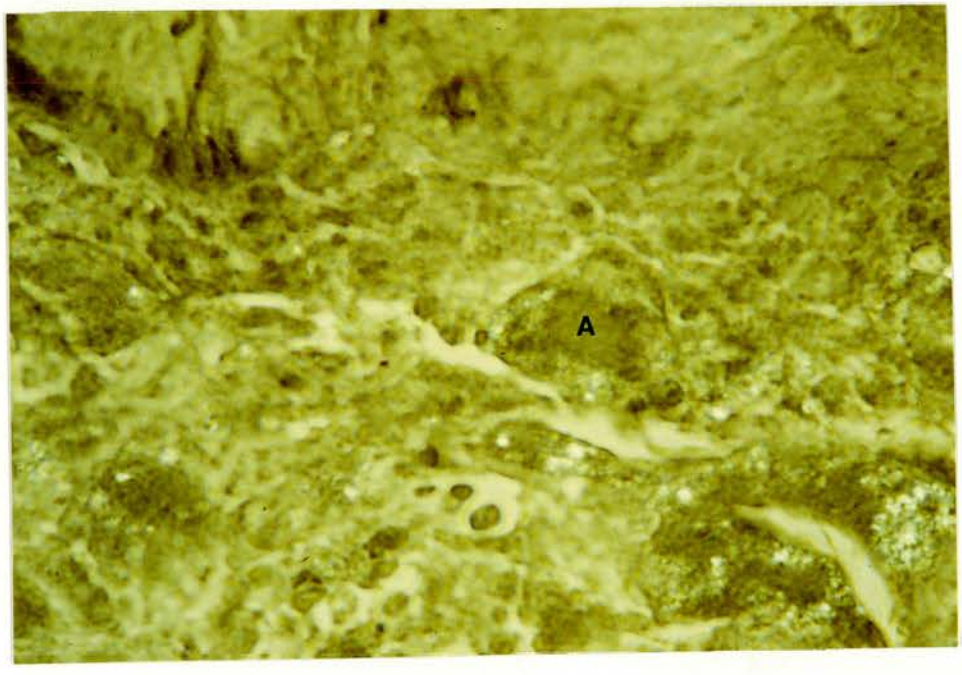
A

Figure 5.8/63

Alsatian (27R2)

Granular staining of the epithelium (A) and occasional regions of the stroma (B) which may represent triglyceride positive material alone, or in combination with other lipids. There are considerable numbers of anisotropic lipid droplets (C) which probably consist mainly of esterified cholesterol, triglyceride lacks such properties. Rather sparse aggregates of free cholesterol crystals (D) are also present.

Calcium Lipase - Lead Sulphide, Nomarski Differential Interference Contrast X 110 (4)

Figure 5.8/64

Old English Sheepdog (38R)

Round cells containing mainly well emulsified anisotropic lipid droplets. Blood vessel lumen (A).

Oil Red O, Polarised Light X 125 (4)

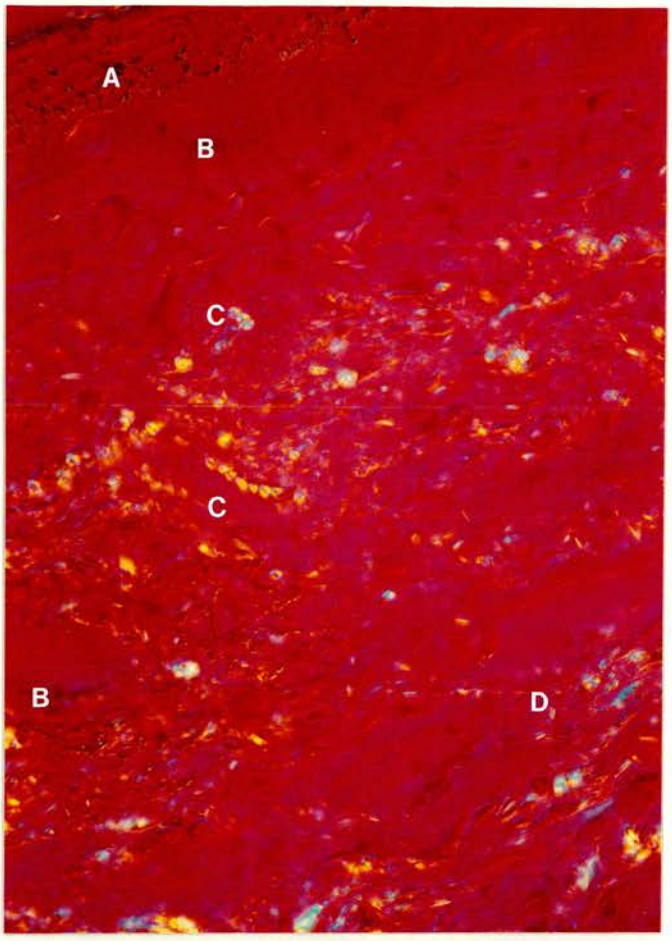
A
B
C
C
B
D

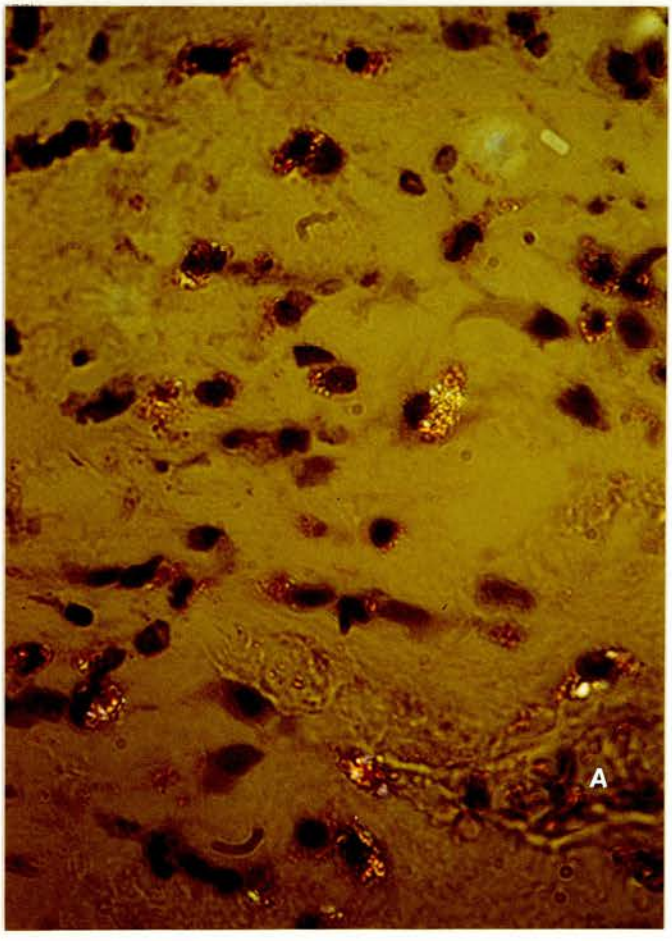
A

Figure 5.8/65

Alsatian (27R2)

Free cholesterol appears black in this section which has been treated with aqueous digitonin to precipitate cholesterol.

0.5% Digitonin, Nomarski Differential
Contrast X 110 (4)

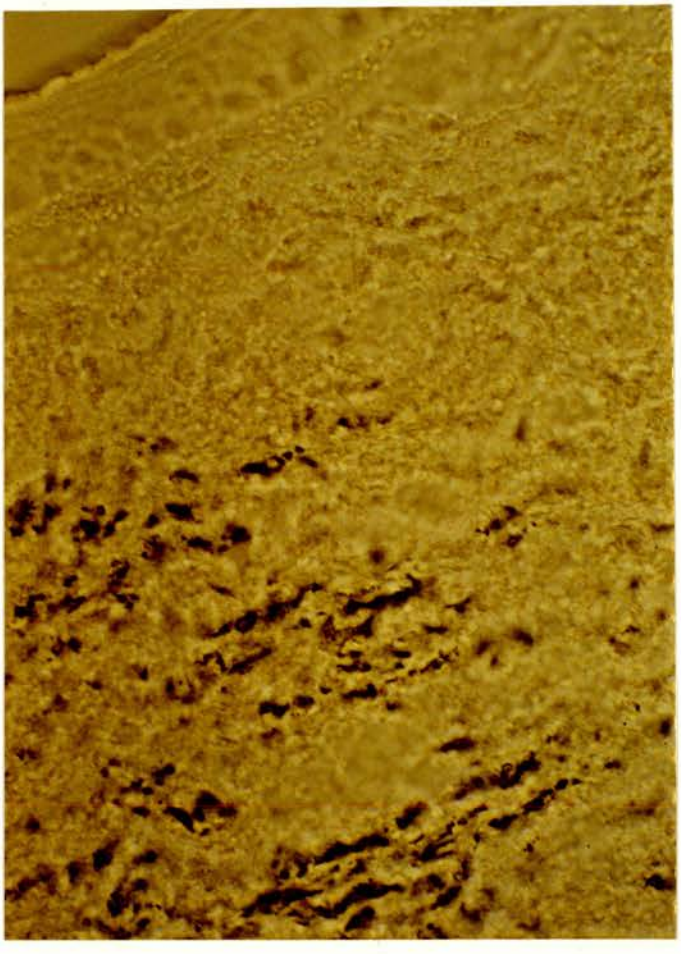

Figure 5.8/66

Old English Sheepdog (38R)

Intracellular phospholipid.

Acetone - Nile Blue Sulphate X 60 (4)

Figure 5.8/67

Alsatian (27L2)

Mixed hydrophobic and hydrophilic lipid. Two giant cells are indicated (arrows). A cholesterol crystal is present in the lower one and peripherally disposed lipid droplets in the upper one.

Nile Blue Sulphate X 60 (4)

Figure 5.8/68

Welsh Springer Spaniel (42R3)

Leakage of dark staining phospholipid-rich lipid into the pre-corneal tear film (A). Mixed hydrophilic and hydrophobic lipids (B) surround cholesterol clefts. Phospholipid positive red blood cells are present in blood vessels (C).

Acid Haematein-Oil Red O X 125 (4)

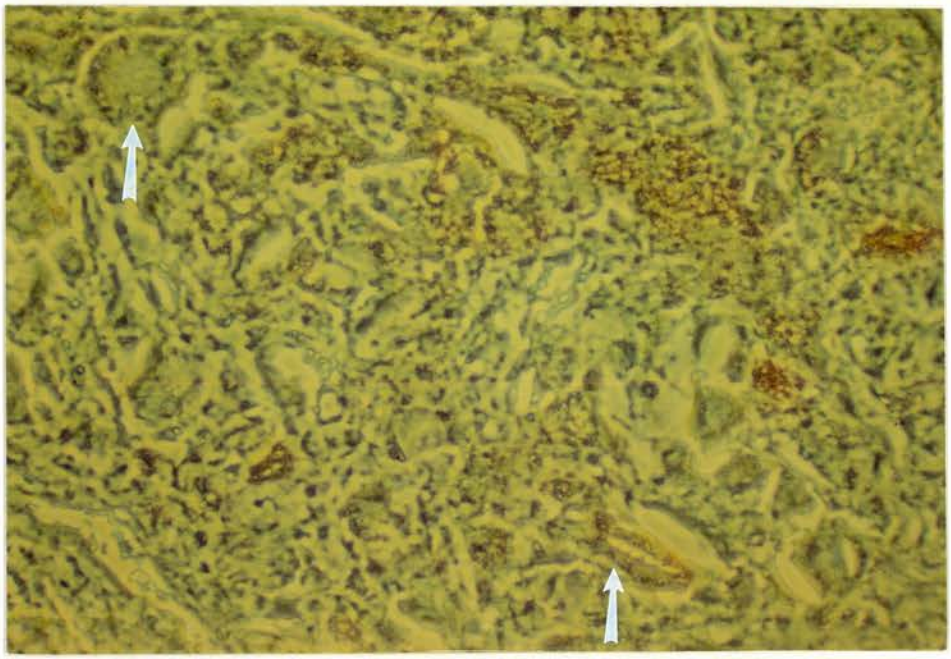

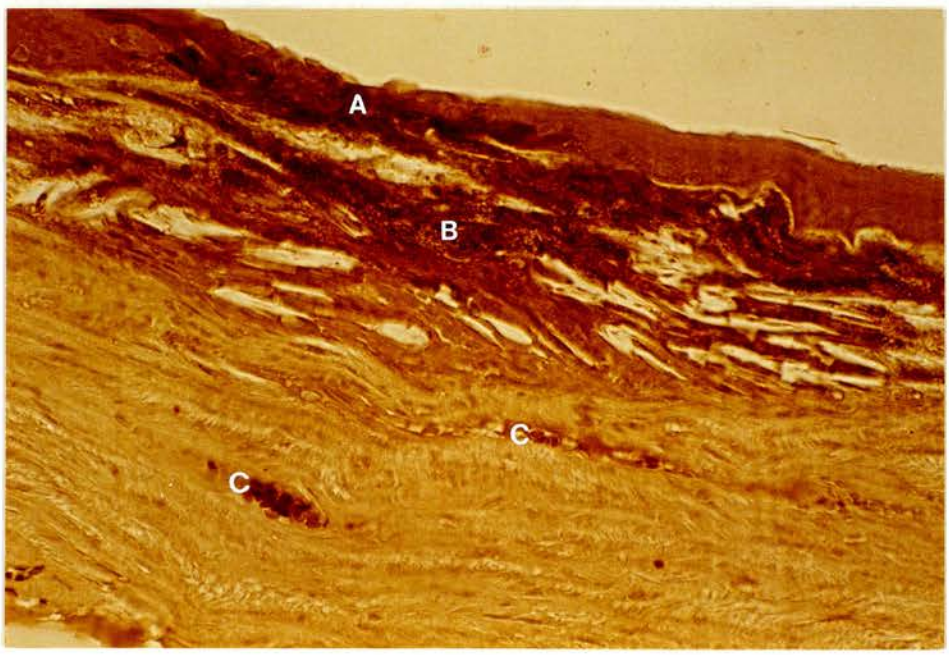
A
B
C
C

Figure 5.8/69

Old English Sheepdog (38R)

Cholesterol crystals surrounded by darkly staining cells.

OTAN, Polarised Light X 40 (4)

Figure 5.8/70

Old English Sheepdog (38R)

Intracellular, unsaturated, or polyunsaturated lipids in a region corresponding to the OTAN positive cells of Figure 5.8/69.

Osmium Tetroxide X 30 (4)

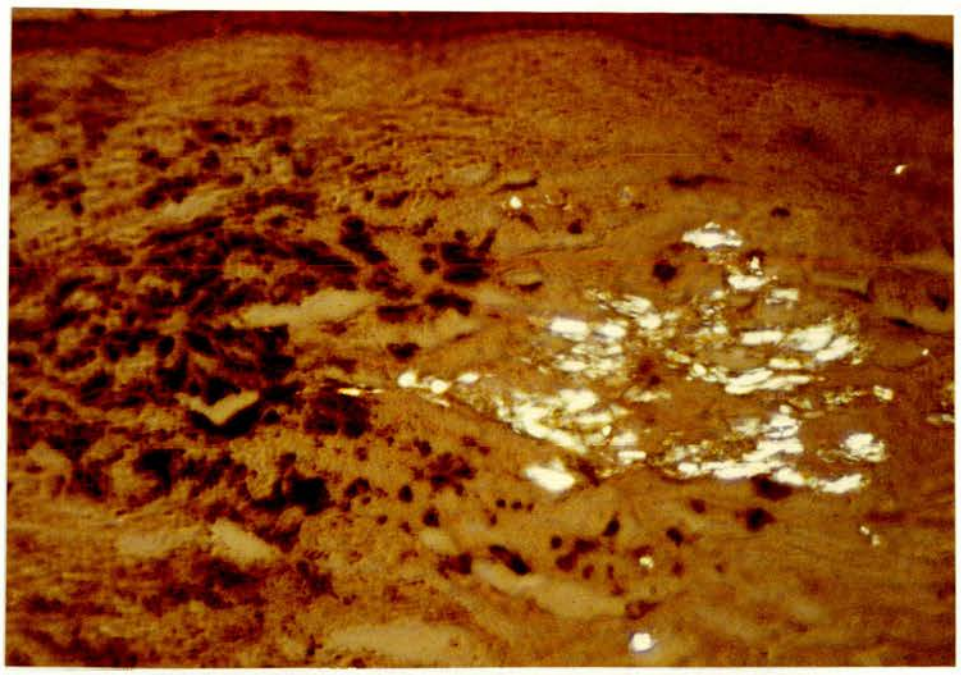

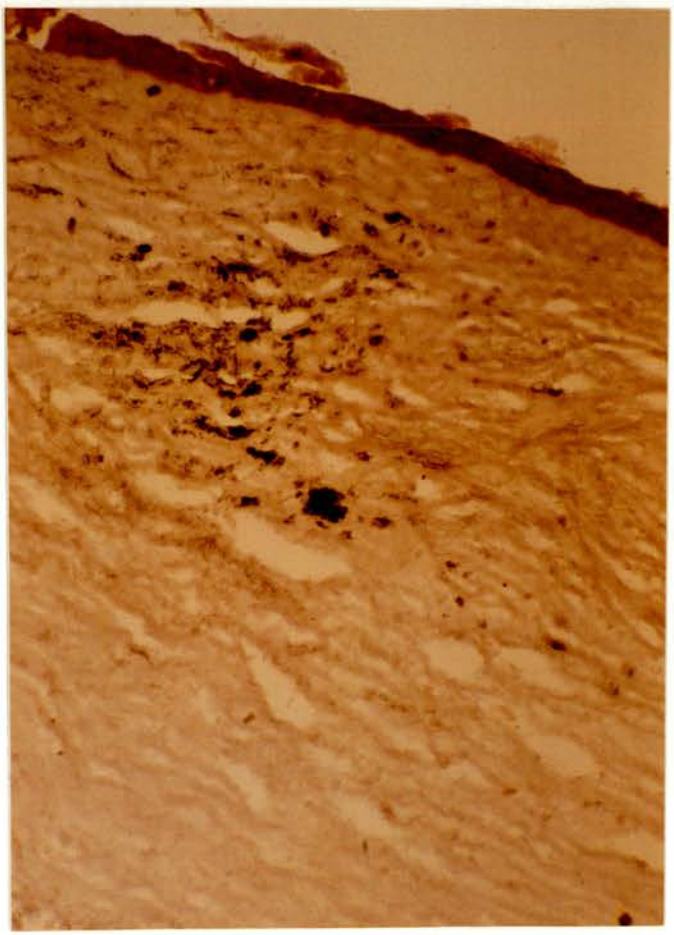

Figure 5.8/71

Alsatian (160R)

Extensive staining in the anterior stroma.

Sudan Black B X 60 (4)

Figure 5.8/72

Old English Sheepdog (38R)

More discrete staining of cells which are predominantly round cells on higher power examination.

Sudan Black B X 70 (4)

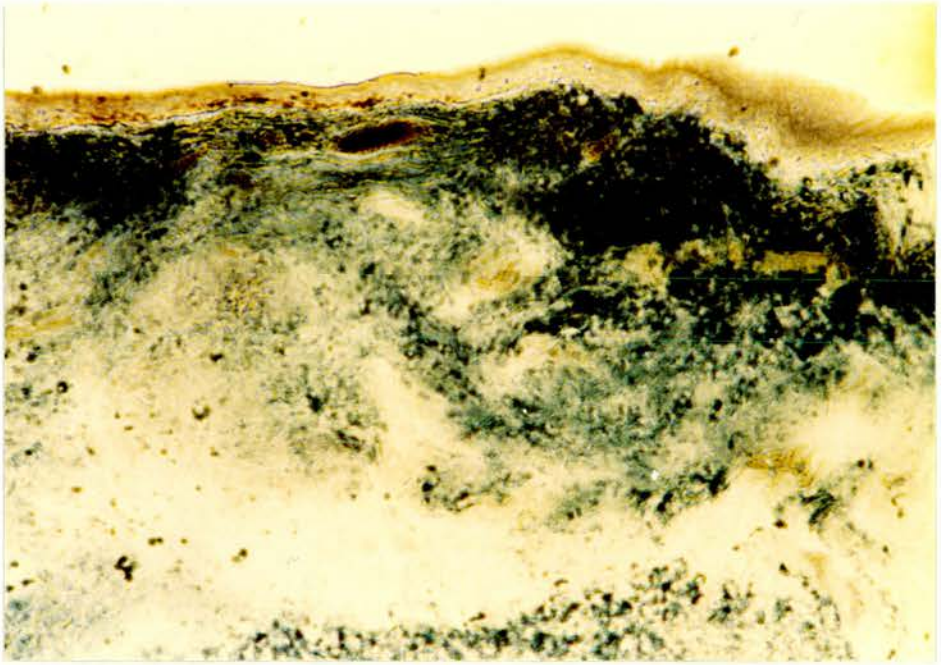

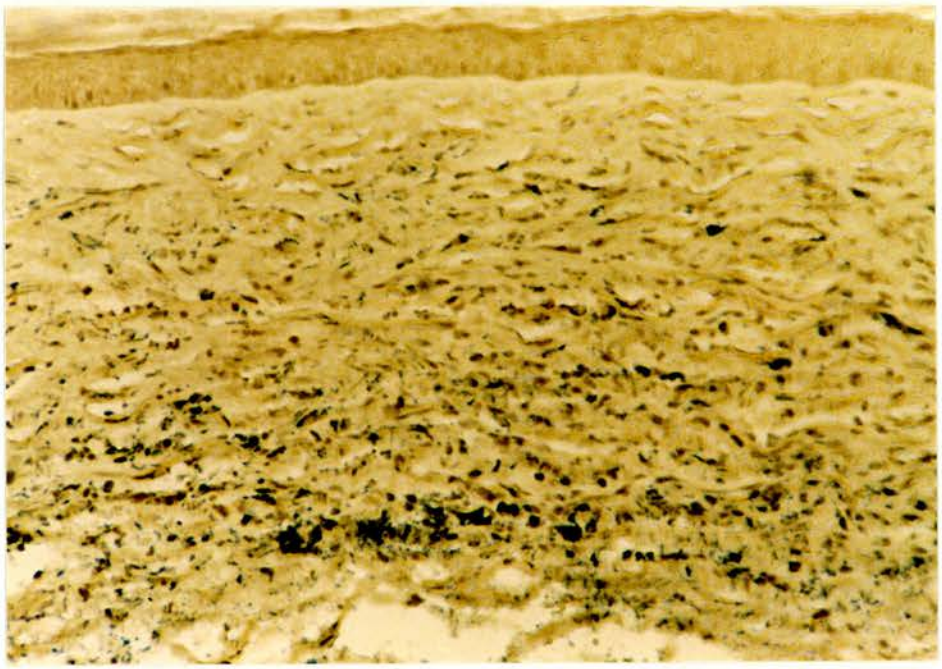

Figure 5.8/73

Old English Sheepdog (38L)

The darkly staining cells in epithelium and stroma are positive for lipase.

Tween Method, Partially Crossed Polarisers X 40 (5)

Figure 5.8/74

Old English Sheepdog (38L)

A parallel section to Figure 5.8/73 stained for non-specific esterases demonstrates widespread enzyme activity, including blood vessels (arrow).

Alpha Naphthyl Acetate Method for Non Specific Esterases X 30 (4)

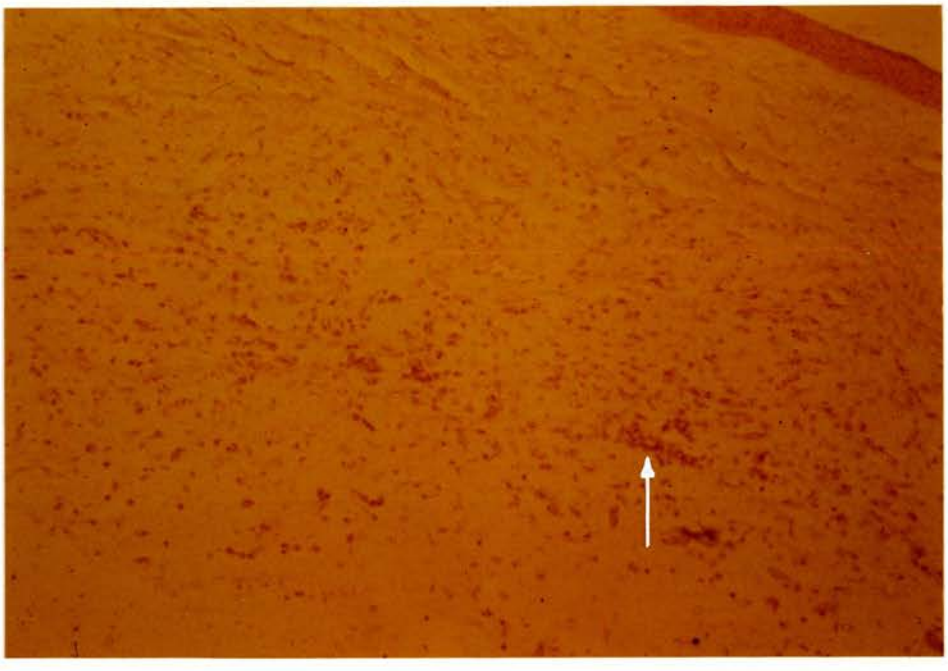

Figure 5.8/75

Rough Collie (73L2)

Considerable non-specific esterase activity between and surrounding cholesterol clefts.

Alpha Naphthyl Acetate Method X 110 (4)

Figure 5.8/76

Rough Collie (73L2)

Demonstration of lysosomal esterases in a parallel section following incubation with E600.

Alpha Naphthyl Acetate with 10^{-5} M E600 at pH 5.8 X 110 (4)

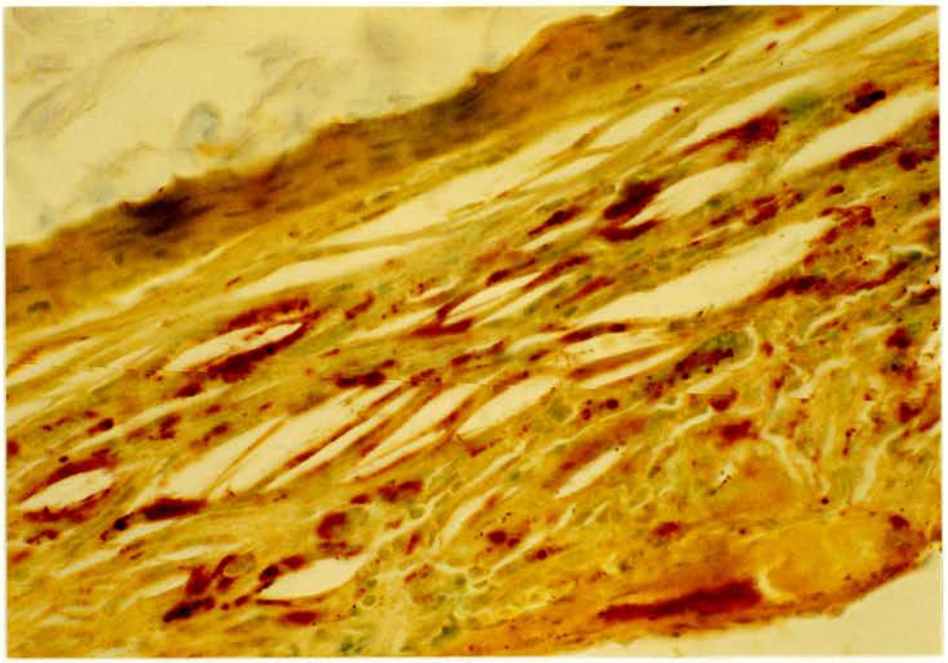

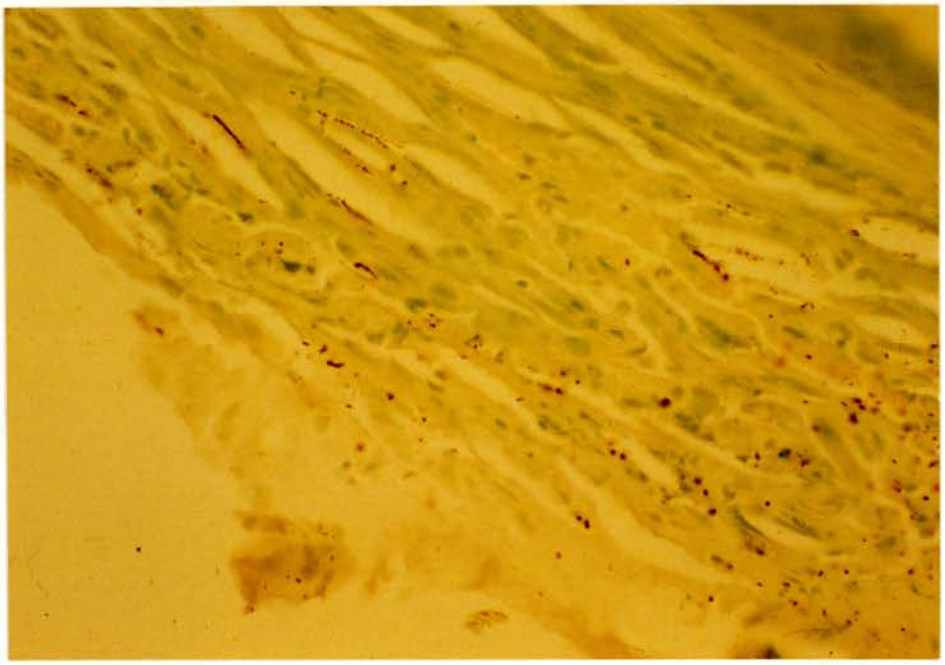

Figure 5.9/1

Alsatian X (150L)

Epithelial and anterior stromal involvement in lipid keratopathy associated with chronic superficial keratitis. Spaces indicative of previous occupancy by lipid droplets are present within a proportion of corneal epithelial cells and adventitial cells.

Toluidine Blue X 280 (5)

Figure 5.9/2

Golden Retriever (14L)

Mid-stromal involvement in lipid keratopathy associated with scleritis. The numerous rhombic and acicular spaces are indicative of previous occupancy by free cholesterol crystals. A proportion of the fibroblasts in the upper part of the micrograph are vacuolated.

Toluidine Blue X 280 (5)

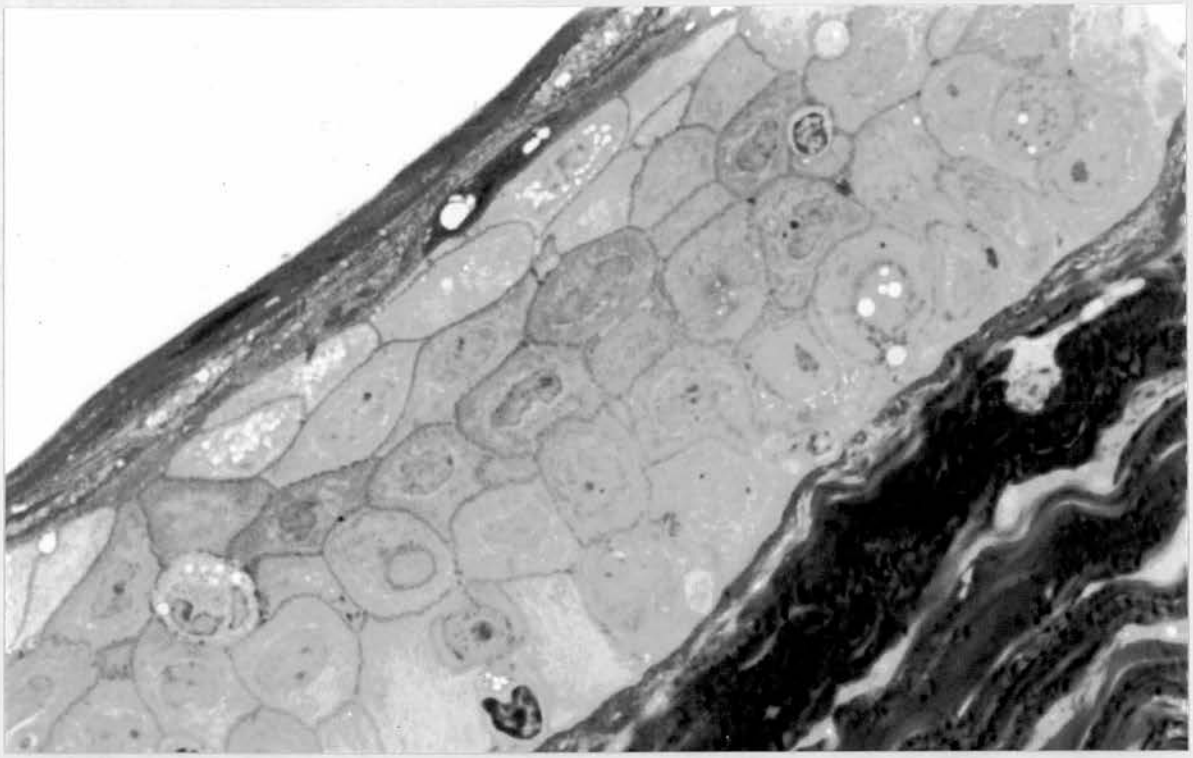

Figure 5.9/3

Alsatian (36L)

Considerable stromal involvement and some epithelial involvement in lipid keratopathy following recurrent episcleritis in an animal with hyperlipoproteinaemia and a vascularised, rather oedematous cornea. The section is slightly tangential.

Toluidine Blue X 100 (4)

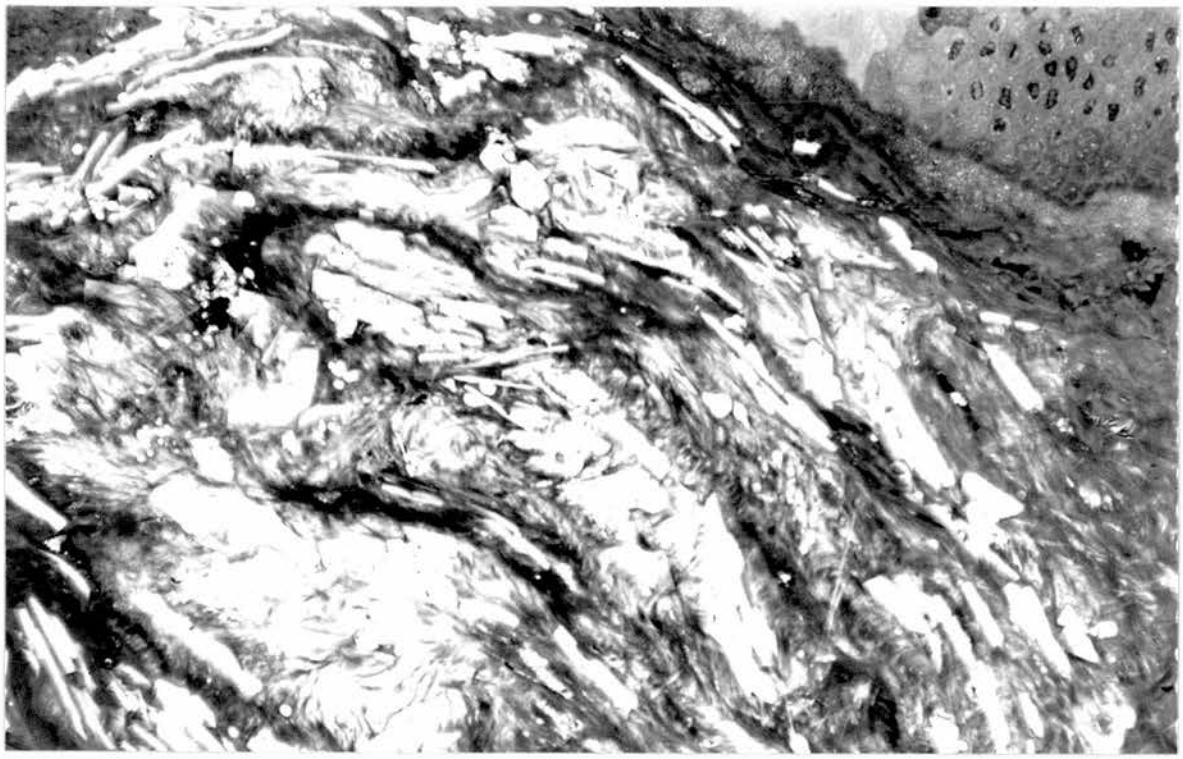

Figure 5.9/4

Alsatian (27L1)

The epithelium is of relatively normal appearance and there are some spaces within the stroma indicative of previous occupancy by lipid.

TEM X 1,650 (2)

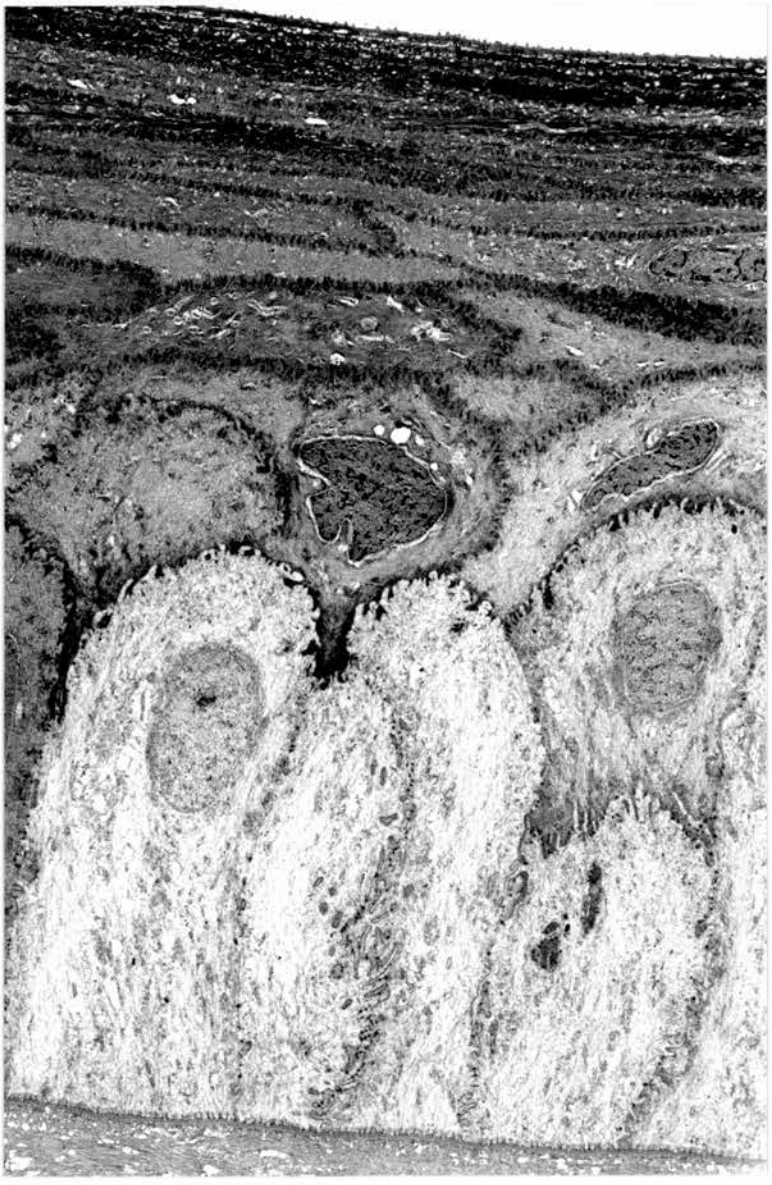

Figure 5.9/5

Alsatian X (150L)

In the anterior corneal epithelium there are whorled membranous lamellae, round clear spaces and increased superficial desquamation. There is also dark staining material with round, clear, spaces in the region of the pre-corneal tear film and between the surface microplicae and microvilli.

TEM X 21,500 (2)

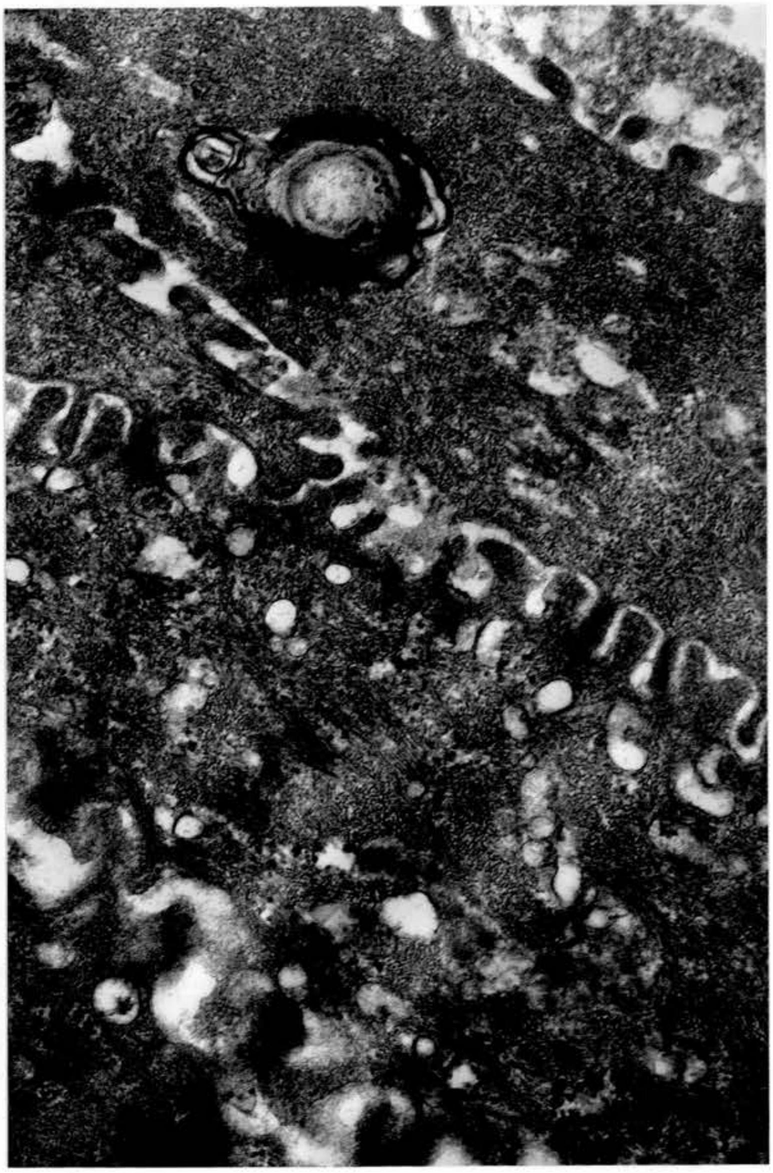

Figure 5.9/6

Alsatian (36L)

Tangential section of the corneal epithelium, the stroma is just visible in the lower left hand corner. In addition to numerous clear spaces within the cells there is great variation of staining intensity, which probably corresponds with degenerative changes in the cells.

Toluidine Blue X 225 (5)

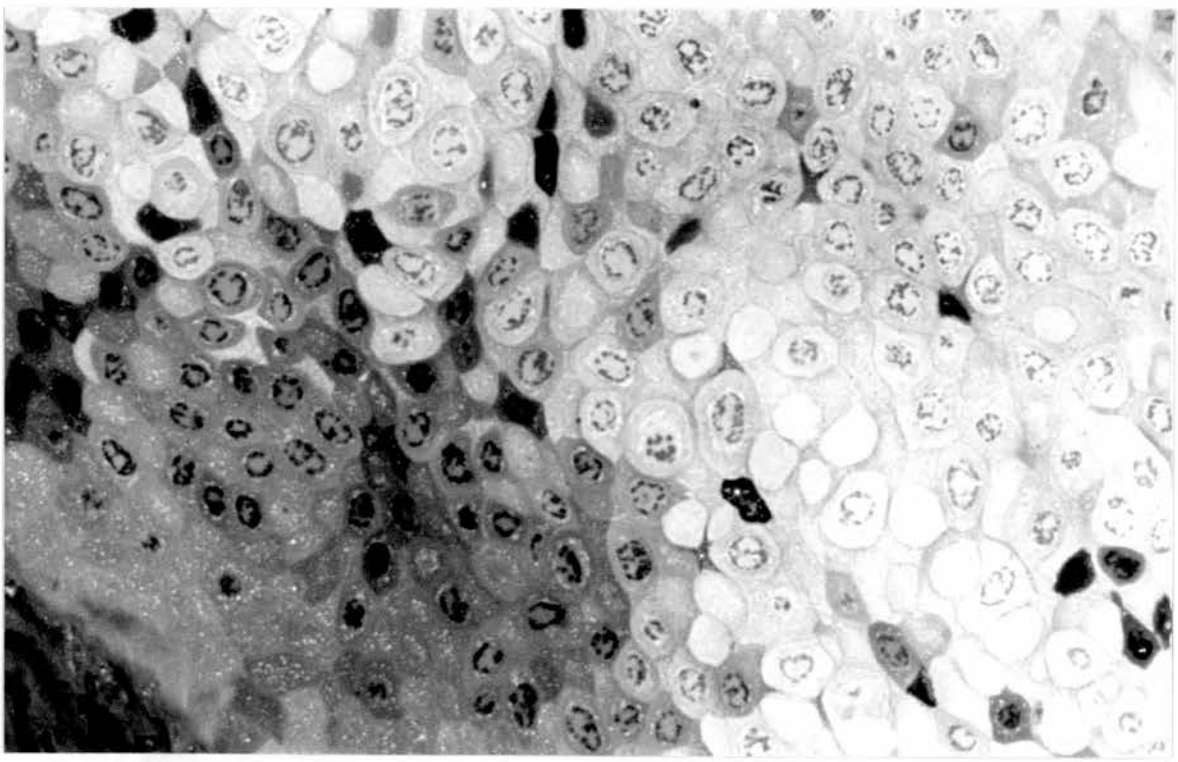

Figure 5.9/7

Jack Russell Terrier (132L)

A darkly staining, degenerate basal epithelial cell is prominent with a polymorphonuclear leukocyte above it. The basal lamina is somewhat irregular and appears discontinuous in places (arrowed). The basal epithelial cells have finger-like projections within the stroma and a proportion of the amorphous material in the anterior stroma may also have originated from the basal epithelial cells. A degenerate fibroblast is also present in the stroma (A).

TEM X 1650 (2)

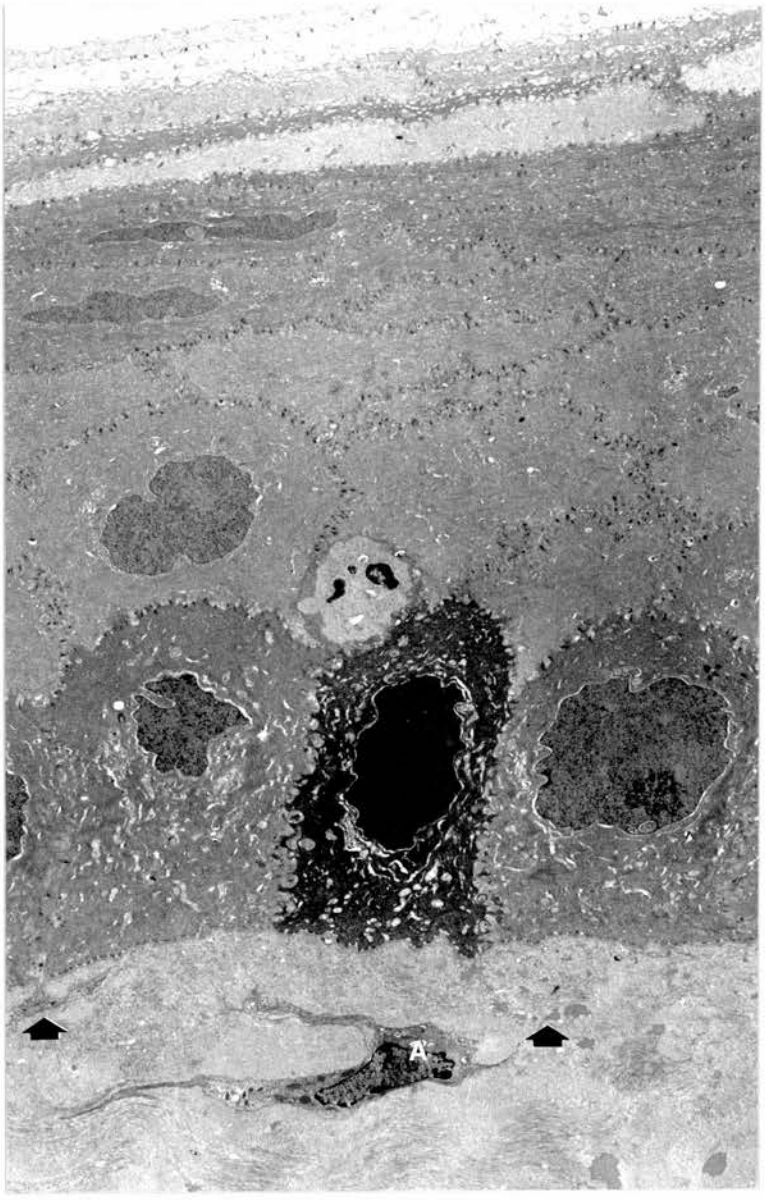
A

Figure 5.9/8

Welsh Springer Spaniel (42R1)

The basal lamina is of normal appearance in this micrograph taken from the edge of the opacity. In the subepithelial zone there appear to be slightly greater numbers of clear spaces, some defined by an osmiophilic rim, than are normally present in control animals of similar age.

TEM X 35,500 (2)

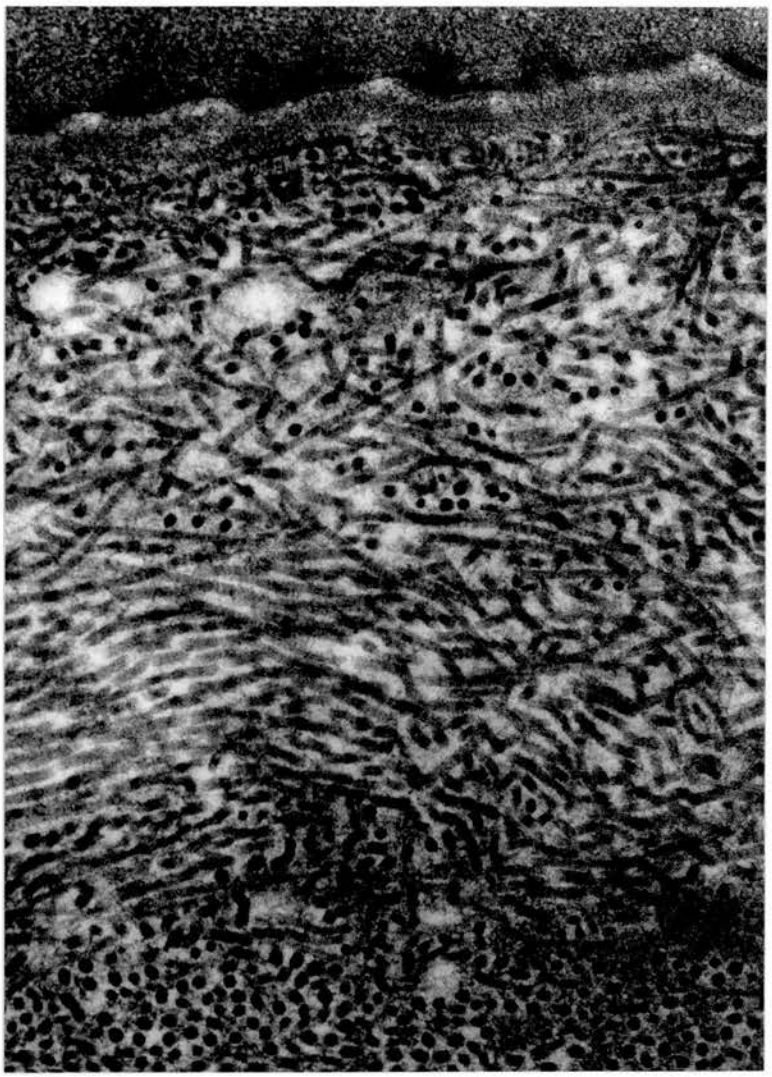

Figure 5.9/9

Alsatian X (150L)

The epithelial cells (A) overlying the abnormal basal lamina (B) are rich in tonofilaments and clear round spaces. Hemidesmosomes of the basal lamina are not clearly defined. There are numerous empty, or almost empty, spaces (C) in the subepithelial zone.

TEM X 27,500 (2)

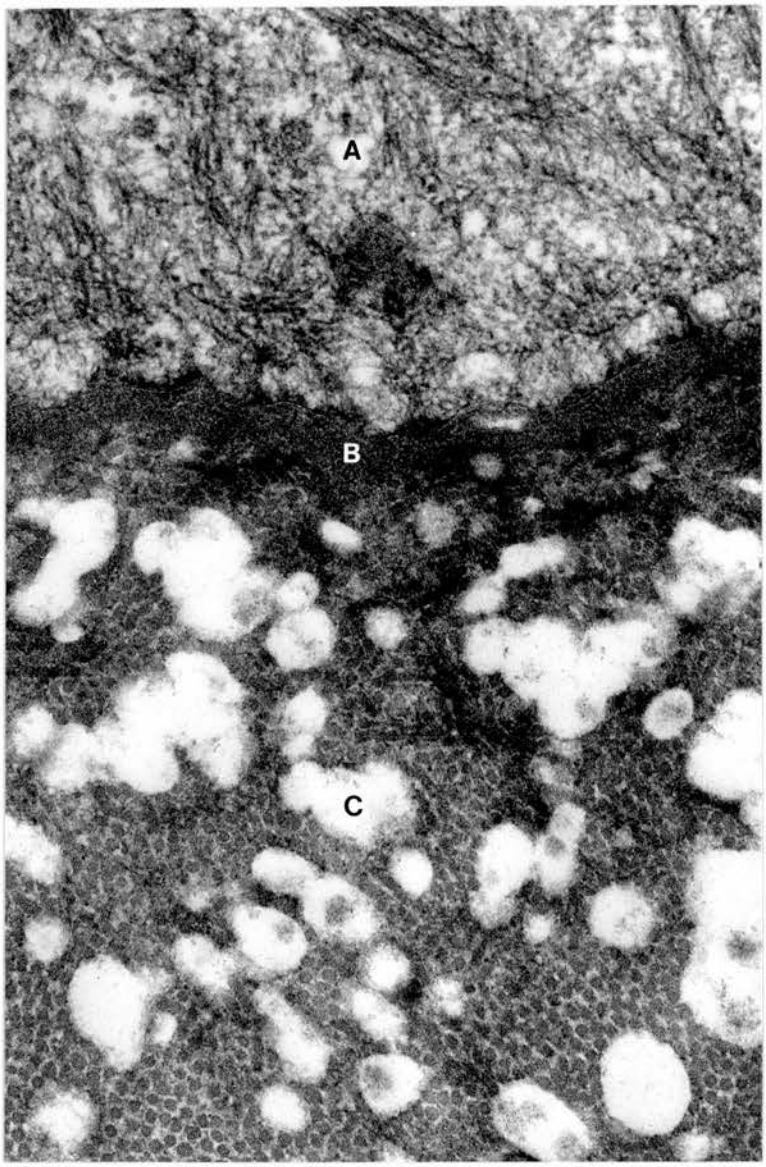
A
B
C

Figure 5.9/10

Alsatian (36R)

The epithelium (A) is on the left, the basal lamina (B) is discontinous. There are round spaces (C) within the stroma, some of which contain membranous lamellae. There is also a single, needle-like space (D) which was probably occupied previously by a crystal of free cholesterol.

TEM X 27,500 (2)

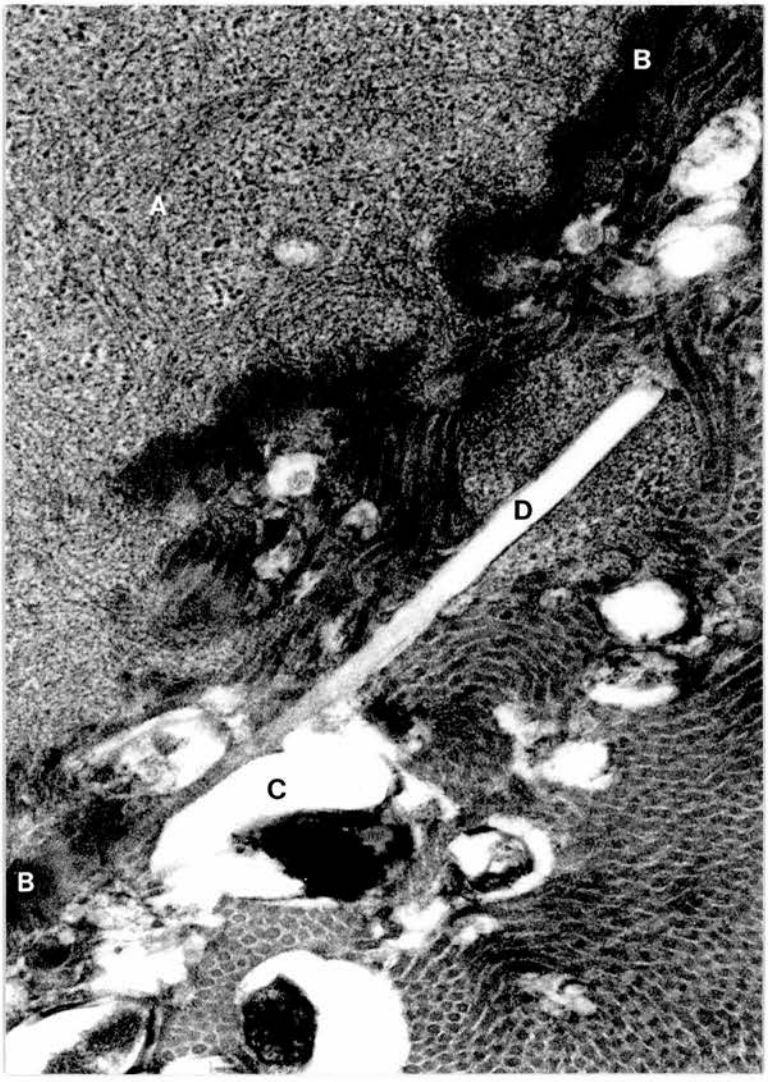
B
A
D
C
B

Figure 5.9/11

English Cocker Spaniel (24L)

Ruthenium red staining gives some indication of the variation in interfibrillar spacing which seems to be present, even in early, non-vascularised, corneal opacities. The ruthenium red positive proteoglycan particles, or granules, between fibrils are also not as regularly disposed as those of normal, control, cornea in an animal of similar age and breed.

TEM, Ruthenium Red X 60,000 (4)

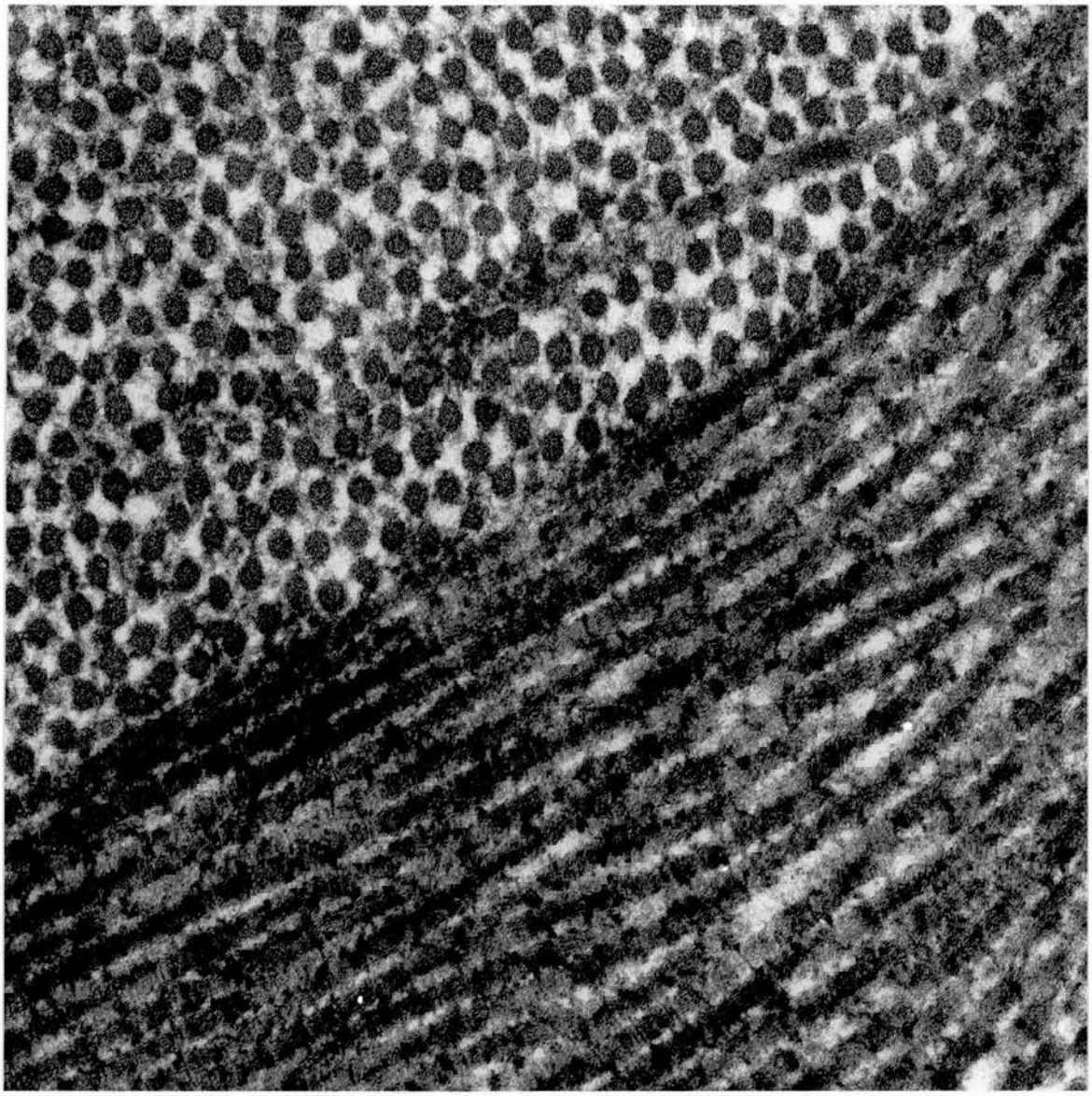

Figure 5.9/12

Alsatian X (150R)

There are numerous melanin granules and tonofilaments in the corneal epithelium on the left. The basal lamina is intact and the subepithelial zone is filled with numerous empty, or partly empty, clear spaces of a variety of shapes and sizes. All the fibroblasts visible are abnormal.

TEM X 2,750 (4)

Figure 5.9/13

Bearded Collie (26L)

Fibroblasts of varied appearance in the mid-stroma. A proportion contain lysosomes and the majority are degenerate.

TEM X 1,650 (2)

Figure 5.9/14

English Cocker Spaniel (24R)

An activated fibroblast from the periphery of an opacity which encroached upon perilimbal territory. It appears that microgranular material has been released into the stroma and a number of pinocytotic vesicles are present. The clear and osmiophilic spaces within the stroma are indicative of previous occupancy by lipid.

TEM X 27,500 (2)

Figure 5.9/15

Alsatian (27R1)

A fibroblast, with centriole, in the perilimbal region at the periphery of the lesion.

TEM X 35,500 (2)

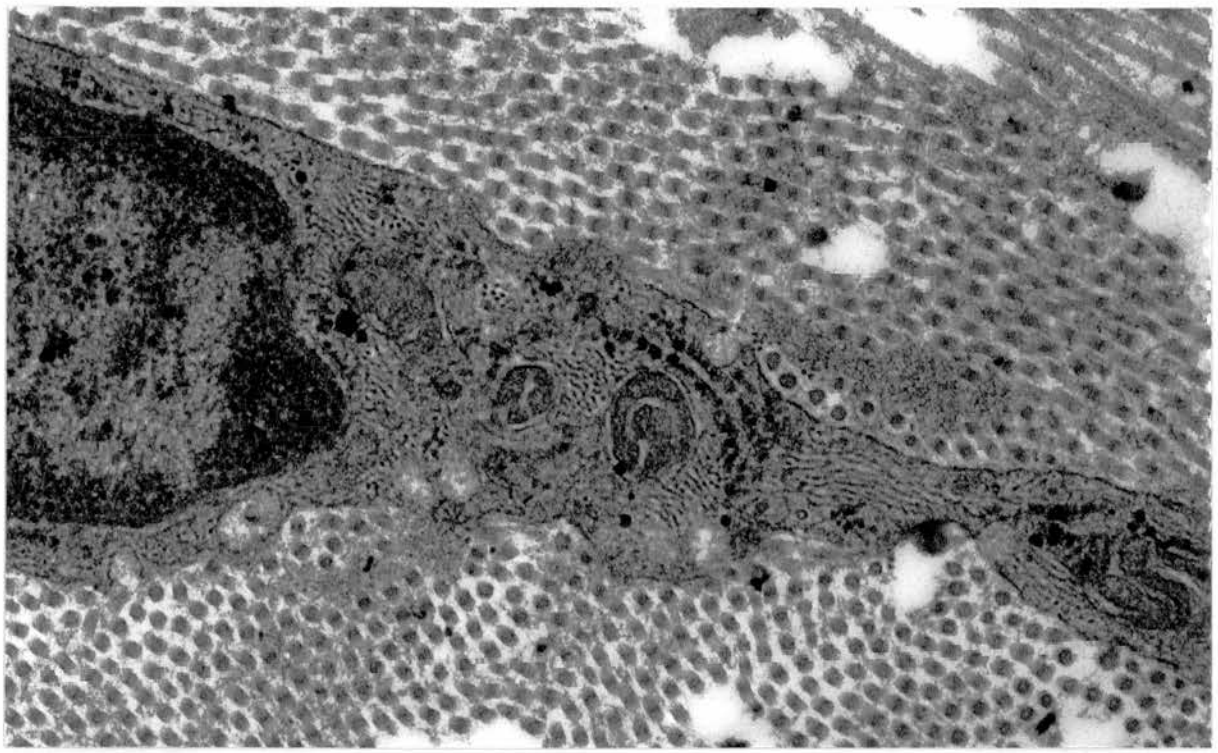

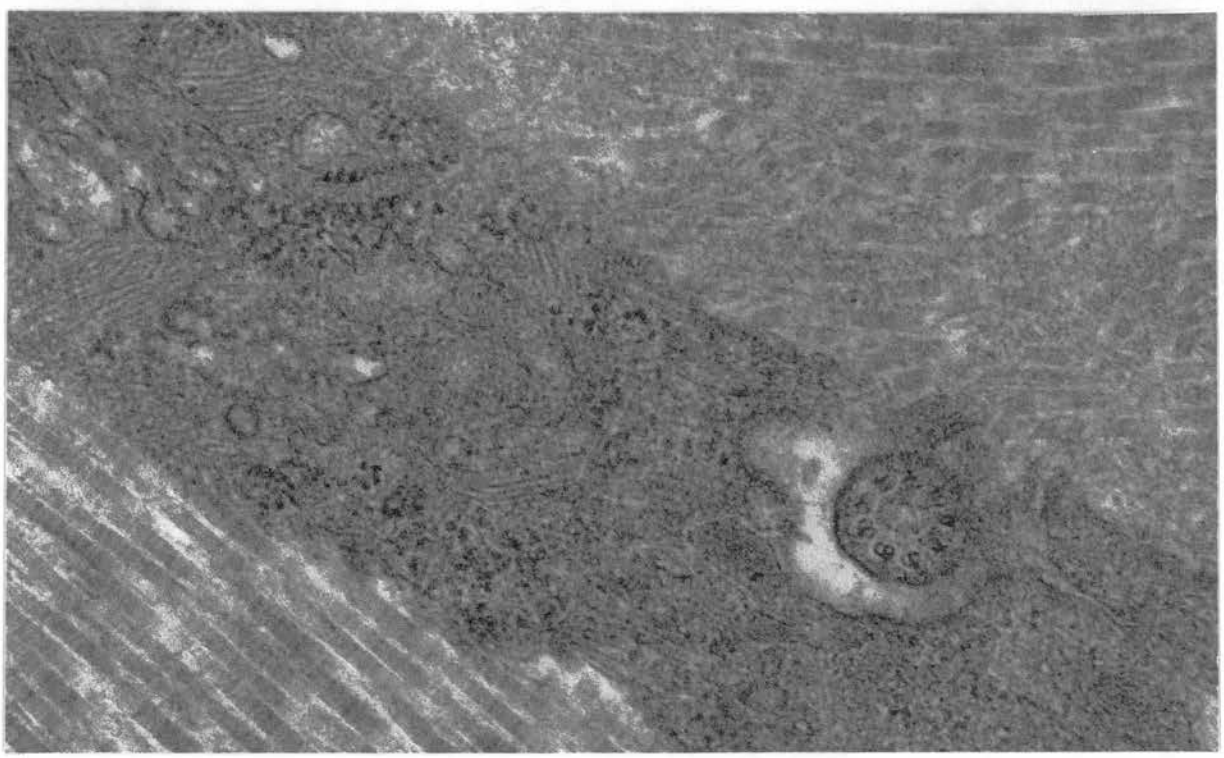

Figure 5.9/16

Golden Retriever (4L)

Degenerate fibroblast. A proportion of the vesicles and vacuoles present may be derived from pinched off swellings which appear to bud off from the endoplasmic reticulum (arrowed).

TEM X 6,000 (2)

Figure 5.9/17

Alsatian (160R)

A degenerating fibroblast demonstrating intracisternal sequestration (arrow).

TEM X 27,500 (2)

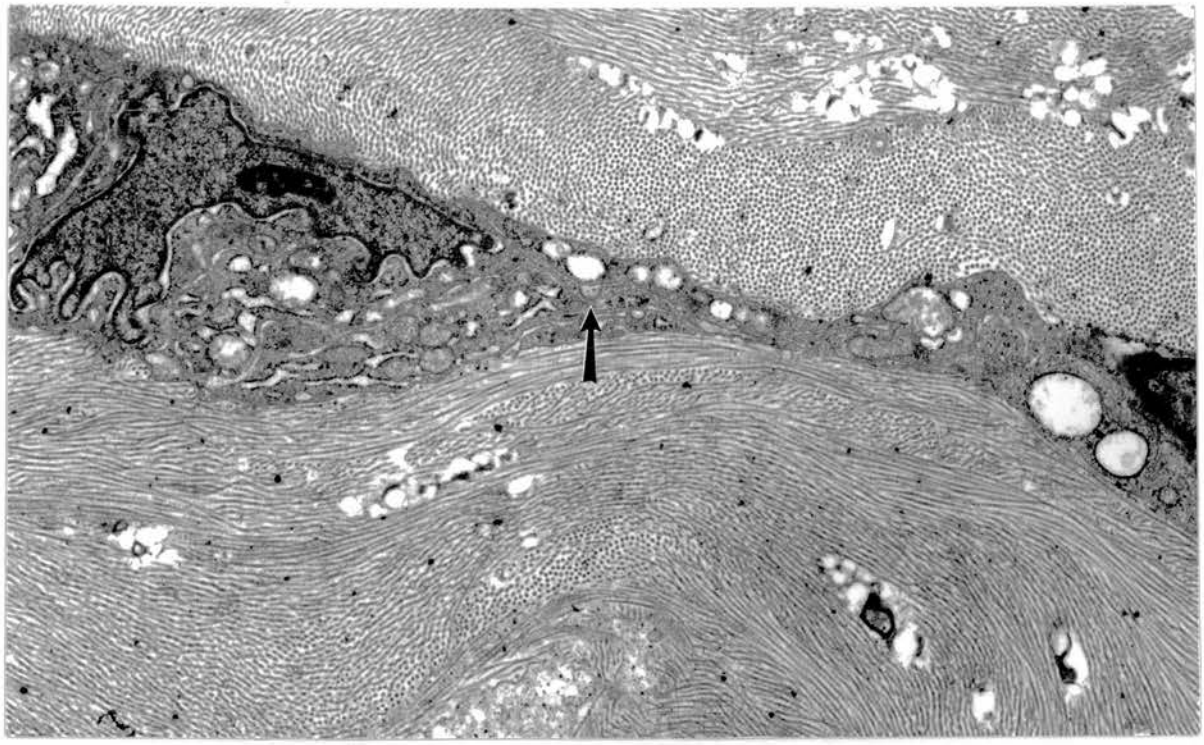

Figure 5.9/18

Alsatian X (150L)

Ruthenium red preparation to show that the ruthenium red positive material present within the vacuoles and and endoplasmic reticulum of abnormal fibroblasts corresponds with that released into the stroma and accumulating beneath the basal lamina.

TEM, Ruthenium Red X 4,600 (2)

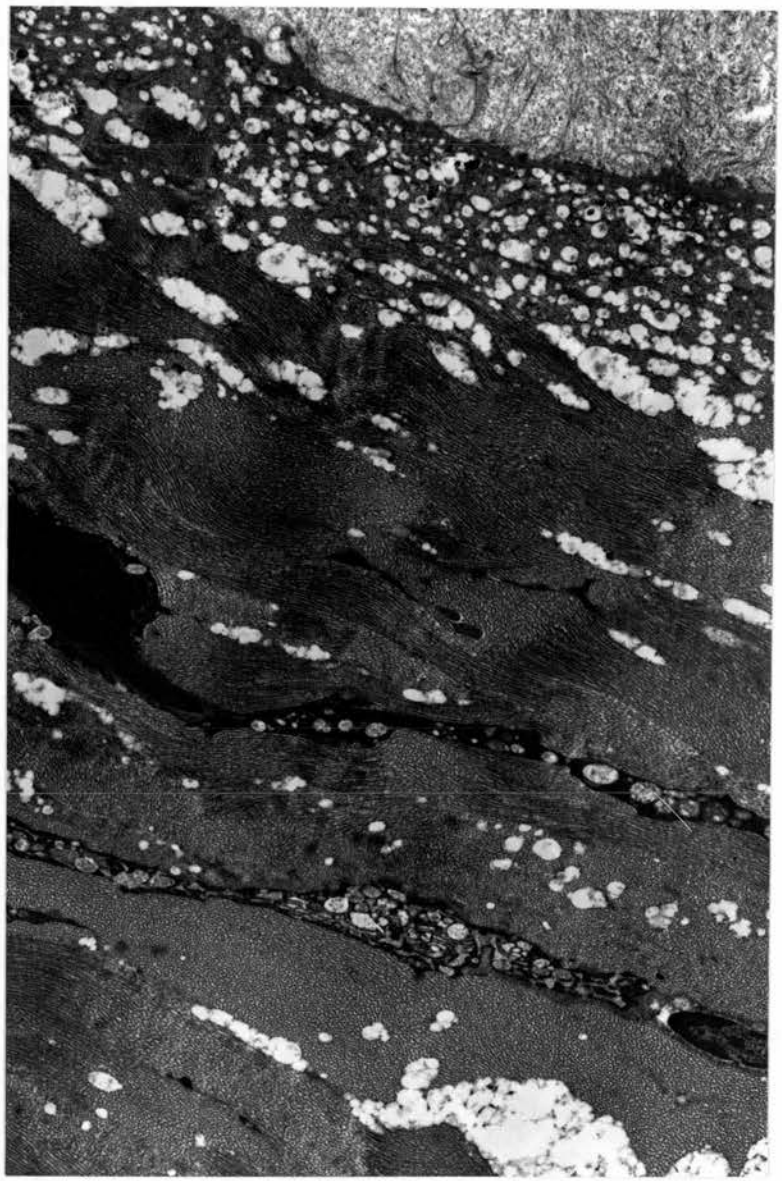

Figure 5.9/19

Golden Retriever (4R)

Oblong spaces with osmiophilic borders which, from the results of light microscopy, were previously occupied by solid crystals of lipid rich in esterified cholesterol. The lipid material labelled (A) is similar to that labelled (B) and (C). The fibroblast may be engaged in either lipid release or lipid uptake from the appearance of this micrograph. The lipid labelled (B) is closely associated with a pit, or invagination, of the plasma membrane.

TEM X 60,000 (2)

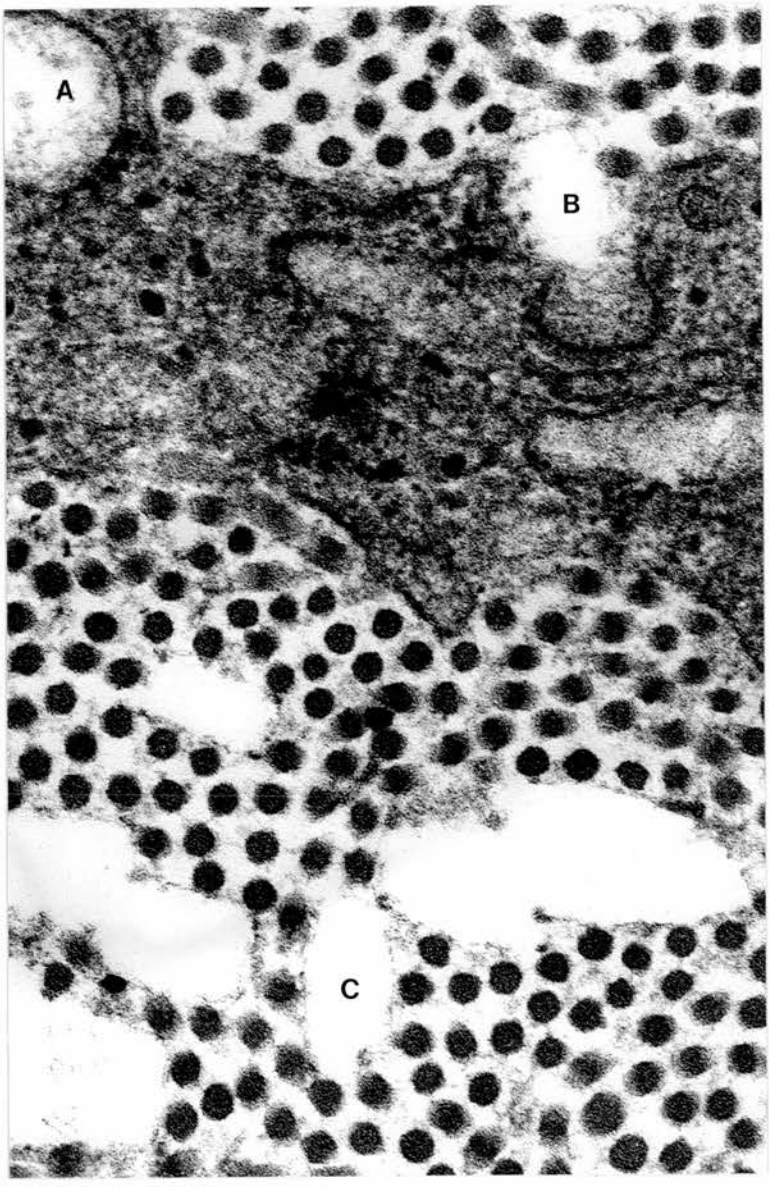
A
B
C

Figure 5.9/20

English Springer Spaniel (66R)

Appearance of mitochondria (A) and granular endoplasmic reticulum (B) in a degenerating fibroblast.

TEM X 46,000 (2)

Figure 5.9/21

Alsatian (36R)

Membranous lamellae in a degenerating fibroblast.

TEM X 12,500 (2)

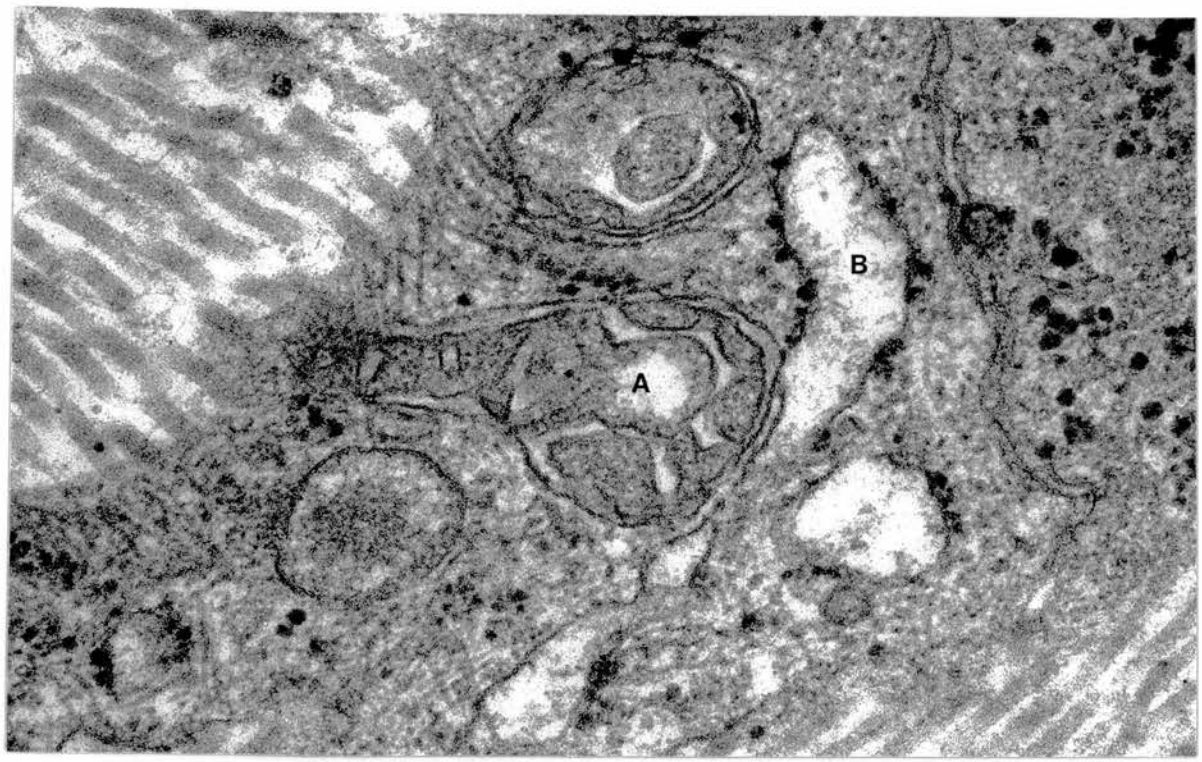
A
B

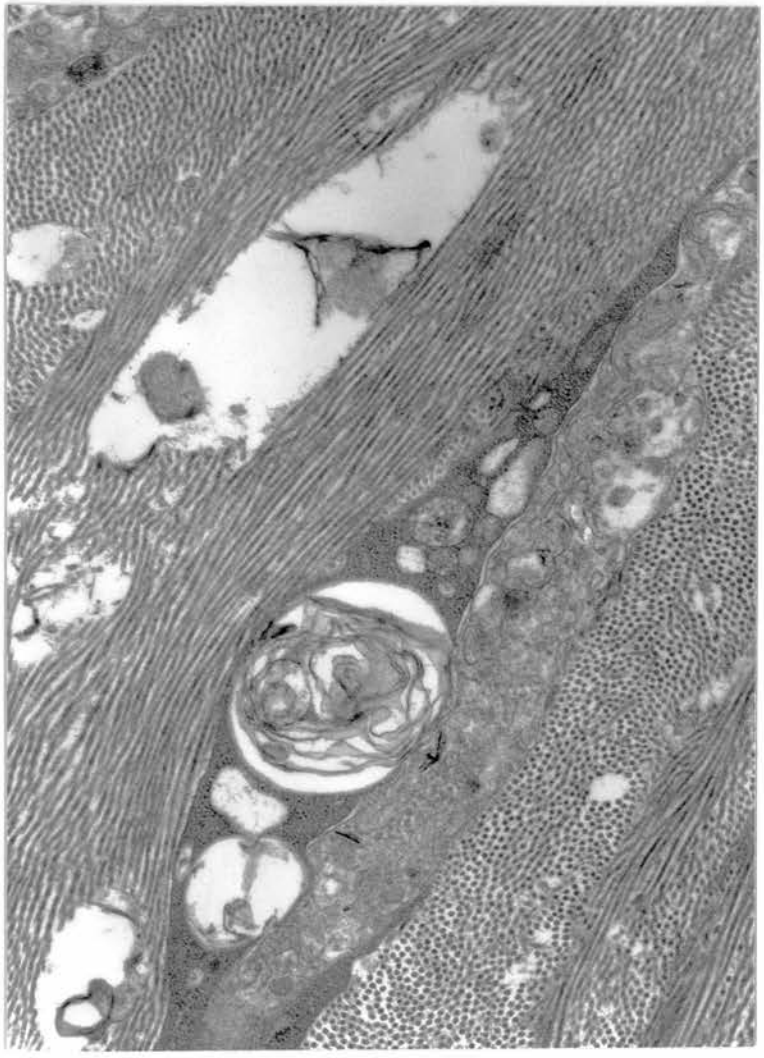

Figure 5.9/22

Golden Retriever (9L)

Membranous lamellae closely associated with an abnormal corneal fibroblast. The dark stripe of the lamella is of approximately 30 Å thickness.

TEM X 35,500 (2)

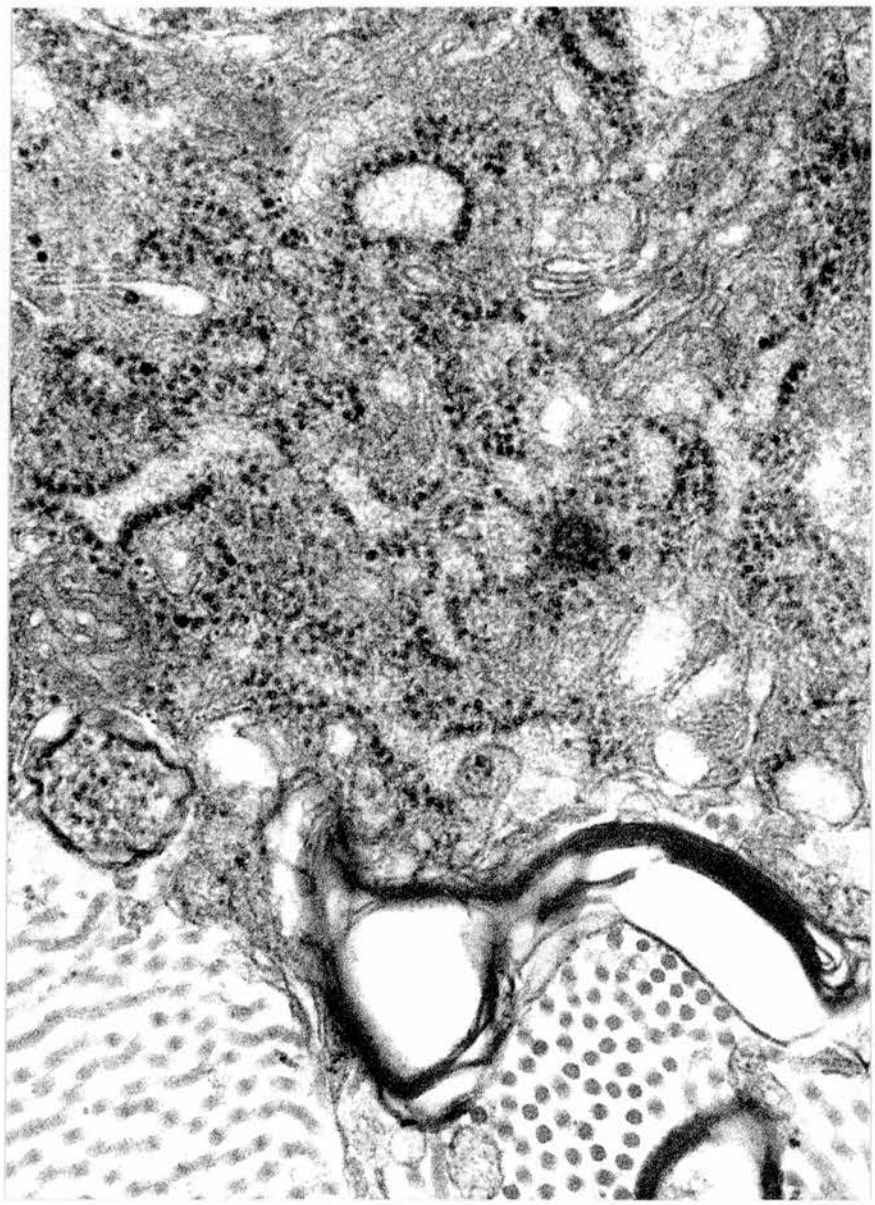

Figure 5.9/23

Golden Retriever (151R)

Degenerate fibroblast associated with ruthenium red positive material (A), round spaces (B) and an oblong space which is notched (C). The latter was previously occupied by free cholesterol.

TEM, Ruthenium Red X 21,500 (2)

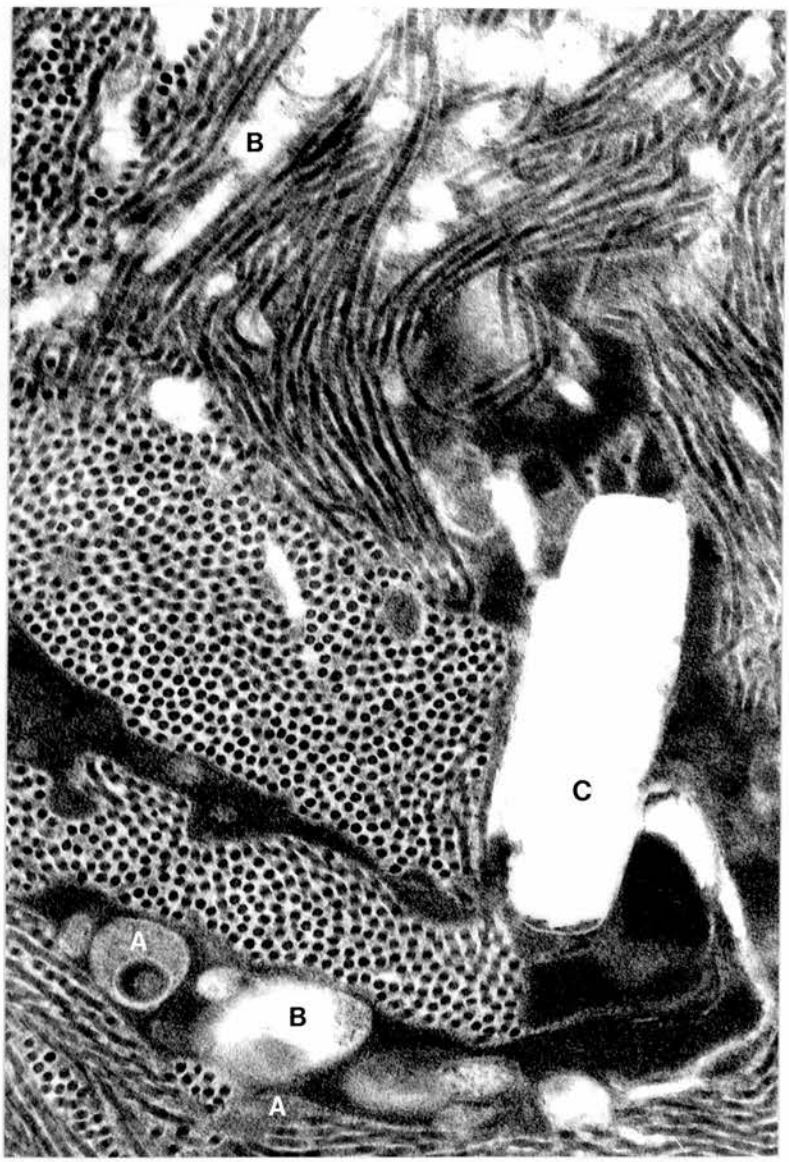
B
C
A
B
A

Figure 5.9/24

Old English Sheepdog (13R)

Tangential section mid-stroma, to demonstrate the extent of cholesterol clefts and stromal disruption in a cornea which was oedematous on slit lamp examination.

TEM X 2,750 (2)

Figure 5.9/25

Old English Sheepdog (13R)

Tangential section of the basal epithelial cells, basal lamina and anterior stroma from the same dog.

TEM X 2,750 (2)

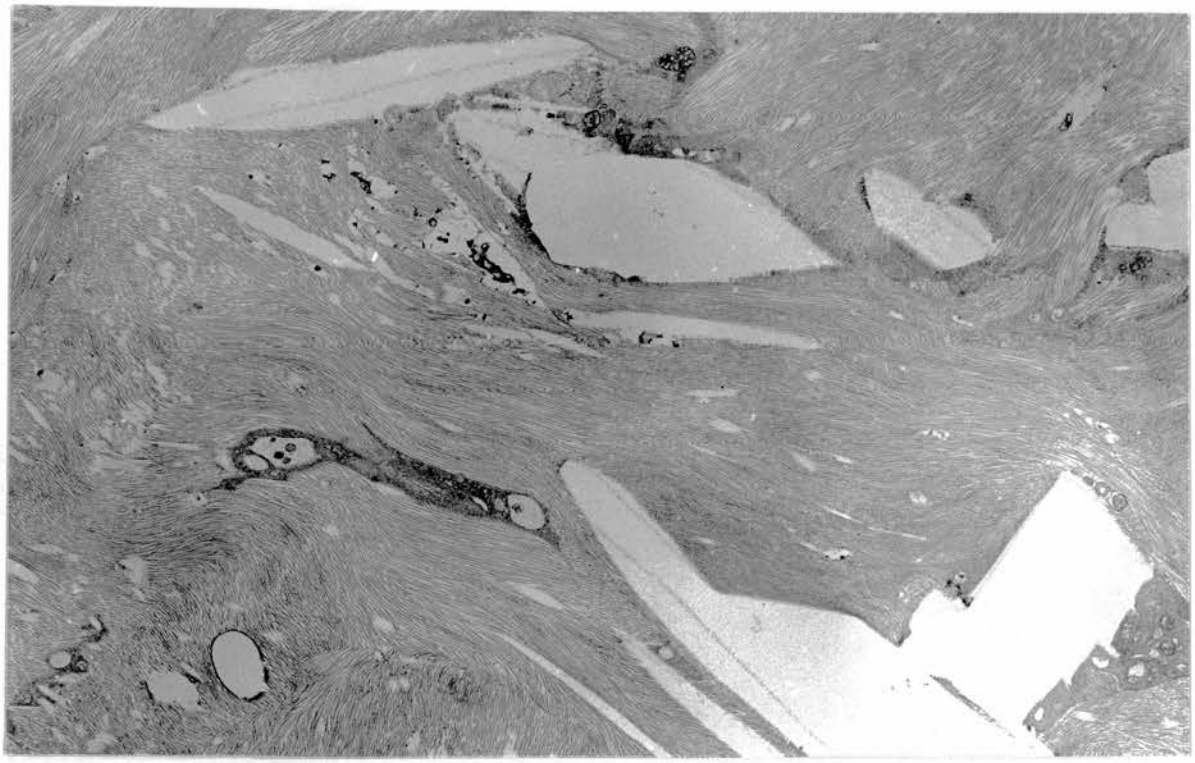

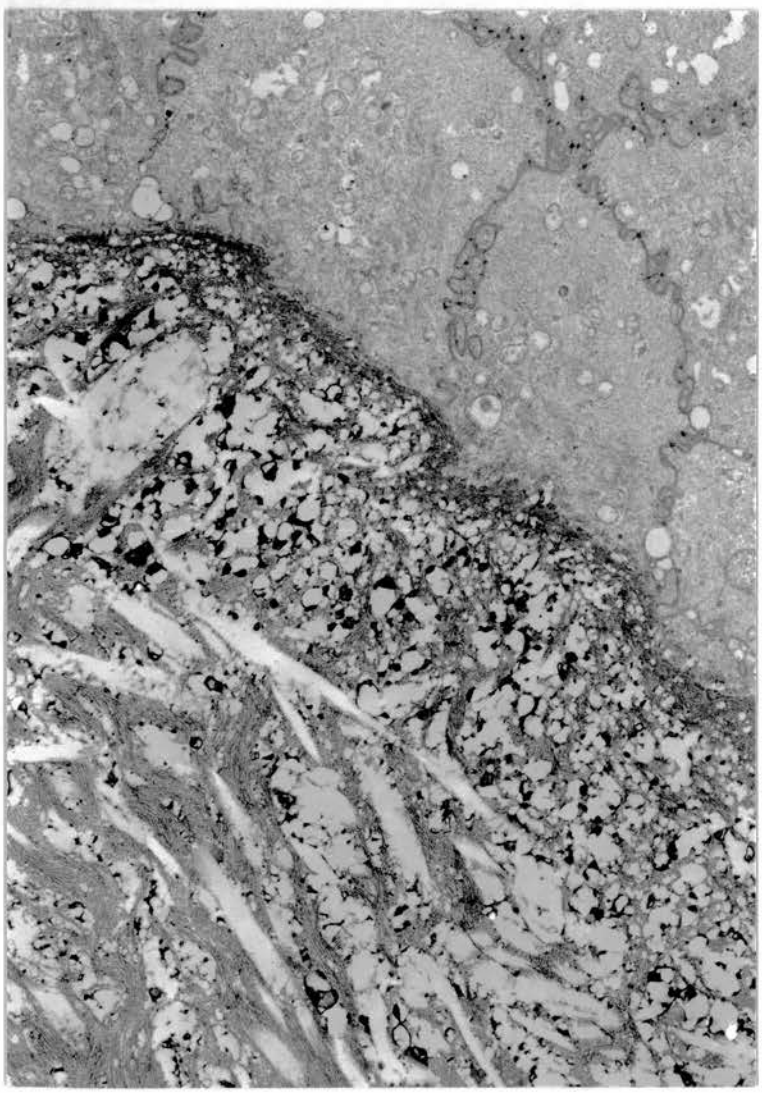

Figure 5.9/26

Alsatian (36R)

Necrotic fibroblasts associated with cholesterol clefts and membranous lamellae.

TEM X 4,600 (2)

Figure 5.9/27

Welsh Springer Spaniel (42R2)

Lysosome-containing fibroblasts and fibroblasts containing circular spaces. The circular spaces were identified as containing mainly esterified cholesterol globules with earlier histochemical methods.

Granular material is apparent within the stroma and, particularly, accumulating beneath the basal lamina. The appearance of the granular material is consistent with lipid released by degenerating globule-containing fibroblasts, as identified with earlier lipid histochemistry.

TEM X 1,650 (2)

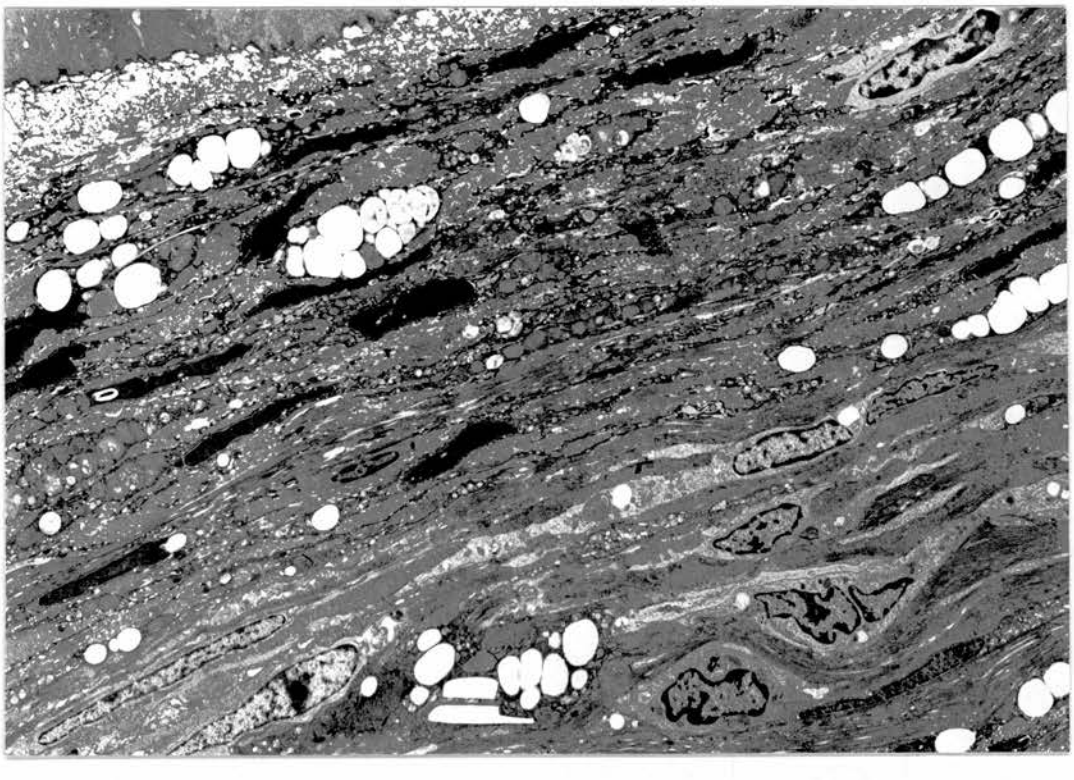

Figure 5.9/28

Welsh Springer Spaniel (42R2)

Abnormal fibroblast containing large lysosomes. The structure labelled (1) may indicate a primary lysosome, whereas (2) and (3) may represent stages in secondary lysosome development.

TEM X 16,500 (2)

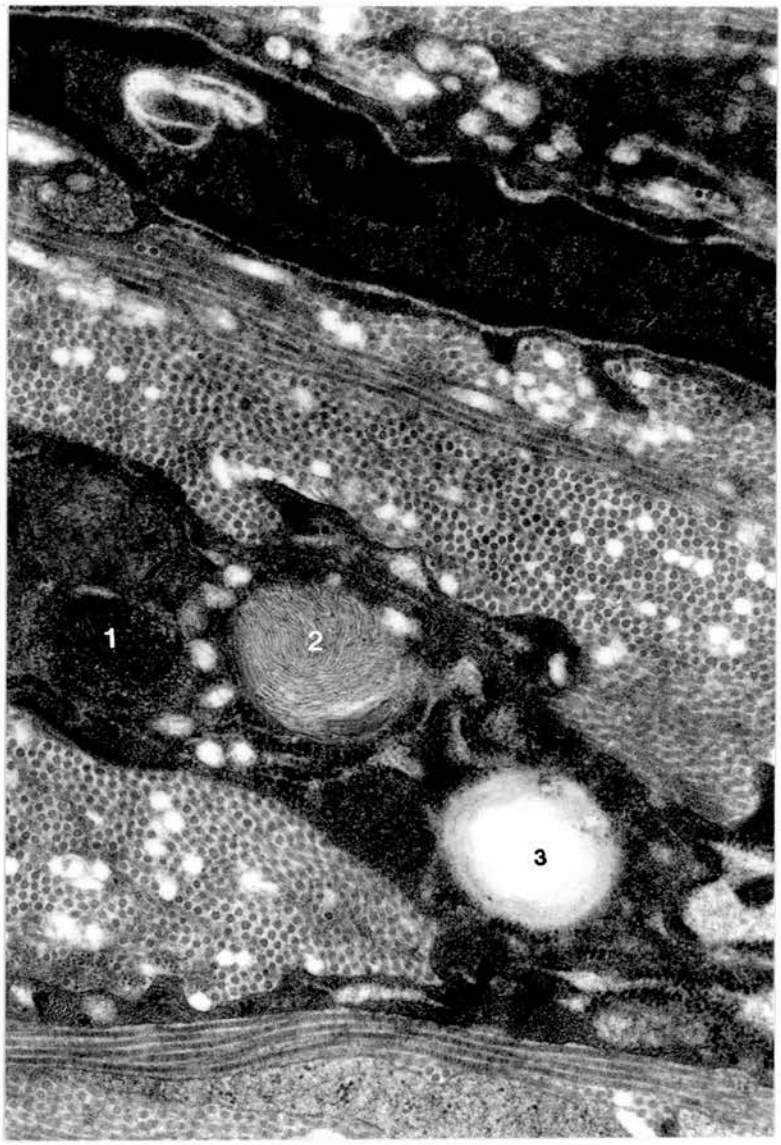
1
2
3

Figure 5.9/29

Alsatian (27L2)

Acid phosphatase positive material present within primary lysosomes (1) and secondary lysosomes (2) and (3) at various stages of development.

TEM, Lead Capture Method for
Acid Phosphatase X 21,500 (2)

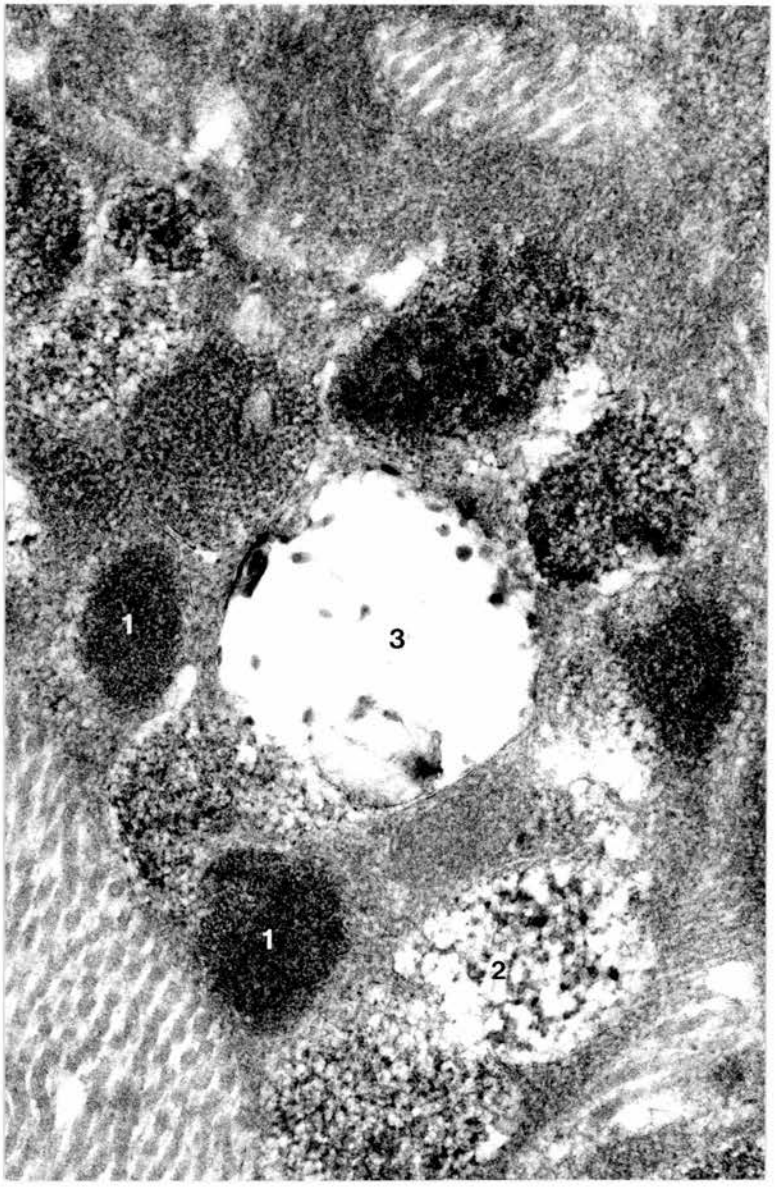
1
3
1
2

Figure 5.9/30

Golden Retriever (9R)

Extracellular membranous lamellae within the anterior stroma. The dark stripe is of approximately 30 Å diameter.

TEM X 165,000 (2)

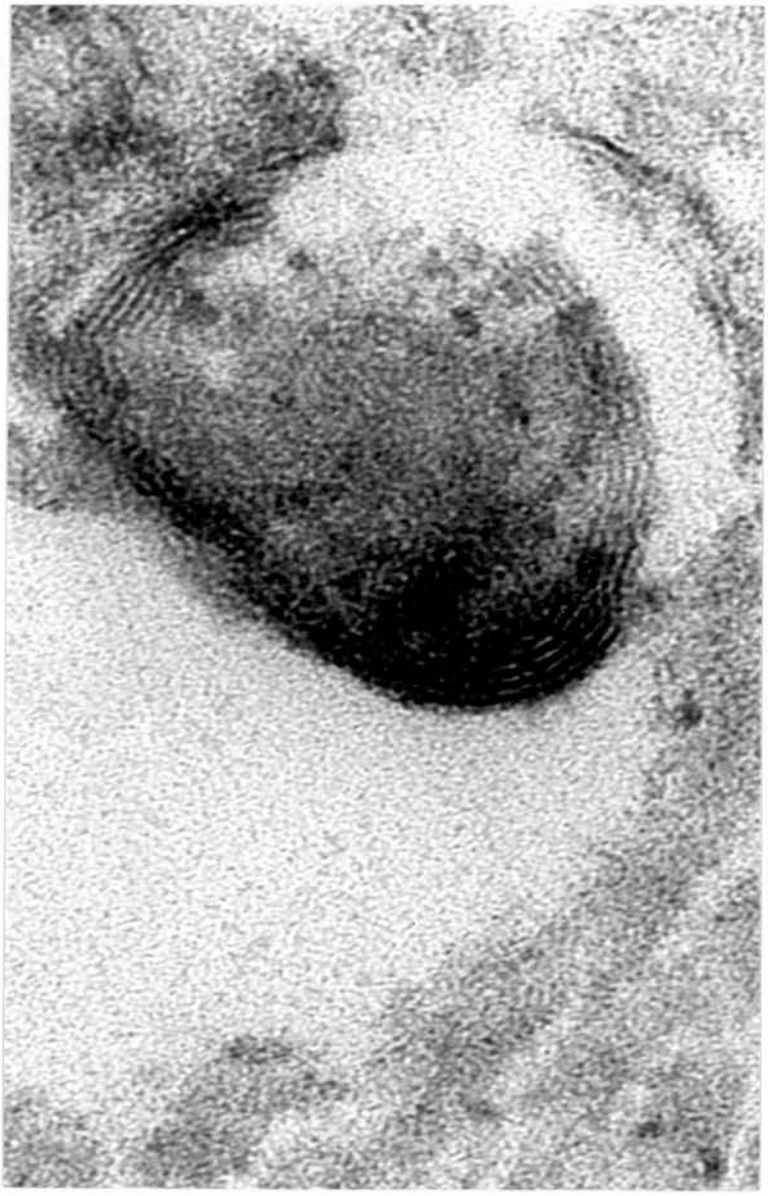

Figure 5.9/31

Old English Sheepdog (38L)

Fibroblasts of more normal appearance in a regressing lesion. The lamellar arrangement is not quite as regular as that of normal control cornea and there is quite dense ground substance throughout the meridional section.

TEM X 4,600 (2)

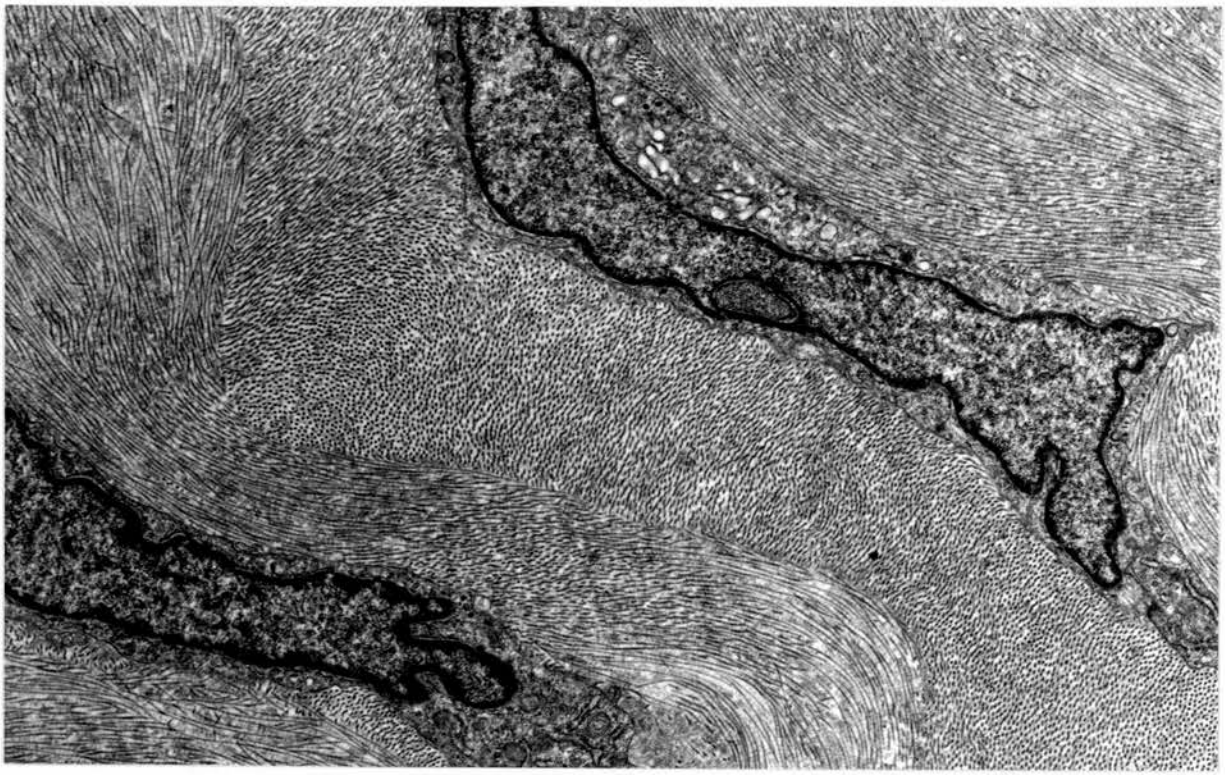

Figure 5.9/32

Alsatian (36L)

Superficial corneal neovascularisation derived from conjunctival vessels (A). The endothelium is usually lost during processing as it is fragile as well as leaky.

SEM X 400 (3)

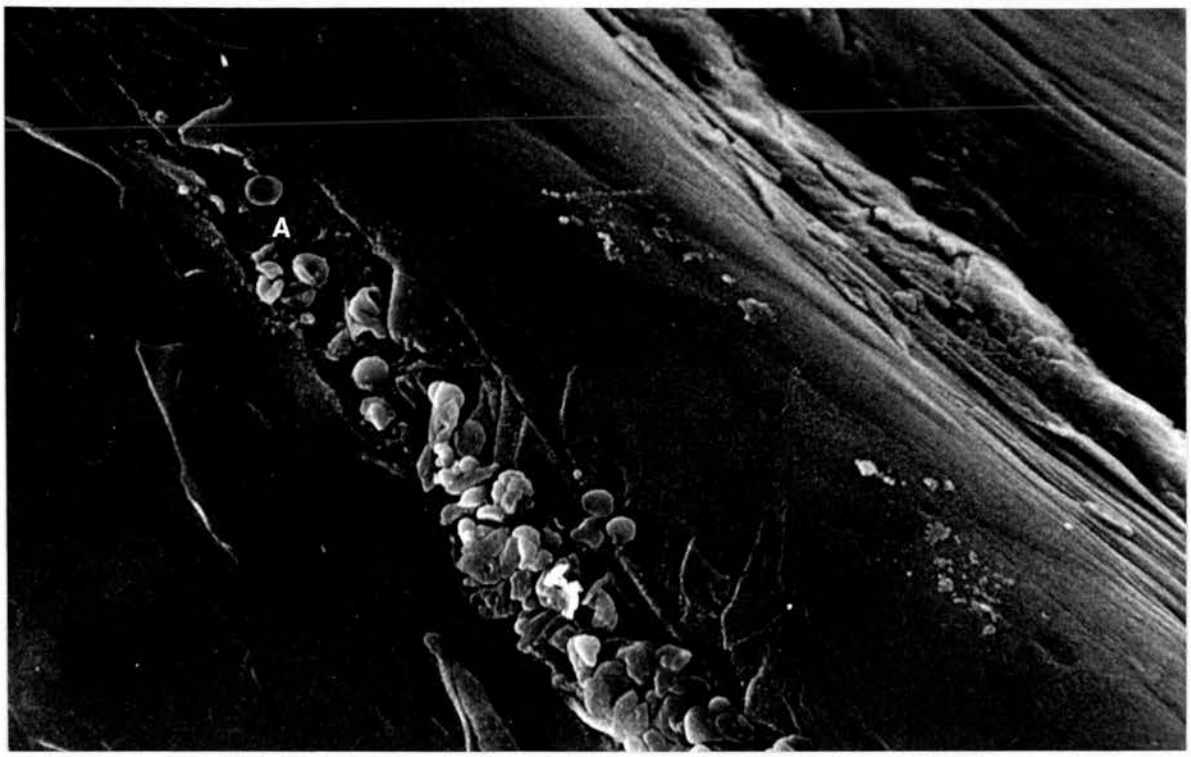
A

Figure 5.9/33

Golden Retriever (4R)

Vascularisation in an area of epithelial erosion (A).

SEM X 1000 (3)

Figure 5.9/34

Welsh Springer Spaniel (42R3)

Vascularisation in mid stroma. There is considerable collagen damage and disruption and the regular arrangement of the collagen present in Figure 5.9/33 has been lost. The collagen fibrils are of varied diameter and broader spacing was apparent in the fibrils of TEM preparations.

SEM X 4000 (3)

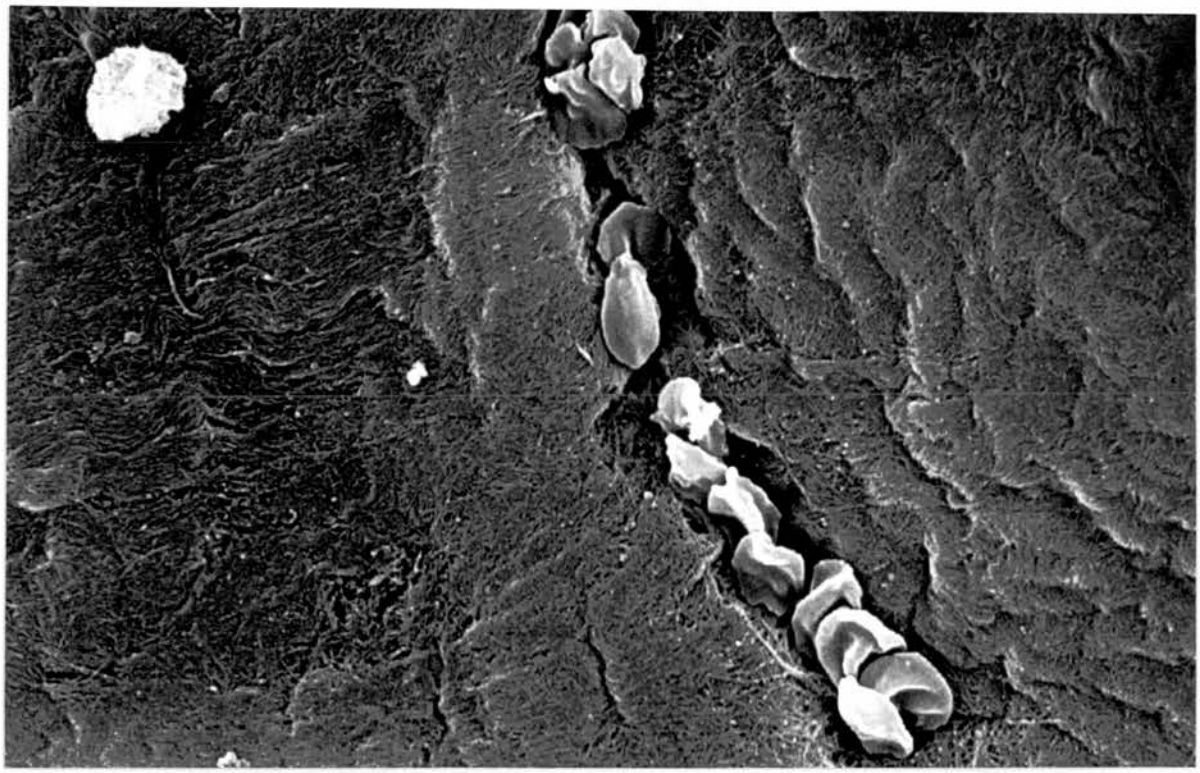

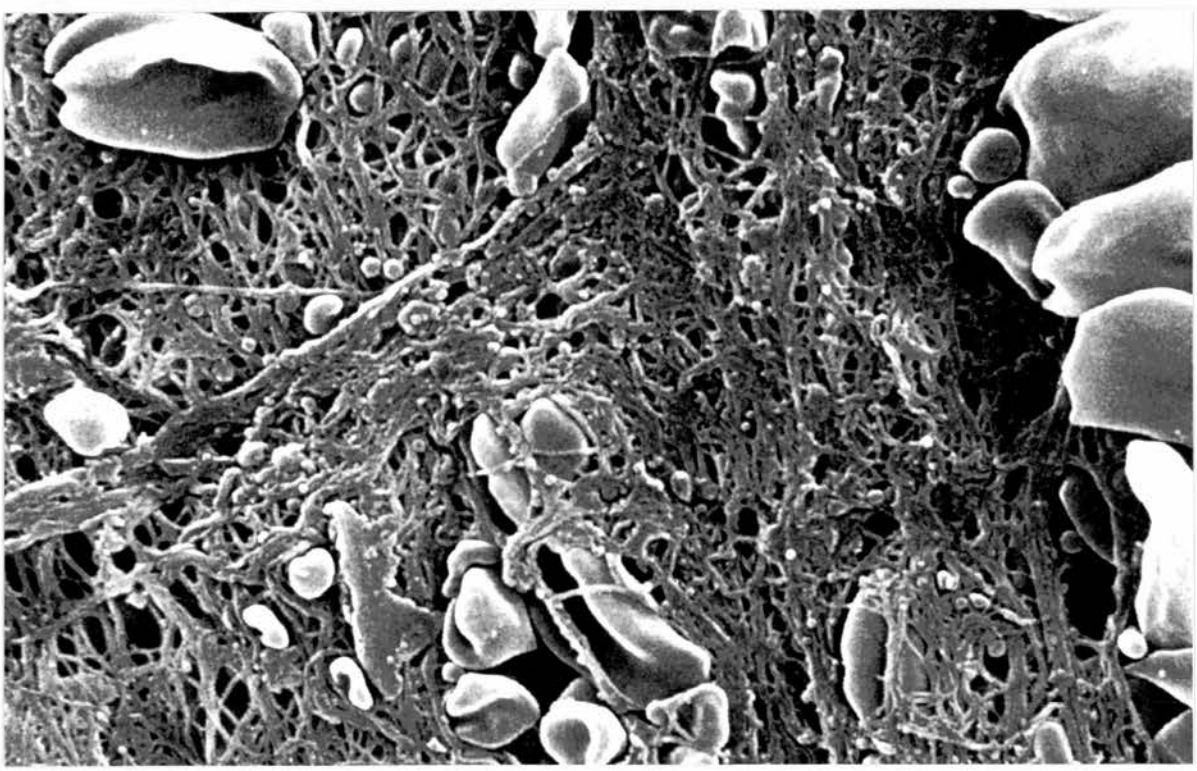

Figure 5.9/35

Alsatian (27R1)

Newly formed stromal capillary. Lumen containing red blood cell (A). The endothelial cells (B) are plump with numerous pinocytotic vesicles. Pericytes (C) are also present.

TEM X 4,600 (2)

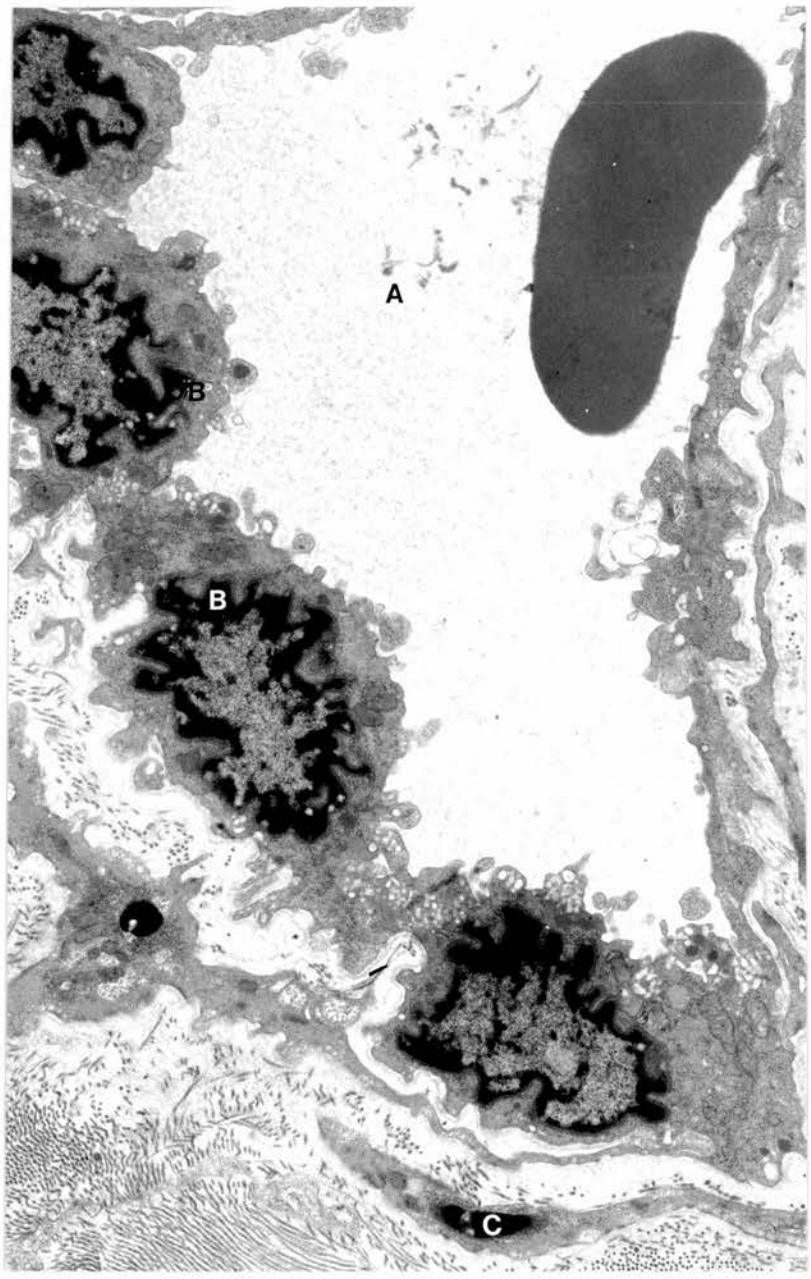
A
B
B
C

Figure 5.9/36

Alsatian (36R)

Non-convoluted appearance of basal surface of endothelial cells in an established stromal capillary. Red blood cells (A) and a polymorphonuclear leukocyte (B) are present within the blood vessel lumen. The arrowed material has characteristics of fibrin. There are also considerable quantities of irregularly shaped clear spaces surrounding the vessel which correspond with both hydrophobic and hydrophilic lipids identified with histochemical methods in this patient.

TEM X 7,700 (2)

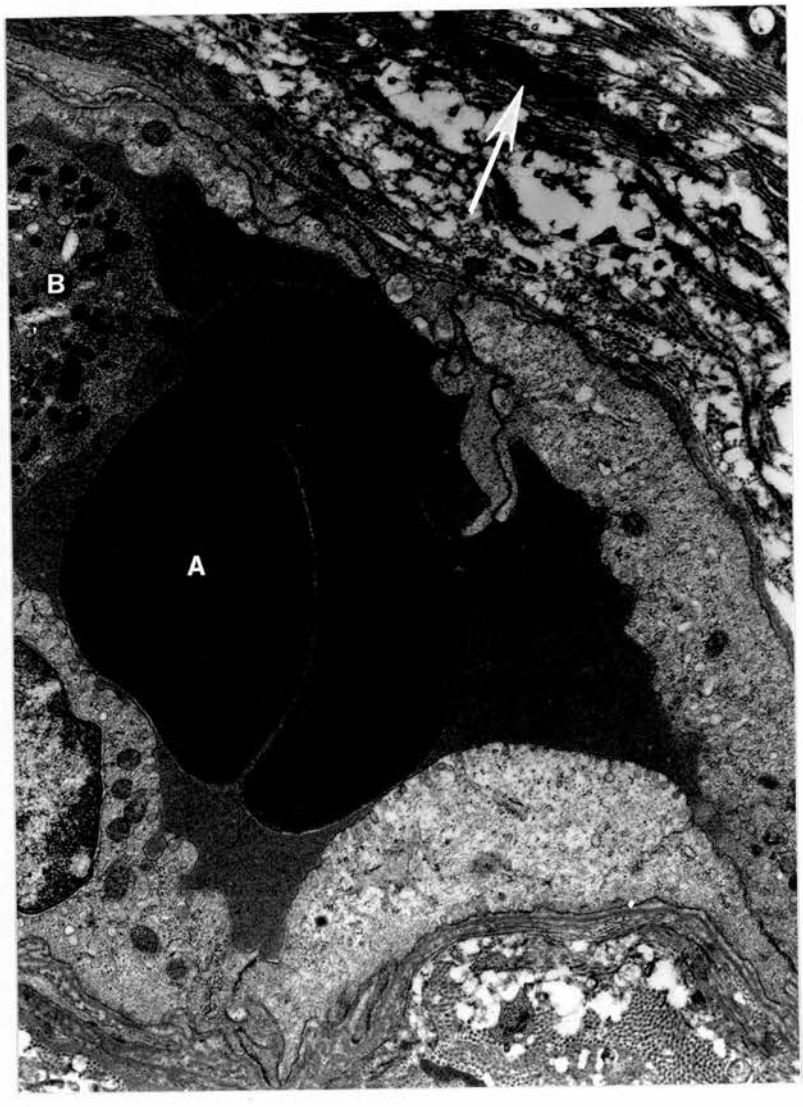
B
A

Figure 5.9/37

Alsatian (150R)

Capillary and post-capillary venule. In this dog there is less indication of lipid perivascularly, and this accords with the serum lipid and lipoprotein levels at the time of keratectomy. There is also no evidence of perivascular fibrin in this micrograph.

TEM X 2,750 (2)

Figure 5.9/38

English Springer Spaniel (65R)

Ruthenium red preparation which demonstrates the extensive reduplication of the basal lamina (arrows). There is separation of the pericytes and endothelial cells by translucent circular spaces which correspond with the lipid droplets of light microscopy. Similar spheres are seen within and near the basal lamina.

TEM X 10,000 (2)

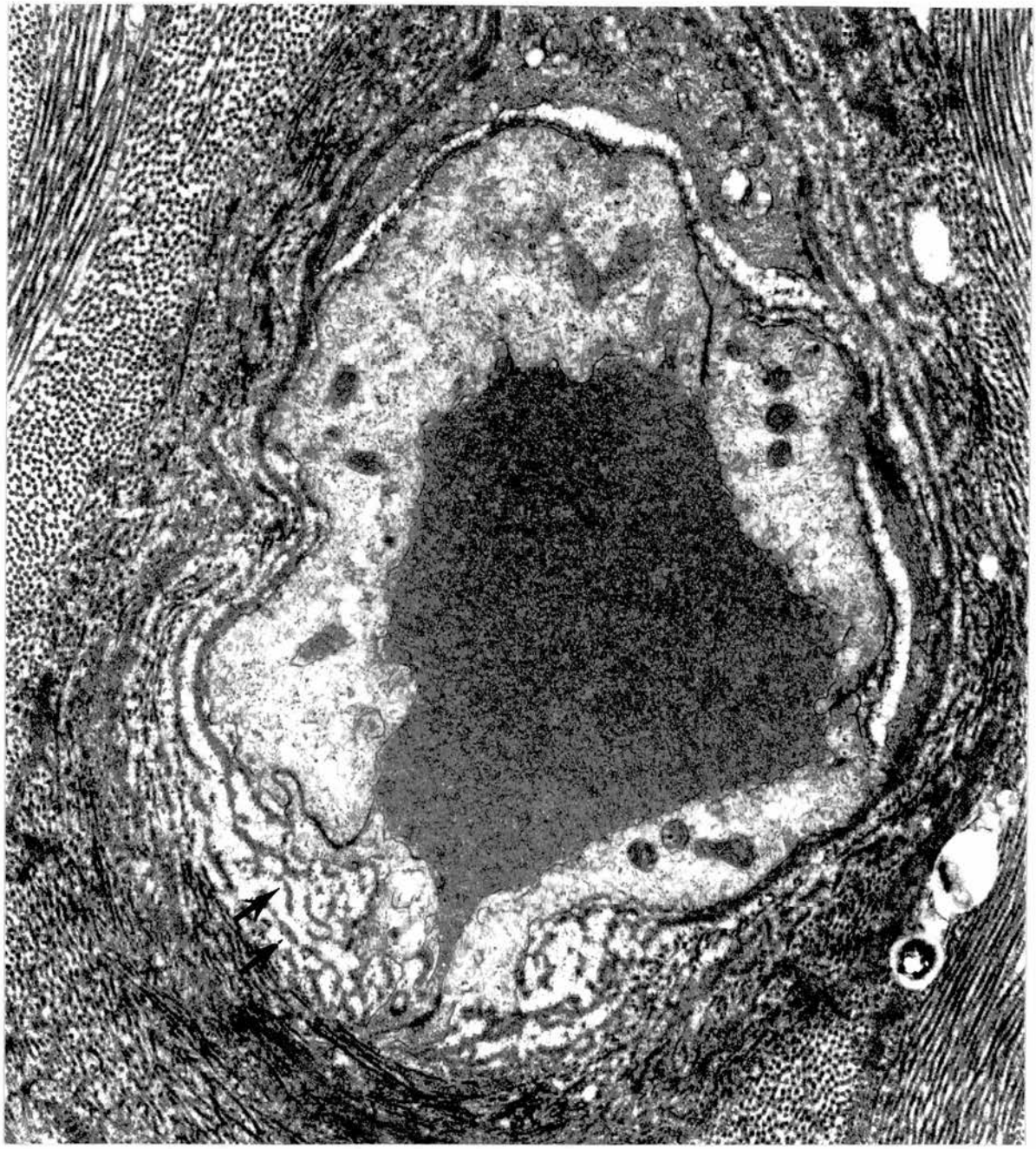

Figure 5.9/39

Alsatian (27L1)

The diameter of the translucent circles is observed to increase with increasing distance from the blood vessel lumen (A). There are also translucent circles within the pericytes (B), whereas a more distant fibroblast (C) is less affected.

TEM X 6,000 (2)

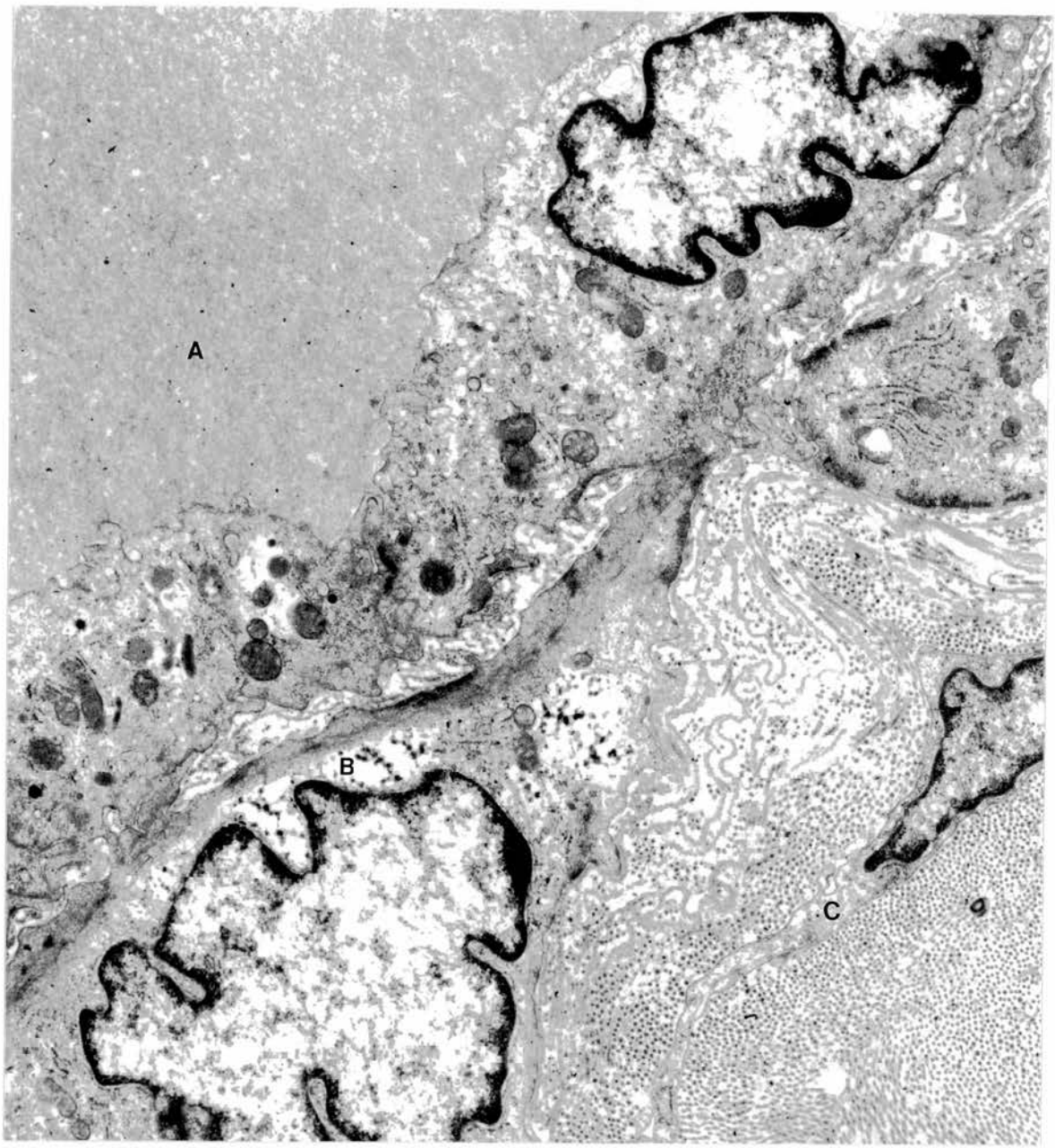
A
B
C

Figure 5.9/40

Welsh Springer Spaniel (42R2)

Red blood cell in the corneal stroma.

TEM X 12,500 (2)

Figure 5.9/41

Alsatian X (150R)

Degenerating red cell in the corneal stroma.

TEM X 12,500 (2)

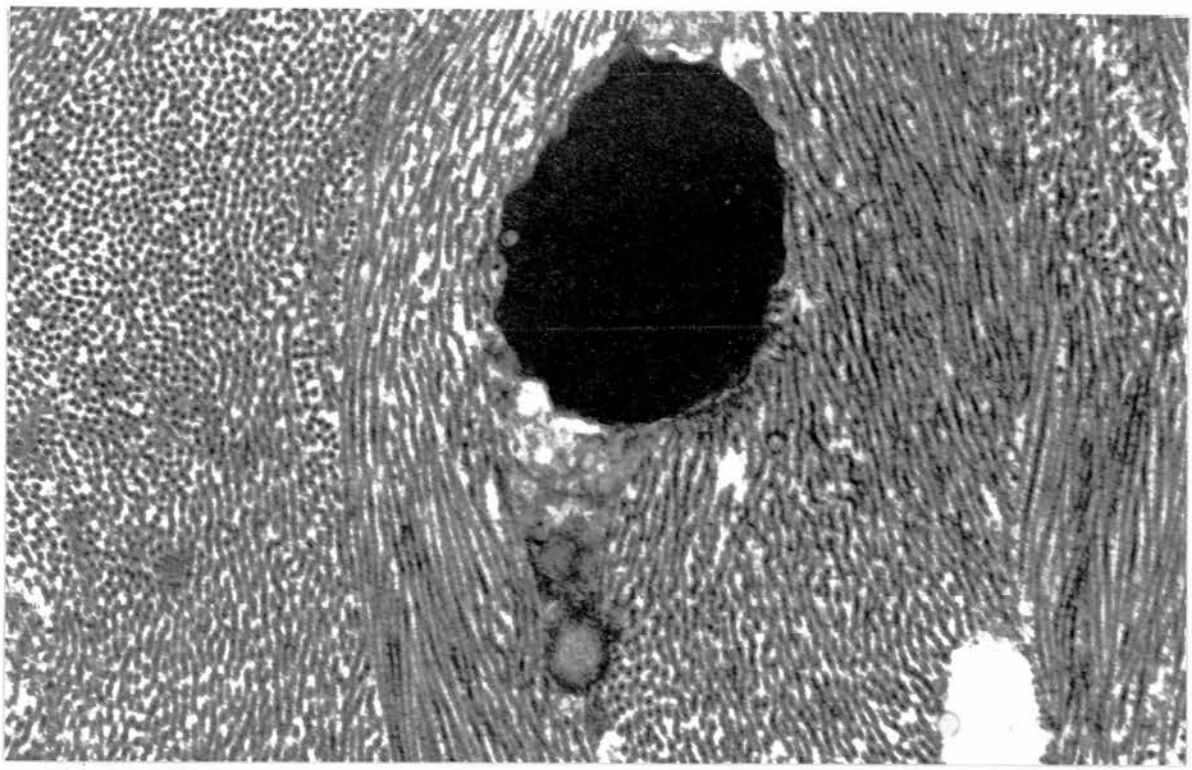

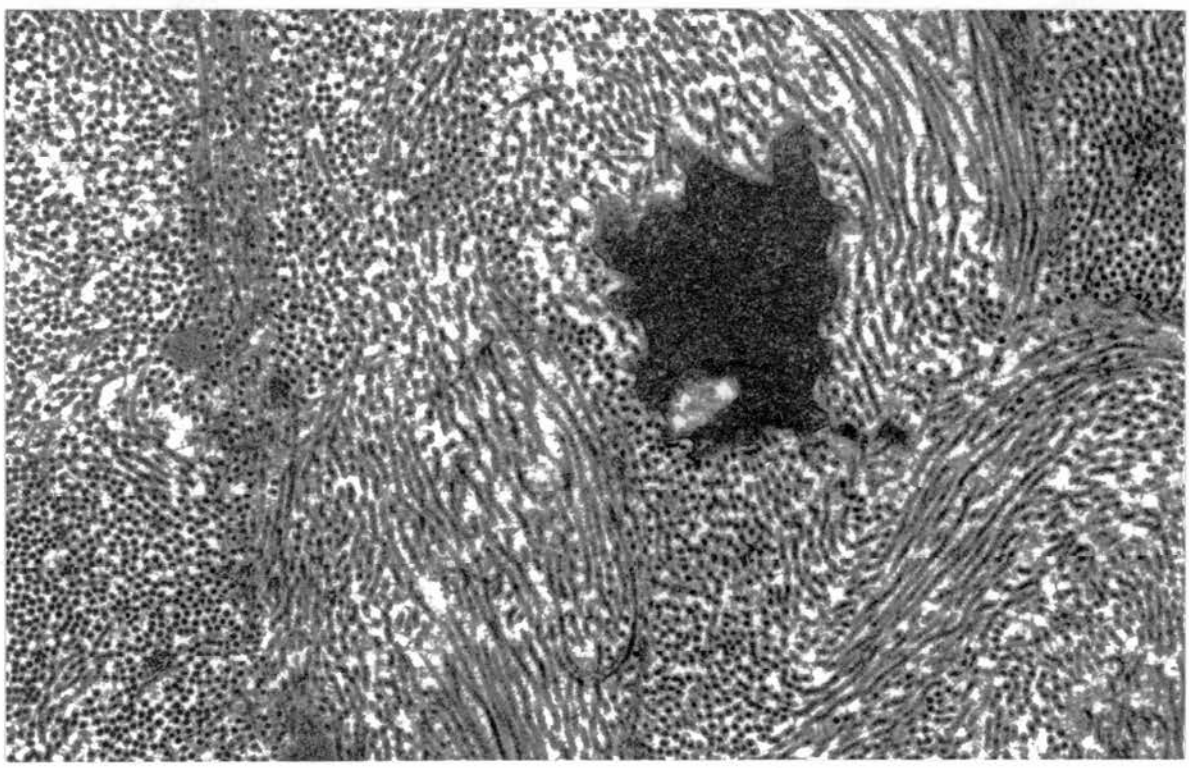

Figure 5.9/42

Bearded Collie (26L)

Fibrin in the posterior stroma (arrows). There are also round or oval spaces in the stroma and the anterior part of Descemet's membrane indicative of previous occupancy by lipid, which correlates with the earlier results of lipid histochemistry in which esterified cholesterol and phospholipid had been demonstrated. The periodicity of many of the collagen fibrils is also greater than normal and may be representative of the type of collagen laid down during corneal repair. The collagen lamellae are less regularly arranged than in normal, control, corneas.

TEM X 10,000 (2)

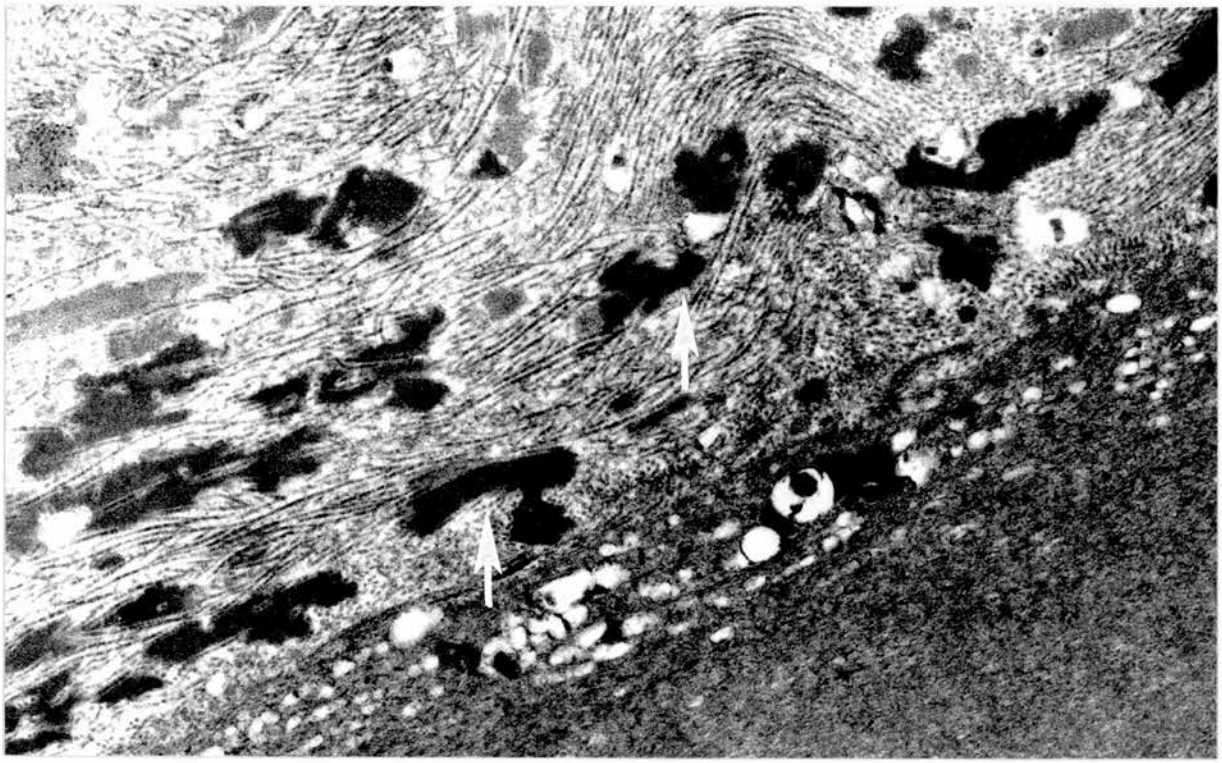

Figure 5.9/43

Alsatian (27L1)

Polymorphonuclear leukocyte (A) closely associated with a fibroblast (B).

TEM X 4,600 (2)

Figure 5.9/44

Golden Retriever (4R)

Polymorphonuclear leukocyte (A) surrounded by poorly differentiated cells. Intracellular and extracellular spaces (characteristic of both liquid and solid lipid and confirmed as such by previous lipid histochemistry). Subsequent micrographs will be presented in conjunction with the findings of earlier lipid histochemistry.

TEM X 2,750 (2)

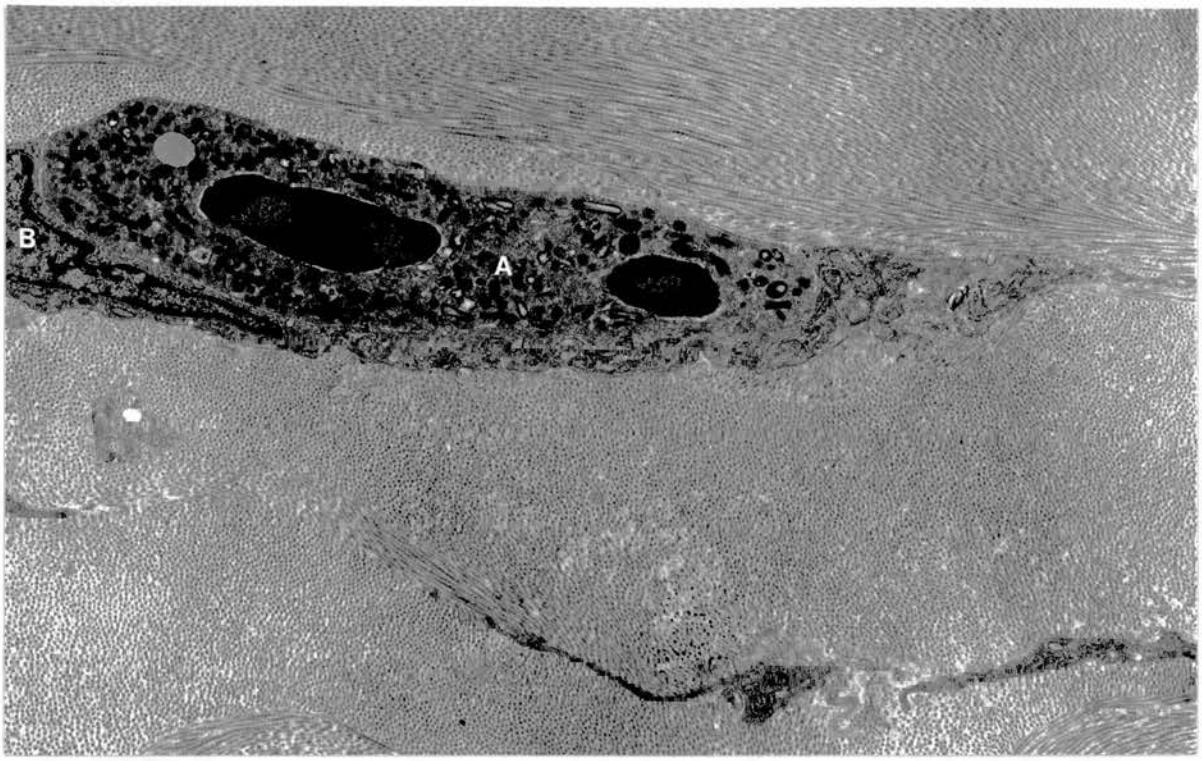
B
A

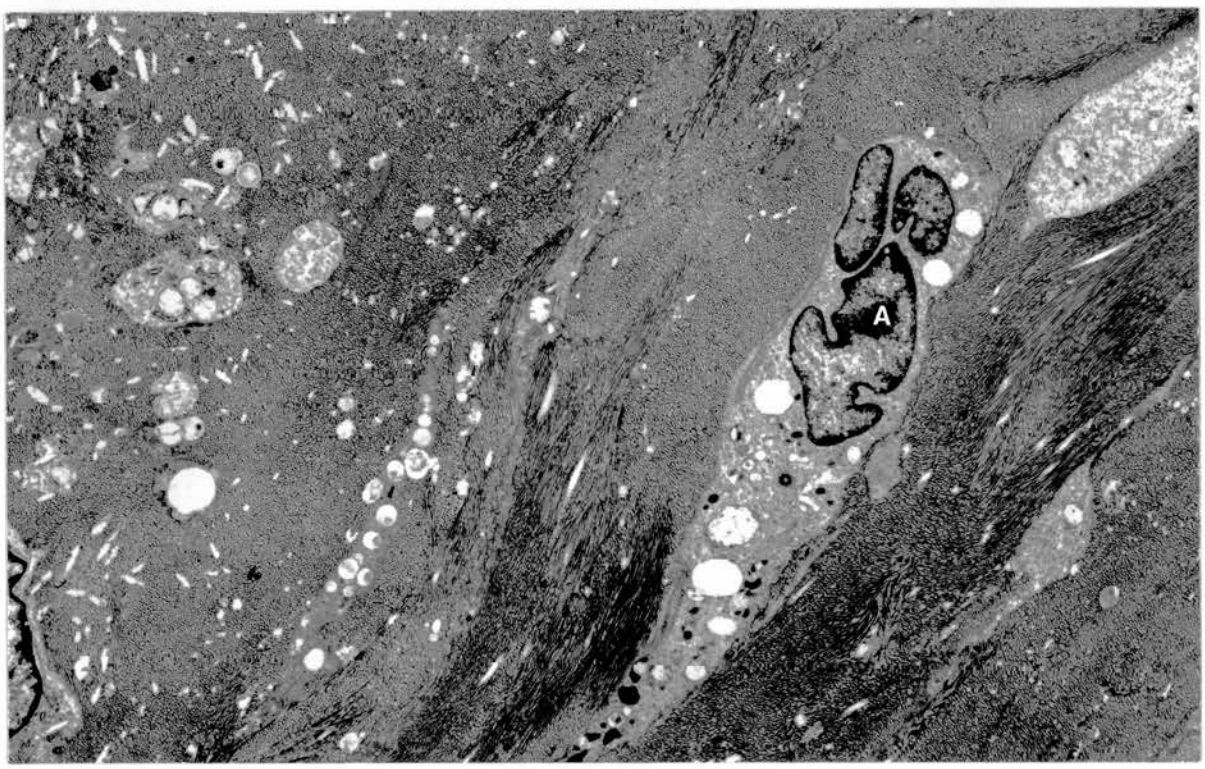
A

Figure 5.9/45

Welsh Springer Spaniel (42R3)

Plasma cells (A) surrounded by masses of granular lipid which consisted of both free and esterified cholesterol. A perineural cell (B) is also present, next to a fibroblast and some unmyelinated nerves.

TEM X 3,550 (2)

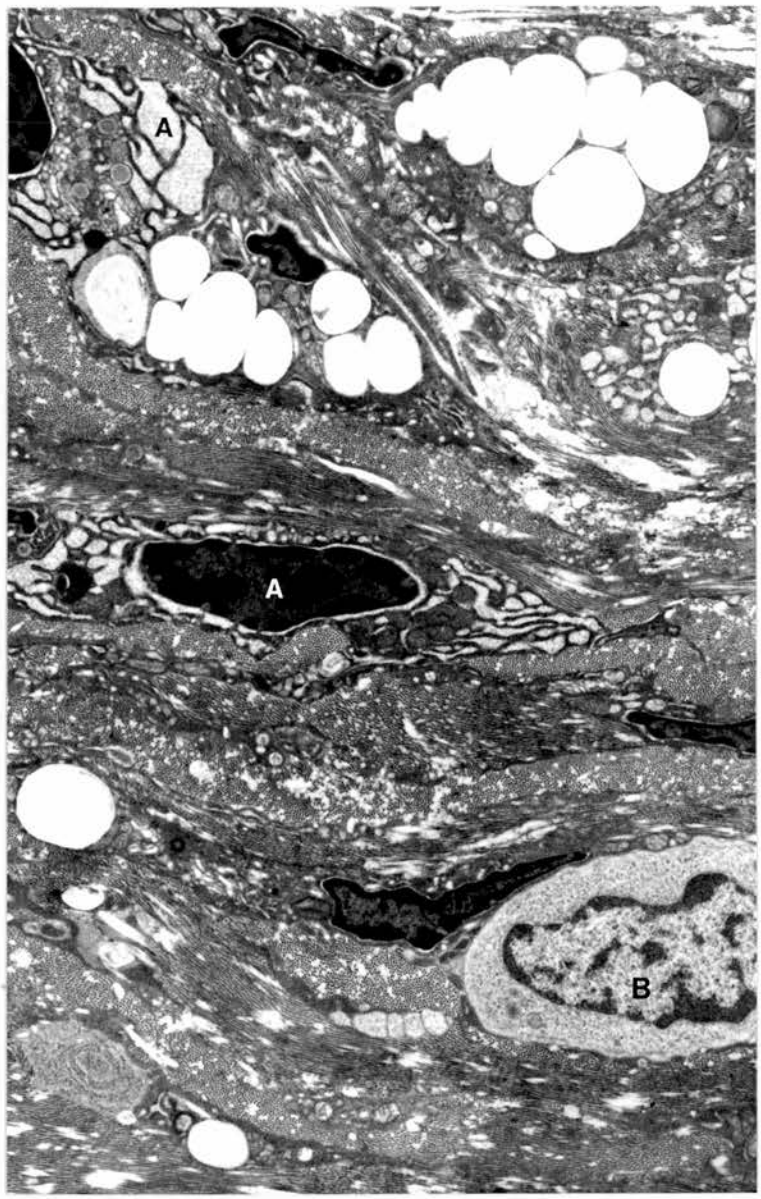
A
A
B

Figure 5.9/46

Alsatian (36R)

Unmyelinated nerves (A) and perineural cell (B). The large intracellular globules were mainly esterified cholesterol.

TEM X 3,550 (2)

Figure 5.9/47

Welsh Springer Spaniel (42R2)

Intracellular and extracellular spaces indicative of liquid and solid lipid, mainly in the form of esterified cholesterol. The cells present are characteristic of fibroblasts.

TEM X 2,750 (2)

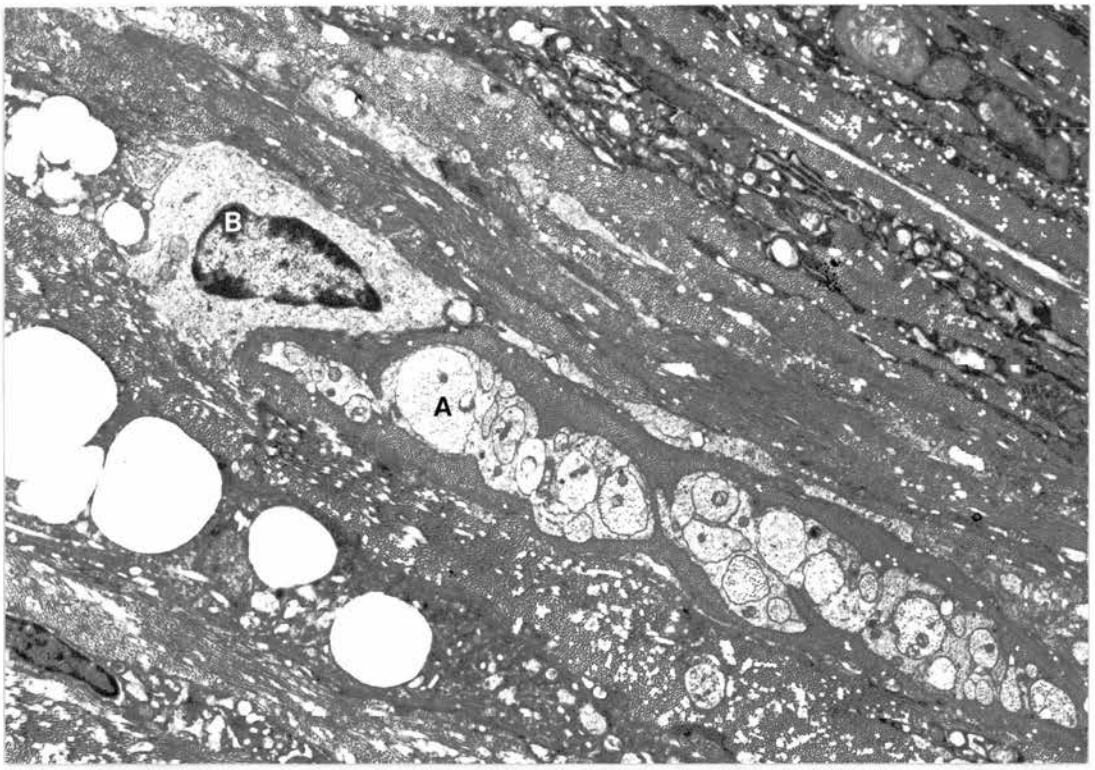
B
A

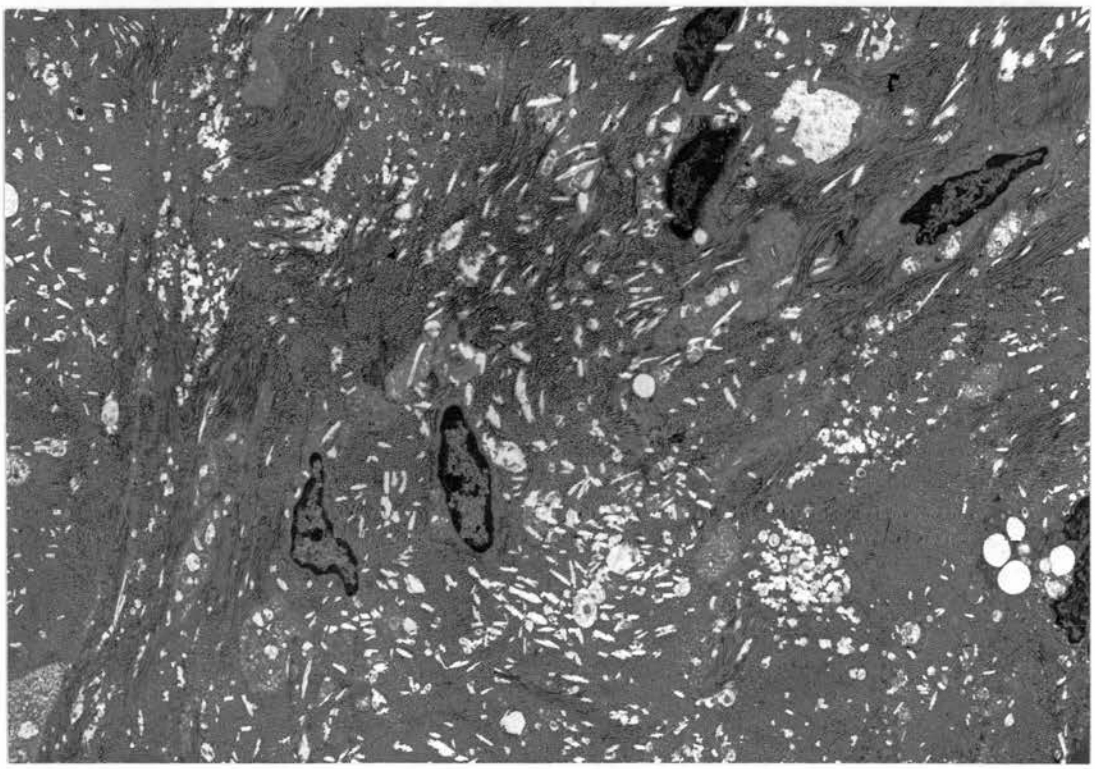

Figure 5.9/48

Golden Retriever (4R)

Mid-stromal appearance of granular lipid derived from degenerate fibroblasts (A). Whilst free cholesterol comprised some of the crystalline lipid the majority of lipid was in the form of esterified cholesterol.

TEM X 2,750 (2)

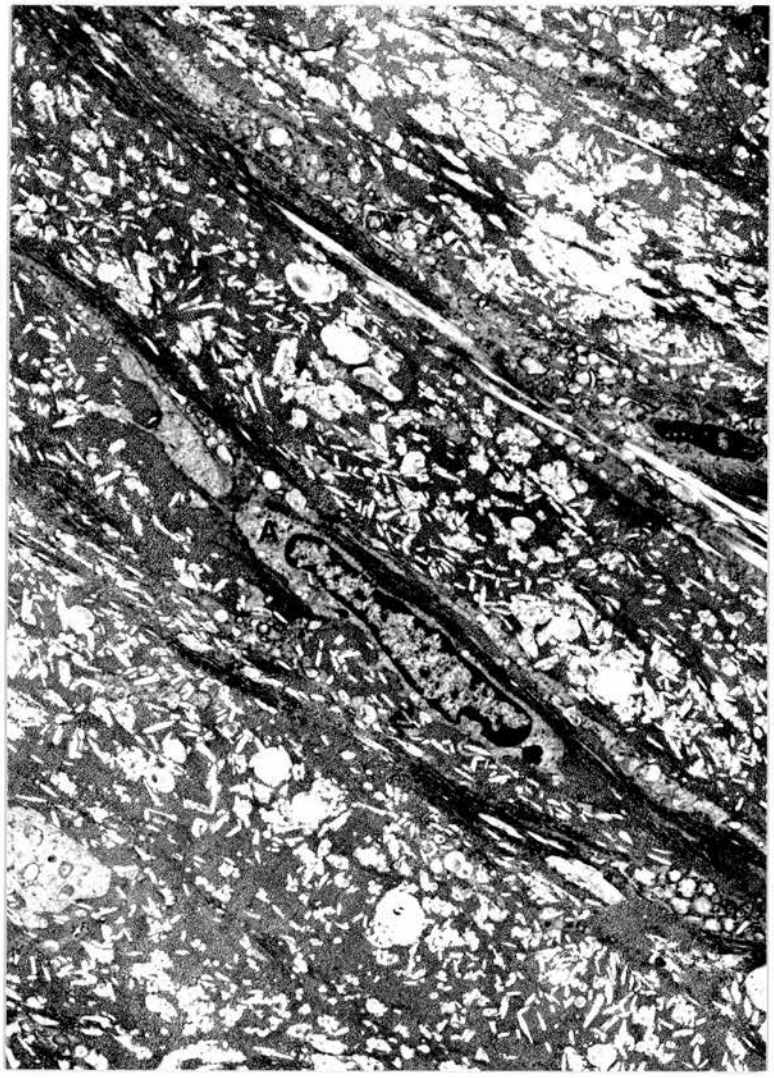

Figure 5.9/49

Alsatian (36L)

A degenerate fibroblast (A) in which crystals of cholesterol are associated with dying back of the extensive cytoplasmic processes. Numerous lipid droplets (which contained esterified cholesterol and phospholipid) have begun to accumulate beneath the basal lamina and they are almost certainly derived directly from fibroblast death.

TEM X 6,000 (2)

Figure 5.9/50

Old English Sheepdog (13L)

Considerable quantities of membranous lamellae composed of esterifed cholesterol and very little phospholipid. More deeply within the stroma crystals of free cholesterol were prominent. The identical appearance of membranous lamellae beneath the basal lamina (A) and within degenerate stromal fibroblasts (B) is clear in this section.

TEM X 7,700 (2)

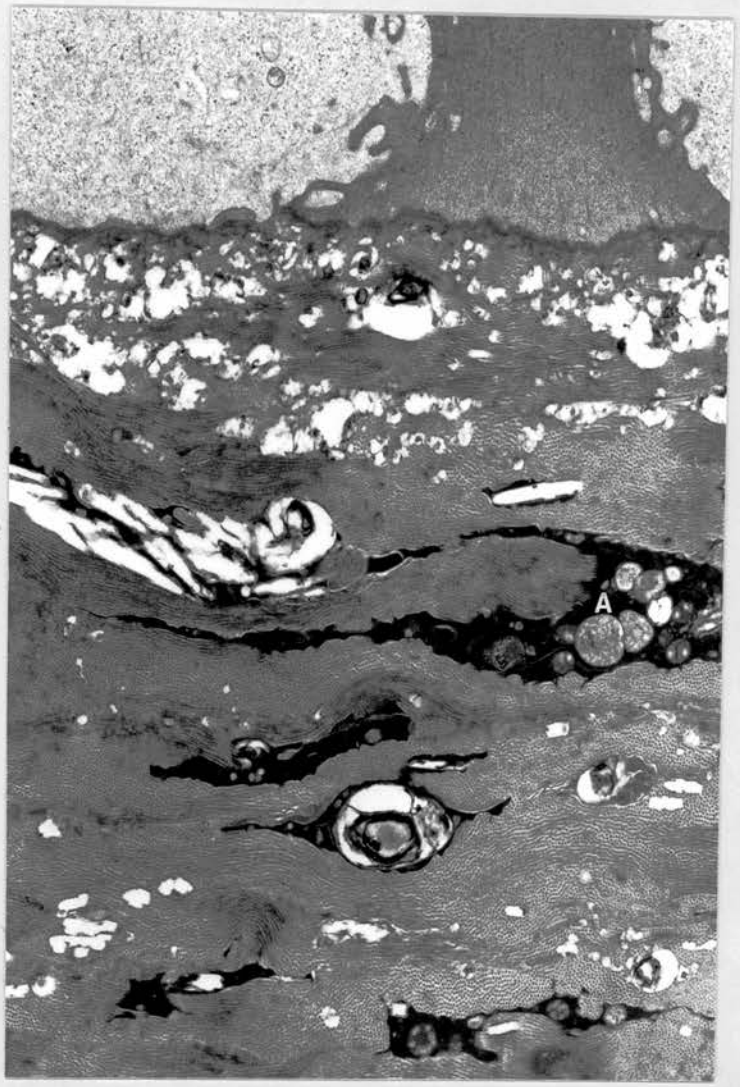
A

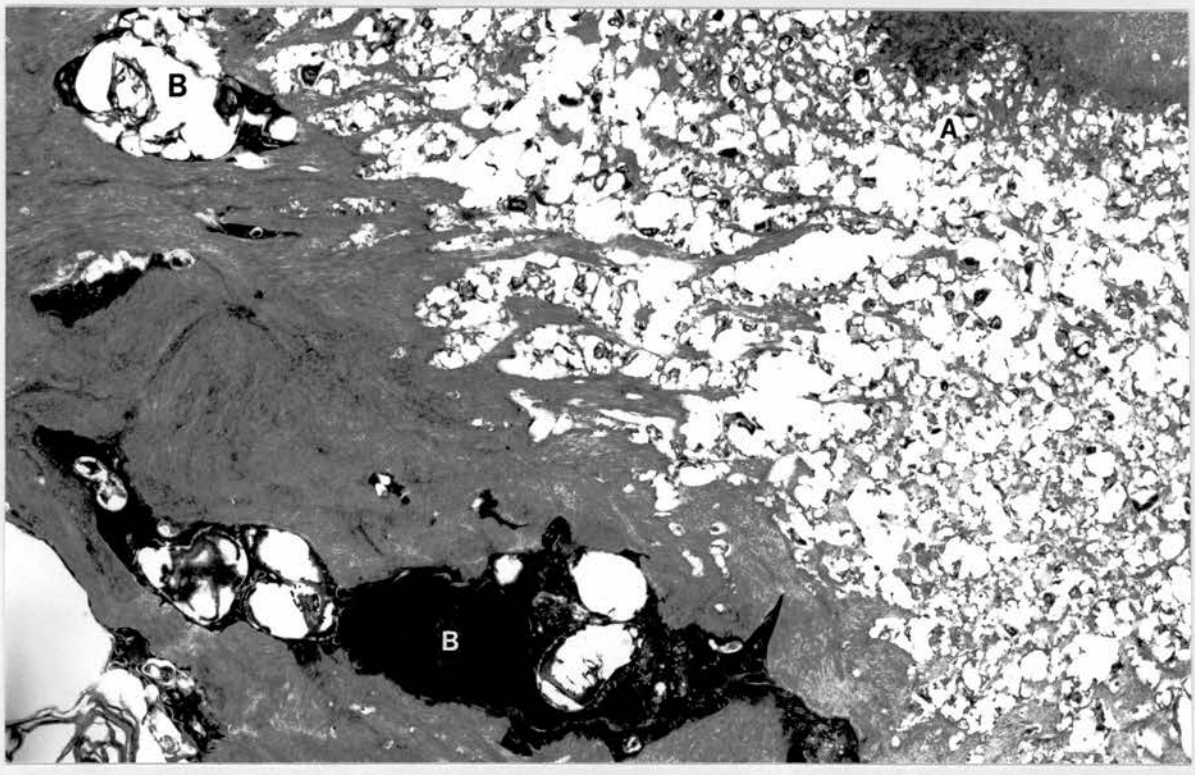
B
A
B

Figure 5.9/51

Alsatian X (150L)

Epithelial melanosis (A). There are also numerous finger-like projections in the basal lamina region.

TEM X 2,150 (2)

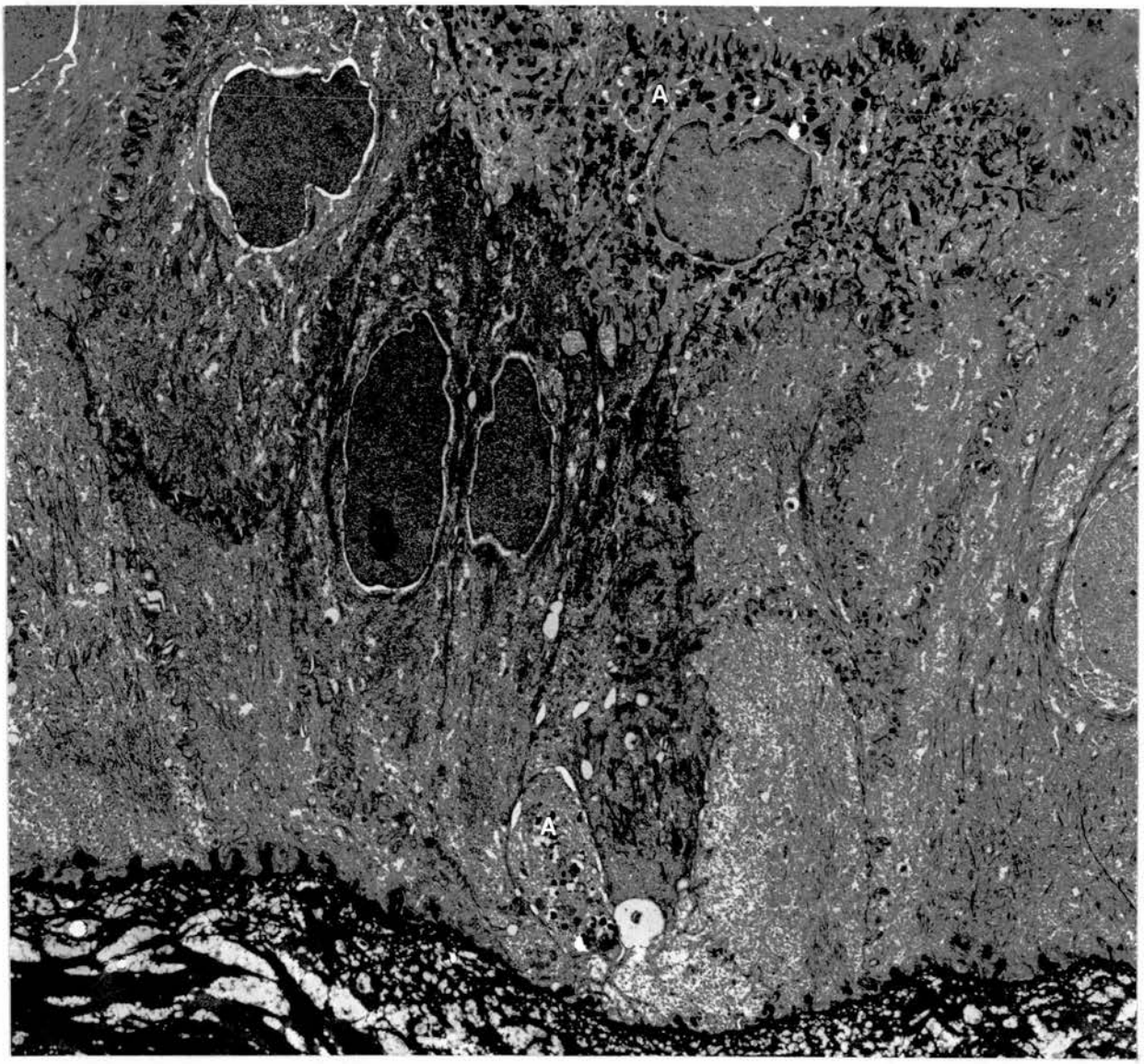
A
A

Figure 5.9/52

Welsh Springer Spaniel (42R2)

Melanocyte (A) in damaged corneal stroma.

TEM X 2,750 (2)

Figure 5.9/53

Jack Russell Terrier (132L)

Melanin granules within a melanocyte in the anterior stroma.

TEM X 21,500 (2)

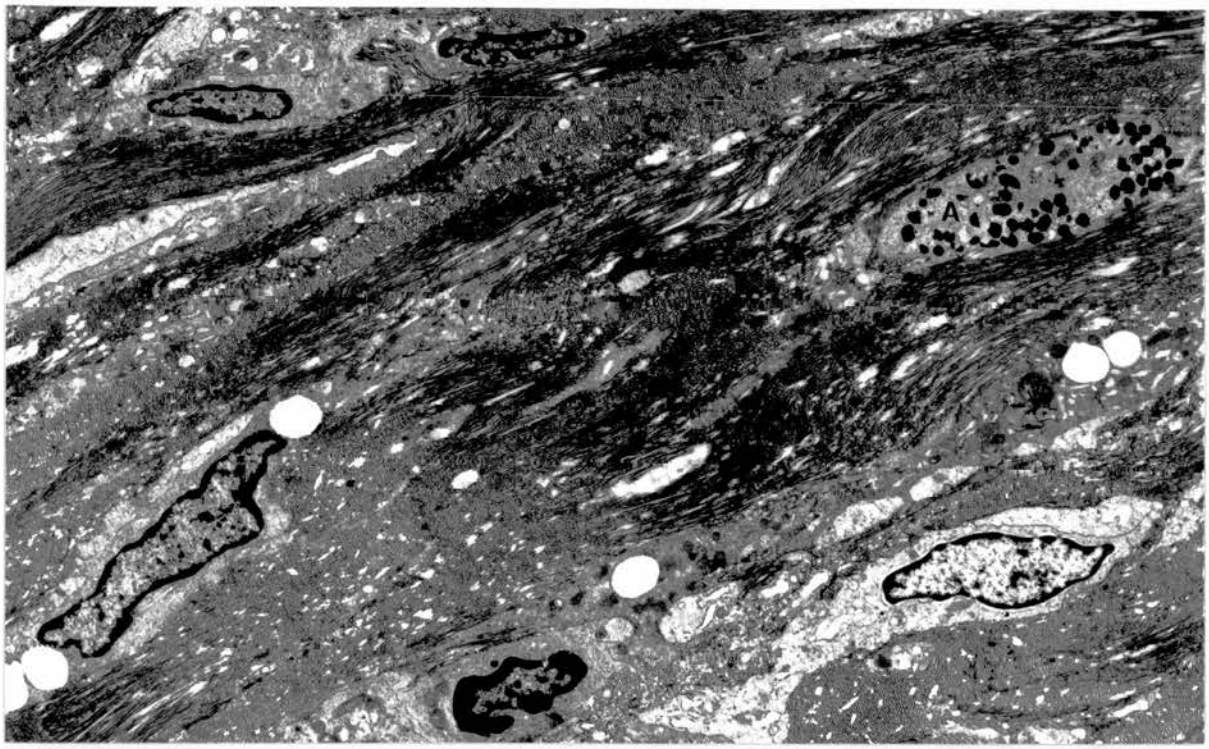
A

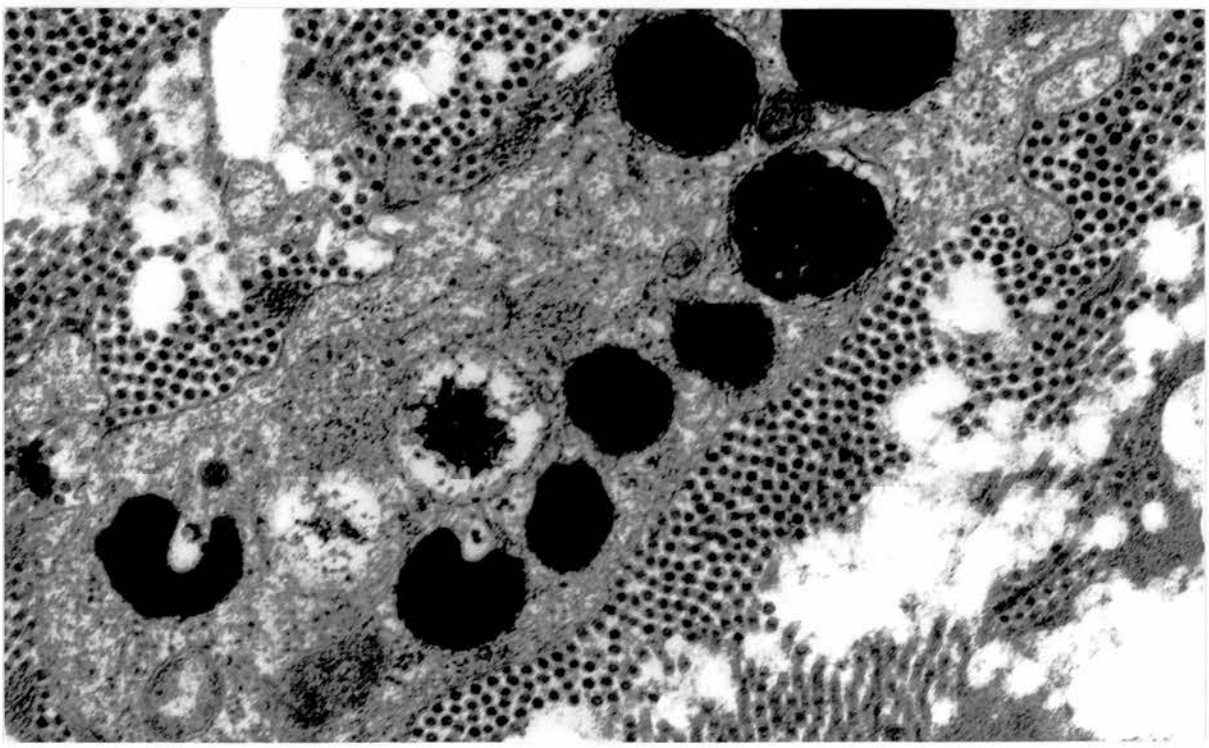

Figure 5.9/54

Alsatian (27R1)

Melanocytes (A) and fibroblasts (B) in the perilimbal stroma.

TEM X 1,650 (2)

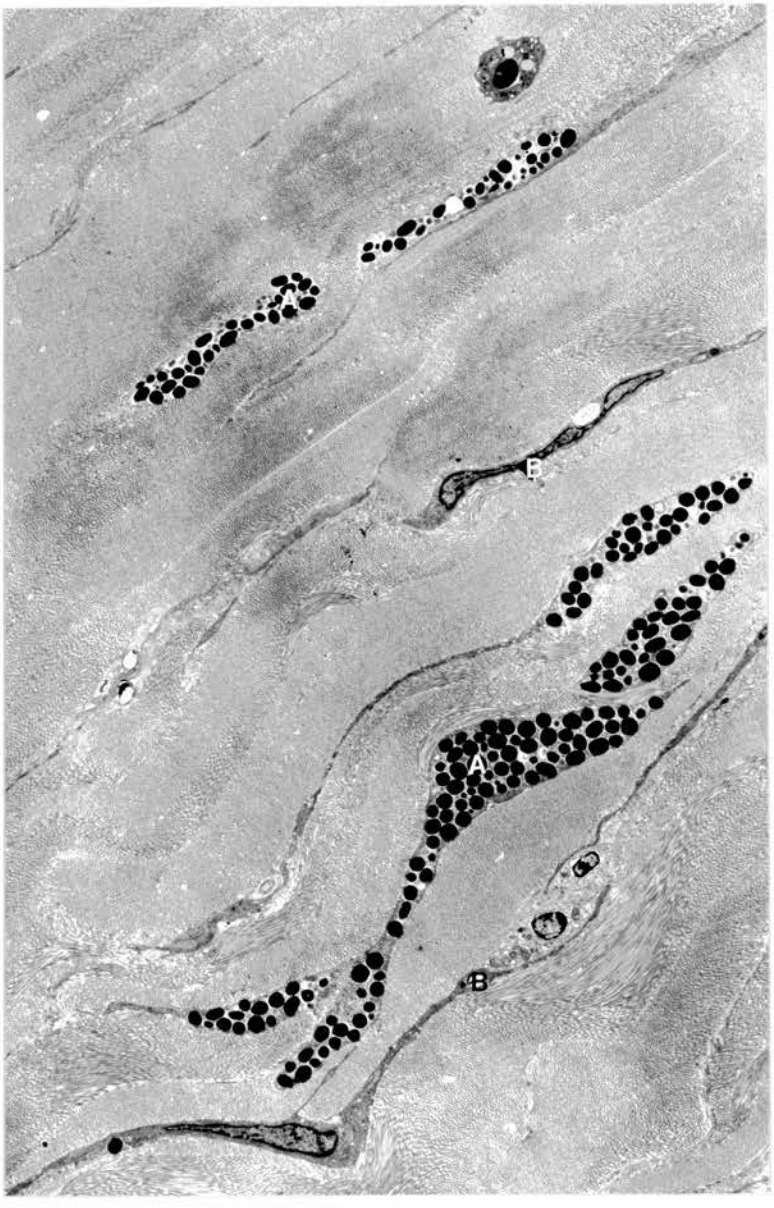
B
A
B

Figure 5.9/55

Old English Sheepdog (38L)

Stromal blood vessel containing red blood cells and a single monocyte (arrowed). The majority of cells within the stroma appear to be fibroblasts.

Toluidine Blue X 225 (4)

Figure 5.9/56

Old English Sheepdog (38L)

Numerous cells within the corneal stroma. There are macrophages of possible haematogenous origin (A) with characteristic lamellipodia (arrows), numerous dense bodies, primary and secondary lysosomes and relatively short chains of rough endoplasmic reticulum sparsely populated with ribosomes.

TEM X 1,650 (2)

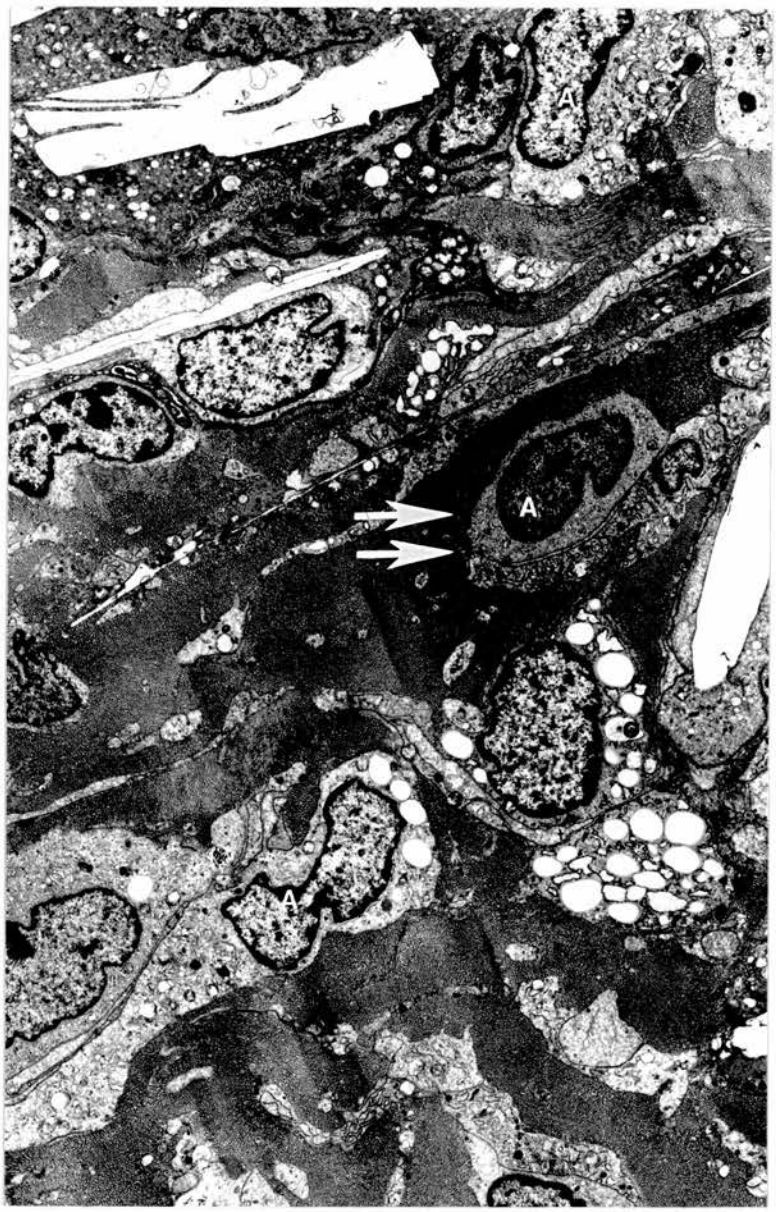
A
A
A

Figure 5.9/57

Golden Retriever (9R)

Immature fibroblasts, or fibroblast-like cells (A) in which the development of rough endoplasmic reticulum is rather poor and lipid is present within single-membrane bound vacuoles. Arrow indicates a possible "coated pit" or invagination of the plasma membrane.

TEM X 3,550 (2)

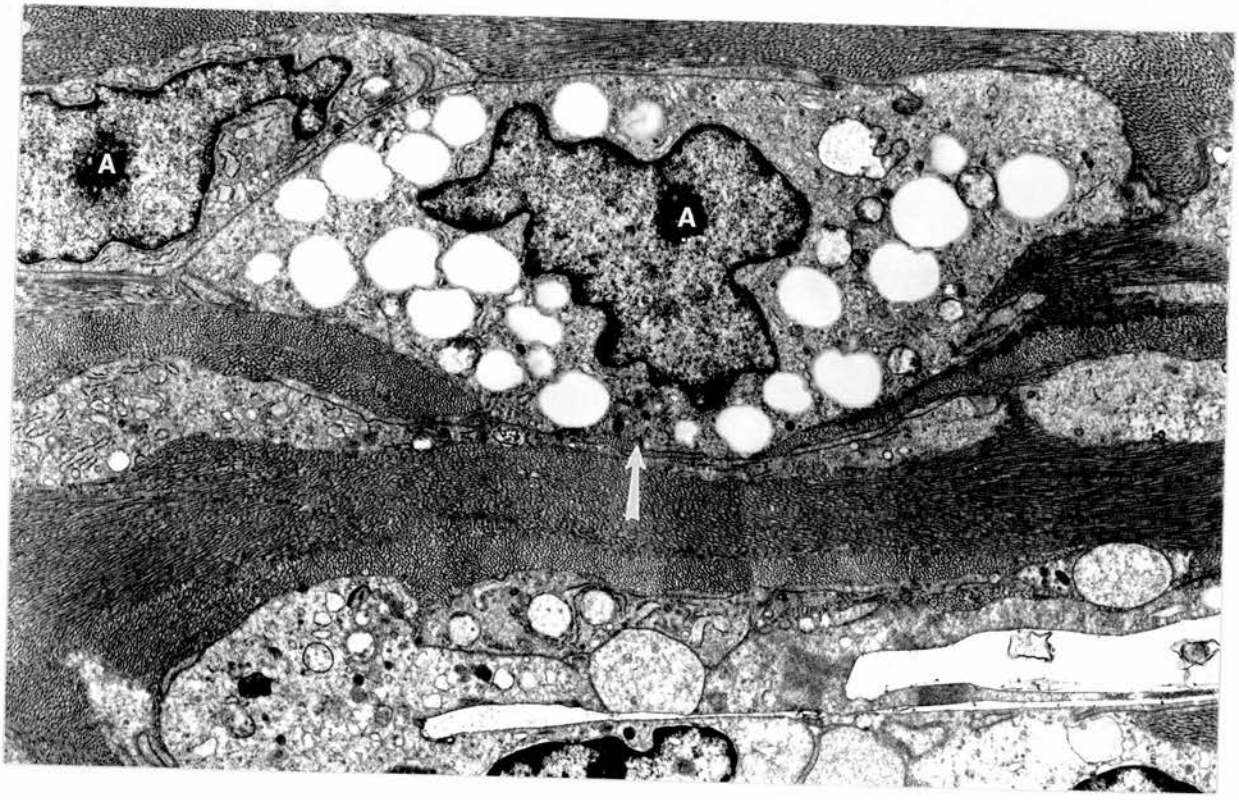
A
A

Figure 5.9/58

Welsh Springer Spaniel (42R2)

Phagocytic cell, the possible stages in endocytosis via a coated pit and lysosome formation are numbered one to four.

TEM X 7,700 (2)

Figure 5.9/59

Welsh Springer Spaniel (42R2)

Residual bodies (A) in phagocytic cells.

TEM X 7,700 (2)

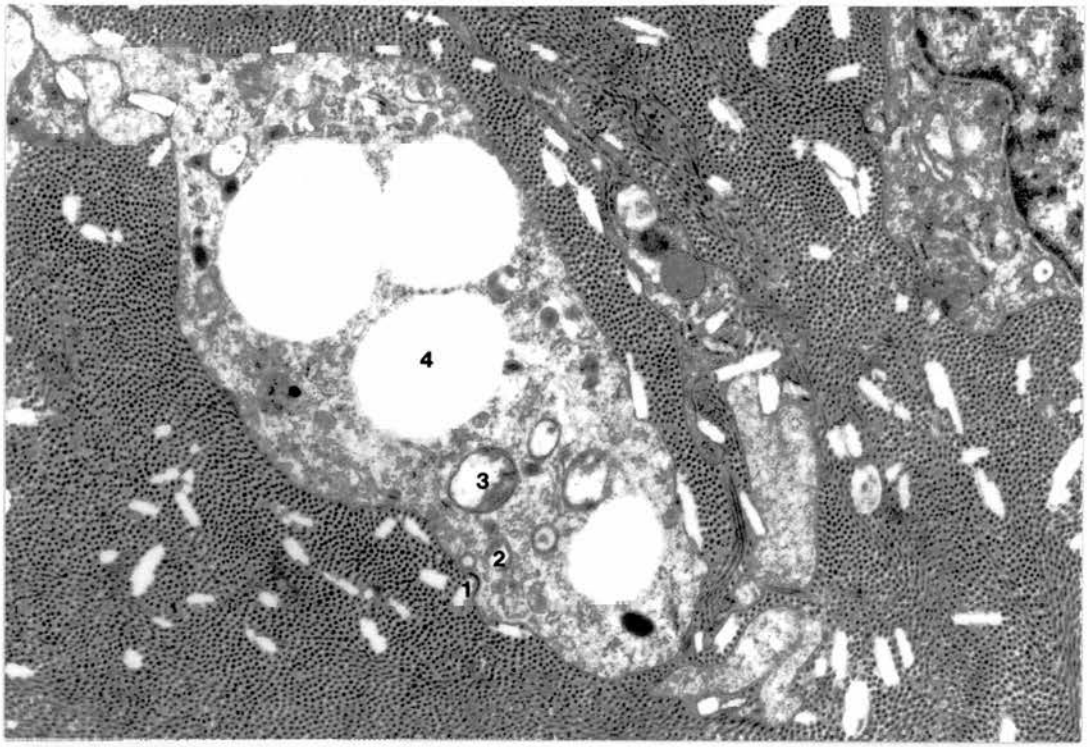
4
3
2
1

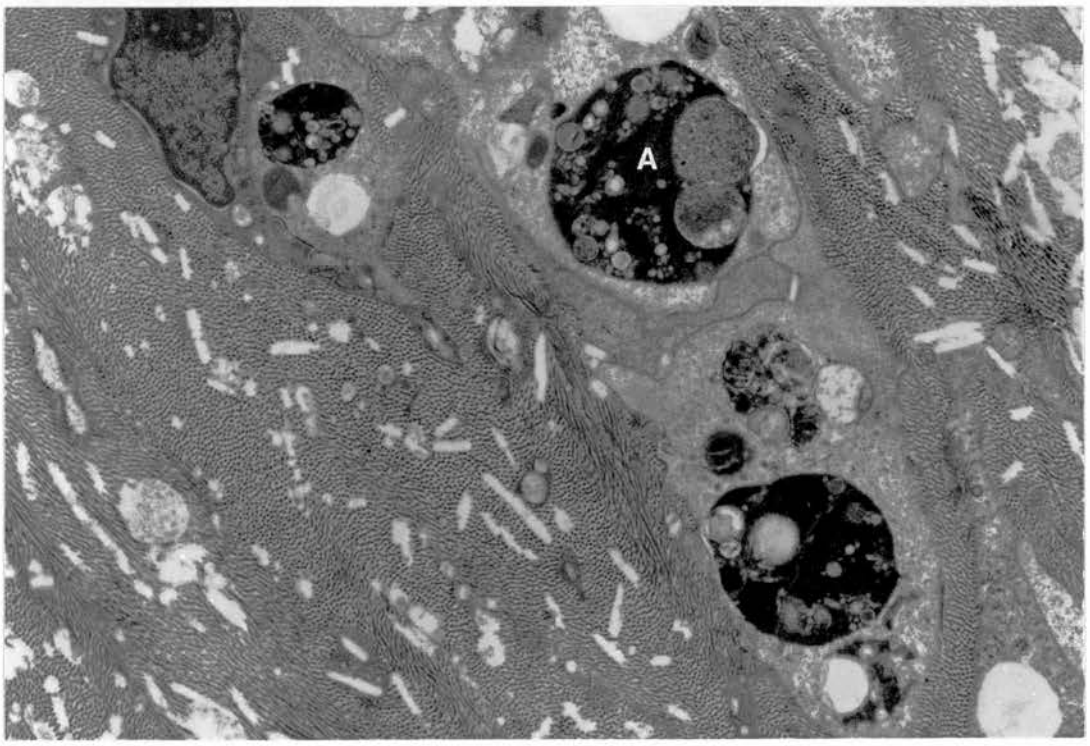
A

Figure 5.9/60

Welsh Springer Spaniel (42R2)

Phagocytic cells containing large quantities of variably sized, poorly separated vacuoles (A). Lipid histochemistry indicated mainly saturated esterified cholesterol. A fibroblast is recognisable (B).

TEM X 3,550 (2)


B
A

Figure 5.9/61

Old English Sheepdog (38L)

Phagocytic cells containing large quantities of clearly separated, small sized, vesicles (1) and well circumscribed vacuoles (2). This material was phospholipid-rich unsaturated or polyunsaturated esterified cholesterol from earlier studies, and the impression was that hydrophilic lipids were a major constituent of small inclusions and decreased relative to non-saturated esterified cholesterol in larger inclusions.

TEM X 3,550 (2)

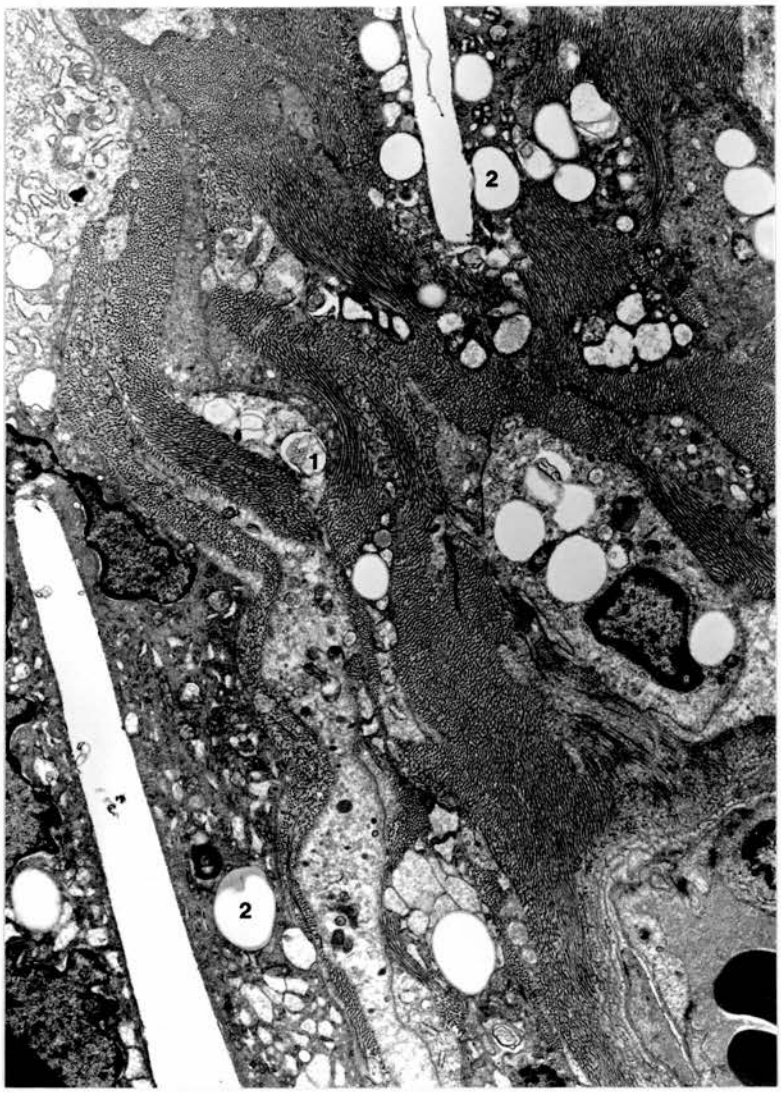
2
1
2

Figure 5.9/62

Old English Sheepdog (38R)

Single membrane bound vacuole (1) containing smaller osmiophilic vesicles, or liposomes. This structure resembles others (2) present in in a perivascular foam cell. Another cell close to the abluminal endothelial cell surface contains numerous circumscribed membranous lamellae or liposomes (3). Endothelial cells (B) and pericytes (C) are also prominent.

TEM X 4,600 (2)

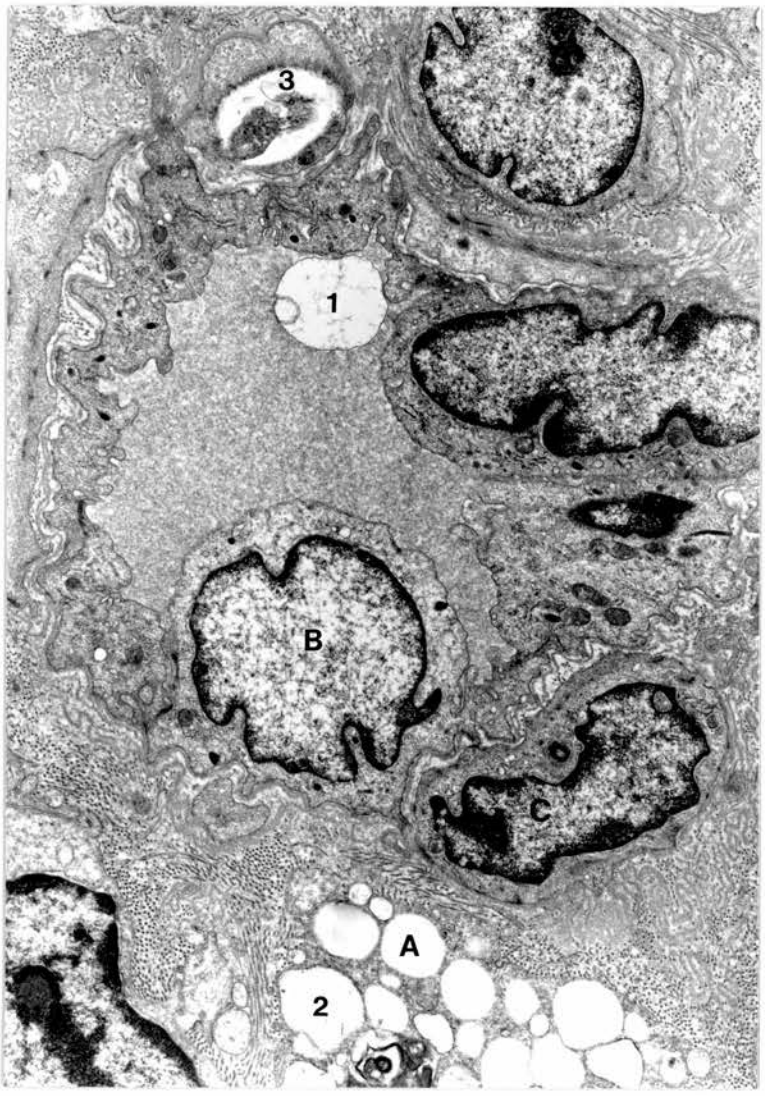
3
1
B
C
A
2

Figure 5.9/63

Old English Sheepdog (38L)

The phagocytic cells in this animal contained mainly phospholipid-rich, non-saturated, esterified cholesterol and there were regions of cornea which were of almost normal appearance. In this section there is a single stromal blood vessel (A) with endothelial cells (B) and a pericyte (C). Macrophages (D) and fibroblasts (E) are recognisable; the origin of foam cells (F) is not so readily determined, although fibroblasts seem likely; the osmiophilic nature of the foam cell contents accords with the findings of lipid histochemistry.

TEM X 1,650 (2)

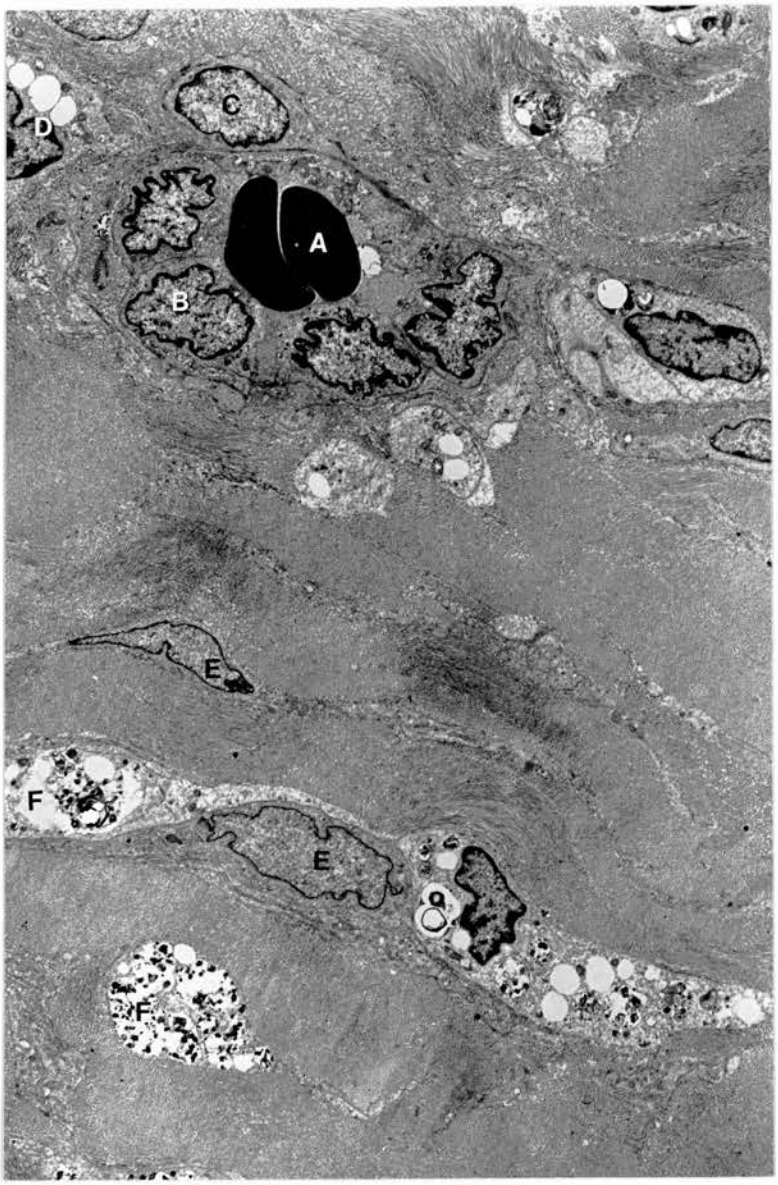
A
B
C
D
E
E
F
F

Figure 5.9/64

Old English Sheepdog (38R)

Giant cell enveloping cholesterol crystals (A). There is also a single macrophage (B) and part of a fibroblast may be present at (C).

TEM X 2,750 (2)


B
A
A
C

Figure 5.9/65

Old English Sheepdog (38L)

Well formed giant cell (A) containing clearly defined vacuoles in which non-saturated esterified cholesterol predominated. Individual macrophages (B) are also present.

TEM X 1,650 (2)

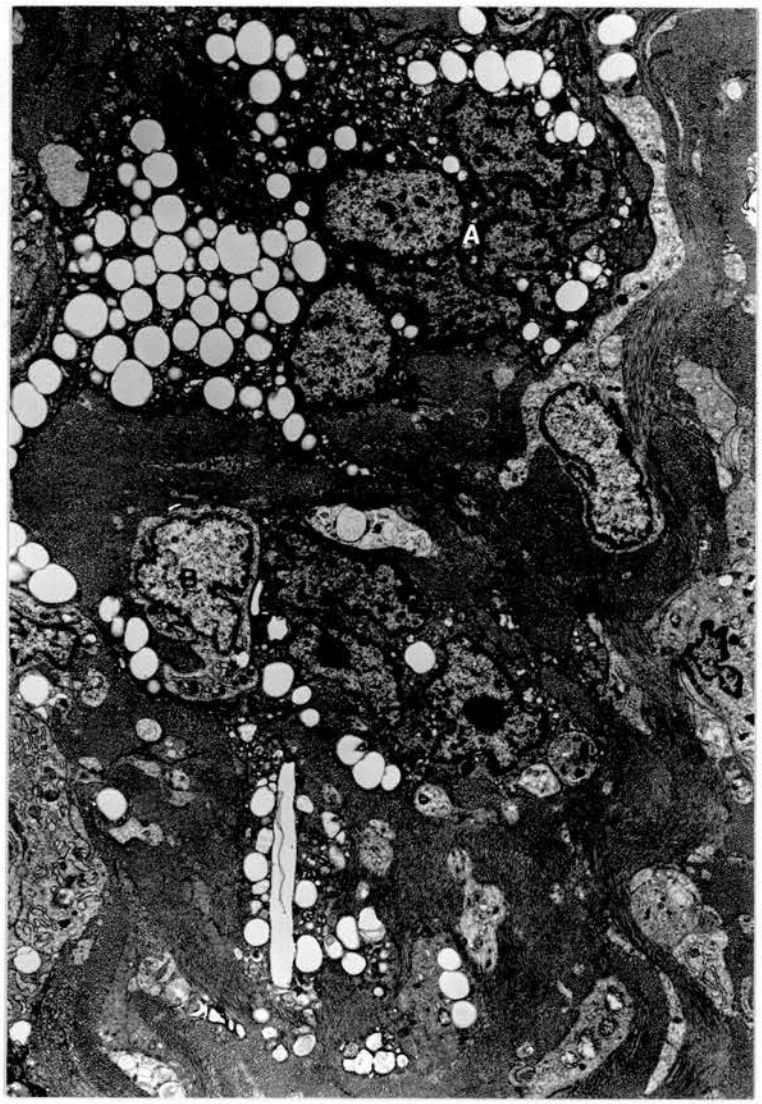
A
B

Figure 5.9/66

Old English Sheepdog (38L)

Part of a giant cell which has enveloped cholesterol crystals (A) next to a small stromal blood vessel. Liposomes can be identified in a variety of sites numbered one to five and may be representative of lipid material in transit.

TEM X 4,600 (2)


5
4
3
2
A
A
A
1

Figure 5.9/67

Old English Sheepdog (38L)

Corneal appearance of a lesion which is regressing in a patient treated for hypothyroidism. Fibroblasts (A) in the upper part of the micrograph are of normal appearance. There are a number of fat-filled cells, confirmed as mainly macrophages (B) and giant cells (C) at greater magnification. The majority of fat-filled cells contain well separated small clear spaces, probably polyunsaturated cholesterol esters; cholesterol crystals are relatively sparse. Lipid histochemistry had also indicated rare globules of triglyceride and these are probably represented by the larger round spaces (arrows). As is typical of a regressing lesion the majority of lipid is intracellular and the majority of cells are of healthy appearance. Extensive stromal vascularisation (D) is also apparent.

Toluidine Blue X 110 (4)

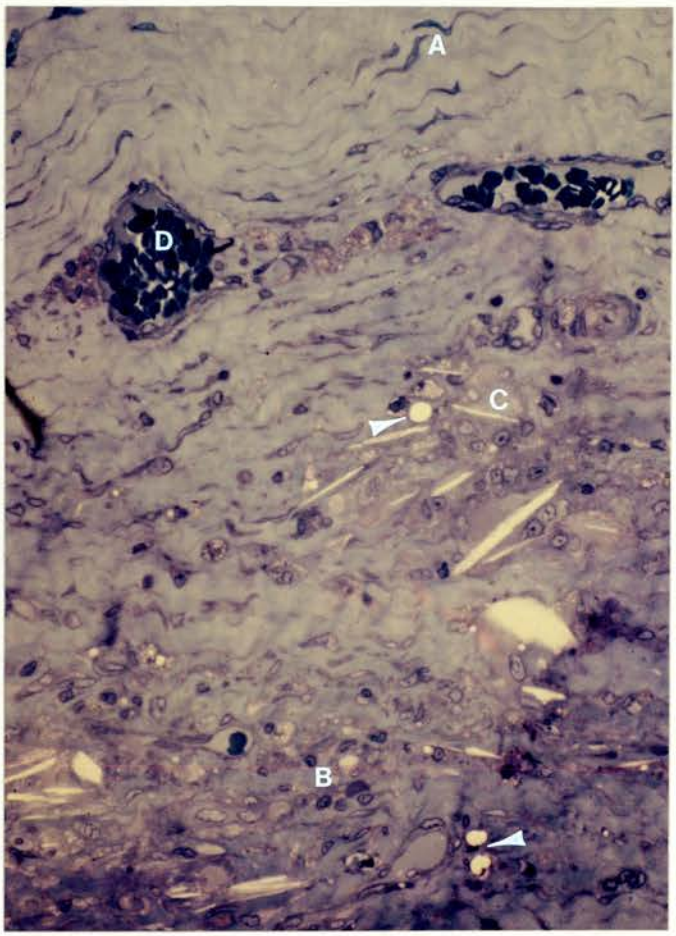
A
D
C
B